

**DEGRADATION OF GUAR-BASED FRACTURING GELS:
A STUDY OF OXIDATIVE AND ENZYMATIC BREAKERS**

A Thesis

by

MUHAMMAD USMAN SARWAR

Submitted to the Office of Graduate Studies of
Texas A&M University
in partial fulfillment of the requirements for the degree of
MASTER OF SCIENCE

December 2010

Major Subject: Petroleum Engineering

**DEGRADATION OF GUAR-BASED FRACTURING GELS:
A STUDY OF OXIDATIVE AND ENZYMATIC BREAKERS**

A Thesis

by

MUHAMMAD USMAN SARWAR

Submitted to the Office of Graduate Studies of
Texas A&M University
in partial fulfillment of the requirements for the degree of

MASTER OF SCIENCE

Approved by:

Chair of Committee,	Hisham Nasr-El-Din
Committee Members,	Stephen A. Holditch
	Mahmoud M. El-Halwagi
Head of Department,	Stephen A. Holditch

December 2010

Major Subject: Petroleum Engineering

ABSTRACT

Degradation of Guar-Based Fracturing Gels:

A Study of Oxidative and Enzymatic Breakers. (December 2010)

Muhammad Usman Sarwar, B.E., Nadirshaw Edulji Dinshaw University of Engineering
and Technology, Karachi, Pakistan

Chair of Advisory Committee: Dr. Hisham Nasr-El-Din

Unbroken gel and residue from guar-based fracturing gels can be a cause for formation damage. The effectiveness of a fracturing treatment depends on better achieving desired fracture geometry, proper proppant placement and after that, a good clean-up. The clean-up is achieved by reducing the fluid viscosity using chemical additives called 'Breakers'. There are many different types of breakers used in the industry, but they can be broadly divided into two categories: oxidizers and enzymes. Breaker performance depends on bottomhole temperature, breaker concentration and polymer loading. Different kind of breakers, used at different concentrations and temperatures, give different kind of 'break' results. Therefore, the amount of unbroken gel and residue generated is also different.

This project was aimed at studying basic guar-breaker interactions using some of the most common breakers used in the industry. The breakers studied cover a working temperature range of 75 °F to 300 °F. The effectiveness of each breaker was studied and also the amount of damage that it causes.

Viscosity profiles were developed for various field concentrations of breakers. The concentrations were tested over temperature ranges corresponding to the temperatures at which each breaker is used in the field. The majority of these viscosity tests were 6 hours long, with a few exceptions. Early time viscosity data, for the initial 10 minutes of the test, was also plotted from these tests for fracturing applications where the breaker is required to degrade the fluid by the time it reached downhole. This was needed to prevent the damage to the pumping equipment at the surface yet still have almost water-like fluid entering into the formation.

The study provides a better understanding of different breaker systems, which can be used in the industry, while designing fracturing fluid systems in order to optimize the breaker performance and achieve a better, cleaner break to minimize the formation damage caused by polymer degradation.

DEDICATION

This thesis is dedicated to my mother, sister and the rest of my family.

ACKNOWLEDGEMENTS

I would like to express my deepest gratitude and appreciation to my advisor and committee chair, Dr. Hisham A. Nasr-El-Din, for his continuous encouragement, guidance, and support. Also, I would like to thank Kay E. Cawiezel for her advice and guidance through the course of this project. I also extend my appreciation to the members of my graduate committee, Dr. Stephen A. Holditch and Dr. Mahmoud M. El-Halwagi, for their help.

Many thanks are due to all my colleagues who helped me during the course of this research. I would like to acknowledge the facilities and resources provided by the BJ Services Company Research and Technology Center in Tomball, Texas. Finally, the facilities and support provided by the Harold Vance Department of Petroleum Engineering of Texas A&M University are gratefully acknowledged.

NOMENCLATURE

ppt	pounds per thousand gallons
gpt	gallons per thousand gallons
T	temperature (°F)
n'	flow behavior index (dimensionless)
K	consistency index (lbf-s ⁿ /ft ²)
RAB	residue-after-break

TABLE OF CONTENTS

	Page
ABSTRACT	iii
DEDICATION	v
ACKNOWLEDGEMENTS	vi
NOMENCLATURE	vii
TABLE OF CONTENTS	viii
LIST OF TABLES	xi
LIST OF FIGURES	xiii
1. INTRODUCTION.....	1
1.1. Introduction	1
1.2. Literature Review	2
1.3. Objectives.....	4
1.4. Thesis Outline	4
2. HYDRAULIC FRACTURING.....	6
2.1. Introduction	6
2.2. History of Hydraulic Fracturing.....	7
2.3. Hydraulic Fracturing Process	8
3. FRACTURING FLUIDS	12
3.1. Introduction	12
3.2. History of Fracturing Fluids.....	13
3.3. Types of Fracturing Fluids	15
3.4. Water-Based Fracturing Fluids	16
3.5. Guar-Based Fracturing Fluids	17
3.5.1. Guar Gum	18
3.5.1.1. Structure of Guar	18
3.5.1.2. Guar Derivatives	20
3.5.2. Crosslinkers.....	22

	Page
3.5.3. Buffers	27
3.5.4. Breakers	27
3.5.4.1. Oxidizers	28
3.5.4.2. Enzymes	30
3.5.5. Biocides	31
3.5.6. Clay Stabilizers	31
3.5.7. Surfactants	32
3.6. Formation Damage Caused by Fracturing Fluids	32
3.7. Rheological Properties of Fracturing Fluids	32
4. EXPERIMENTAL PROCEDURES, RESULTS AND DISCUSSION	34
4.1. Materials	34
4.2. Experimental Procedures	34
4.2.1. Preparing the Gel	34
4.2.2. Viscosity Measurement	37
4.2.3. Residue-After-Break (RAB) Test/ Waterbath-Filtration Test	42
4.2.4. Molecular Weight Cut Off Procedure (MWCO)	45
4.3. Results and Discussion	47
4.3.1. Viscosity Measurement	47
4.3.1.1 Ammonium Persulfate	47
4.3.1.2. Magnesium Peroxide	55
4.3.1.3. Sodium Bromate	60
4.3.1.4. Galactomannanase	65
4.3.1.5. Flow Parameters n' and K	69
4.3.2. Early Time Data	74
4.4. Breaker Activity Curves (S-Curves)	79
4.4.1. Ammonium Persulfate	79
4.4.2. Magnesium Peroxide	81
4.4.3. Sodium Bromate	84
4.4.4. Galactomannanase	86
4.5. Comparison of Breaker Activity Curves	88
4.6. Ammonium Persulfate – 24 hour Break Tests	90
4.7. Residue-After-Break (RAB) Test	95
5. CONCLUSIONS AND RECOMMENDATION	98
REFERENCES	101
APPENDIX A: FLOW PARAMETERS n' AND K	103
APPENDIX B: EARLY TIME VISCOSITY CHARTS	186

VITA	202
------------	-----

LIST OF TABLES

		Page
Table 3.1	Guar Gel Formulation (45 lb/1000 gal) (Nasr-El-Din et al., 2007)	18
Table 4.1	Flow parameters n' and K for 30 ppt guar gel with 1 ppt ammonium persulfate at 125 °F	70
Table 4.2	Flow parameters n' and K for 60 ppt guar gel with 1 ppt magnesium peroxide at 225 °F	71
Table 4.3	Flow parameters n' and K for 30 ppt guar gel with 1 ppt galactomannanase at 175 °F	72
Table 4.4	Flow parameters n' and K for 30 ppt guar gel with 1 ppt sodium bromate at 250 °F	73
Table 4.5	Lowest viscosity values from ammonium persulfate tests with 30 ppt gel	79
Table 4.6	Lowest viscosity values from magnesium peroxide tests with 30 ppt gel	81
Table 4.7	Lowest viscosity values from magnesium peroxide tests with 60 ppt gel	81
Table 4.8	Lowest viscosity values from sodium bromate tests with 30 ppt gel	84
Table 4.9	Lowest viscosity values from sodium bromate tests with 60 ppt gel	84
Table 4.10	Lowest viscosity values from galactomannanase tests with 30 ppt gel	86
Table 4.11	Residue generated using ammonium persulfate at 125 °F	95
Table 4.12	Residue generated using sodium persulfate at 125 °F	95
Table 4.13	Residue generated using galactomannanase at 125 °F	96

	Page
Table 4.14 Residue generated using ammonium persulfate at 150 °F	96
Table 4.15 Residue generated using sodium persulfate at 150 °F.....	96
Table 4.16 Residue generated using galactomannanase at 150 °F	97

LIST OF FIGURES

	Page
Figure 2.1 Internal pressure breaking the vertical wellbore (Reservoir Stimulation, 2000).....	8
Figure 2.2 Introducing proppant into the fracture (Reservoir Stimulation, 2000).....	10
Figure 3.1 Linear structure of guar polymer	19
Figure 3.2 A single repeating unit of guar (Brannon and Tjon-joe-Pin, 1994).....	20
Figure 3.3 A comparison between guar and its derivatives (Rae and di Lullo, 1996).....	22
Figure 3.4 pH ranges for various crosslinking agents (Rae and di Lullo, 1996).....	23
Figure 3.5 Temperature ranges for various crosslinking agents (Rae and di Lullo, 1996).....	24
Figure 3.6 Structure of borate crosslinked guar (Modern Fracturing, 2007)	26
Figure 3.7 Dimensionless monoborate ion concentration vs pH for various temperatures (Haris, 1993).....	26
Figure 3.8 Radical reaction sites available on a single repeating unit of guar (Brannon and Tjon-joe-Pin, 1994)	28
Figure 4.1 JANKE & KUNKEL overhead mixer	36
Figure 4.2 OFITE M900 Viscometer	38
Figure 4.3 CHANDLER 5550 HPHT Viscometer	39
Figure 4.4 Temperature controlled waterbath	43
Figure 4.5 Filtration process going on in fluid loss cells	44
Figure 4.6 Thermo scientific high speed centrifuge.....	46

	Page
Figure 4.7	Special molecular weight cut off tube 46
Figure 4.8	Viscosity profile of 30 ppt guar gel with 0.25 ppt ammonium persulfate (75 °F – 175 °F) 48
Figure 4.9	Viscosity profile of 30 ppt guar gel with 0.25 ppt ammonium persulfate (200 °F – 250 °F) 48
Figure 4.10	Viscosity profile of 30 ppt guar gel with 0.5 ppt ammonium persulfate (75 °F – 175 °F) 49
Figure 4.11	Viscosity profile of 30 ppt guar gel with 0.5 ppt ammonium persulfate (200 °F – 250 °F) 49
Figure 4.12	Viscosity profile of 30 ppt guar gel with 1 ppt ammonium persulfate (75 °F – 175 °F) 50
Figure 4.13	Viscosity profile of 30 ppt guar gel with 1 ppt ammonium persulfate (200 °F – 250 °F) 50
Figure 4.14	Viscosity profile of 60 ppt guar gel with 1 ppt ammonium persulfate 51
Figure 4.15	Viscosity profile of 30 ppt guar gel with ammonium persulfate at 75 °F 51
Figure 4.16	Viscosity profile of 30 ppt guar gel with ammonium persulfate at 100 °F 52
Figure 4.17	Viscosity profile of 30 ppt guar gel with ammonium persulfate at 125 °F 52
Figure 4.18	Viscosity profile of 30 ppt guar gel with ammonium persulfate at 150 °F 53
Figure 4.19	Viscosity profile of 30 ppt guar gel with ammonium persulfate at 175 °F 53
Figure 4.20	Viscosity profile of 30 ppt guar gel with ammonium persulfate at 200 °F 54

	Page
Figure 4.21	Viscosity profile of 30 ppt guar gel with ammonium persulfate at 225 °F 54
Figure 4.22	Viscosity profile of 30 ppt guar gel with ammonium persulfate at 250 °F 55
Figure 4.23	Viscosity profile of 30 ppt guar gel with 1 ppt magnesium peroxide..... 56
Figure 4.24	Viscosity profile of 60 ppt guar gel with 1 ppt magnesium peroxide..... 56
Figure 4.25	Viscosity profile of 30 ppt guar gel with 5 ppt magnesium peroxide..... 57
Figure 4.26	Viscosity profile of 30 ppt guar gel with 10 ppt magnesium peroxide..... 57
Figure 4.27	Viscosity profile of 30 ppt guar gel with magnesium peroxide at 175 °F 58
Figure 4.28	Viscosity profile of 30 ppt guar gel with magnesium peroxide at 200 °F 58
Figure 4.29	Viscosity profile of 30 ppt guar gel with magnesium peroxide at 225 °F 59
Figure 4.30	Viscosity profile of 30 ppt guar gel with magnesium peroxide at 250 °F 59
Figure 4.31	Viscosity profile of 30 ppt guar gel with 1 ppt sodium bromate 60
Figure 4.32	Viscosity profile of 60 ppt guar gel with 1 ppt sodium bromate 61
Figure 4.33	Viscosity profile of 30 ppt guar gel with 5 ppt sodium bromate 61
Figure 4.34	Viscosity profile of 30 ppt guar gel with 10 ppt sodium bromate 62
Figure 4.35	Viscosity profile of 30 ppt guar gel with sodium bromate at 150 °F..... 62
Figure 4.36	Viscosity profile of 30 ppt guar gel with sodium bromate at 200 °F..... 63
Figure 4.37	Viscosity profile of 30 ppt guar gel with sodium bromate at 225 °F..... 63
Figure 4.38	Viscosity profile of 30 ppt guar gel with sodium bromate at 250 °F..... 64

	Page
Figure 4.39	Viscosity profile of 30 ppt guar gel with sodium bromate at 275 °F..... 64
Figure 4.40	Viscosity profile of 30 ppt guar gel with sodium bromate at 300 °F..... 65
Figure 4.41	Viscosity profile of 30 ppt guar gel with 0.5 gpt galactomannanase..... 66
Figure 4.42	Viscosity profile of 30 ppt guar gel with 1 gpt galactomannanase..... 66
Figure 4.43	Viscosity profile of 30 ppt guar gel with galactomannanase at 75 °F 67
Figure 4.44	Viscosity profile of 30 ppt guar gel with galactomannanase at 100 °F 67
Figure 4.45	Viscosity profile of 30 ppt guar gel with galactomannanase at 125 °F 68
Figure 4.46	Viscosity profile of 30 ppt guar gel with galactomannanase at 150 °F 68
Figure 4.47	Viscosity profile of 30 ppt guar gel with galactomannanase at 175 °F 69
Figure 4.48	Early time viscosity of 30 ppt guar gel with 0.25 ppt ammonium persulfate (75 °F – 175 °F) 75
Figure 4.49	Early time viscosity of 30 ppt guar gel with ammonium persulfate at 225 °F 75
Figure 4.50	Early time viscosity of 60 ppt guar gel with 1 ppt magnesium peroxide..... 76
Figure 4.51	Early time viscosity of 30 ppt guar gel with magnesium peroxide at 200 °F 76
Figure 4.52	Early time viscosity of 30 ppt guar gel with 10 ppt sodium bromate..... 77
Figure 4.53	Early time viscosity of 30 ppt guar gel with sodium bromate at 250 °F 77
Figure 4.54	Early time viscosity of 30 ppt guar gel with 1 gpt galactomannanase.... 78

	Page
Figure 4.55 Early time viscosity of 30 ppt guar gel with galactomannanase at 175 °F	78
Figure 4.56 Breaker activity curves for 30 ppt gel with ammonium persulfate based on temperature.....	80
Figure 4.57 Breaker activity curves for 30 ppt gel with ammonium persulfate based on concentration	80
Figure 4.58 Breaker activity curves for 30 ppt gel with magnesium peroxide based on temperature.....	82
Figure 4.59 Breaker activity curves for 30 ppt gel with magnesium peroxide based on concentration	82
Figure 4.60 Breaker activity curves for 60 ppt gel with magnesium peroxide based on temperature.....	83
Figure 4.61 Breaker activity curves for 30 ppt gel with sodium bromate based on temperature.....	85
Figure 4.62 Breaker activity curves for 30 ppt gel with sodium bromate based on concentration	85
Figure 4.63 Breaker activity curves for 60 ppt gel with sodium bromate based on temperature.....	86
Figure 4.64 Breaker activity curves for 30 ppt gel with galactomannanase based on temperature.....	87
Figure 4.65 Breaker activity curves for 30 ppt gel with galactomannanase based on concentration	87
Figure 4.66 Breaker activity curves for different breakers at 1 ppt concentration tested with 30 ppt gels.....	88
Figure 4.67 Breaker activity curves for different breakers at 1 ppt concentration tested with 60 ppt gels.....	89
Figure 4.68 24 hr viscosity profile of 30 ppt gel without any breaker added at room temperature	91

	Page
Figure 4.69 24 hr viscosity profile of 30 ppt gel with 0.25 ppt ammonium persulfate at room temperature.....	91
Figure 4.70 24 hr viscosity profile of 30 ppt gel with 0.5 ppt ammonium persulfate at room temperature.....	92
Figure 4.71 24 hr viscosity profile of 30 ppt gel with 1 ppt ammonium persulfate at room temperature	92
Figure 4.72 24 hr viscosity profile of 30 ppt gel with 5 ppt ammonium persulfate at room temperature	93
Figure 4.73 24 hr viscosity profile of 30 ppt gel with 10 ppt ammonium persulfate at room temperature	93
Figure 4.74 Breaker activity curve for 24 hr ammonium persulfate test with 30 ppt guar gel at room temperature	94

1. INTRODUCTION

1.1 Introduction

Guar is a naturally occurring polymer used as a gellant in hydraulic fracturing fluids. Natural guar contains some residue which does not contribute to the increase in viscosity. This viscosity is required to carry the proppant into the fracture after the fracture has been created in order to keep it open when the pumping is stopped. Once the proppant is delivered into the fracture, the fluid viscosity needs to be reduced so that it is easy to flow back and clean-up the formation.

Chemical breakers are used in hydraulic fracturing fluids to reduce the molecular weight of guar polymers which reduces fluid viscosity and facilitates the flowback of residual polymer providing rapid recovery of polymer from the proppant pack. Ineffective breakers or misapplication of breakers can result in screenouts or flowback of viscous fluids both of which can significantly decrease the well productivity.

Service companies and operators spend large quantities of time “optimizing” breaker systems for the particular well conditions and fluid requirements. Typically breaker profiles are developed with new product introduction and are optimized for the particular fluid system. A comprehensive study has not been done to evaluate breaker activity as just a function of time and temperature.

This thesis follows the style and format of *SPE Production & Operations*.

1.2 Literature Review

Almond (1982) looked into the effect of breaker concentration, breaker type, break time, crosslinker and pH of guar and cellulose based fracturing fluids; demonstrating that the residual polymer after break can cause flow reduction by plugging the formation.

Almond and Bland (1984) studied the effect of break mechanism on residue generated for cellulose and guar based polymers; stating that the break temperature or breaking mechanism plays a significant role in determining the amount of flow reduction.

Gall and Raible (1985) used size exclusion chromatography (SEC) to determine the decrease in molecular size of the broken polymers. The study showed that unbroken or partially broken polymer can significantly reduce flow through a porous medium and the insoluble residue generated during the degradation of guar polymers can affect the pore size of the medium. This means that polymers containing naturally occurring residue require greater reduction in molecular weight than the ones without residue. The study also states that viscosity reduction does not necessarily mean that proppant pack damage will not occur because the amount of breakers used typically are insufficient to break the polymer completely.

Roodhart et al. (1988) developed a realistic hydraulic fracturing simulator; showing that inadequate degradation of polymer based fracturing fluids can cause a considerable decrease in well productivity.

Craig et al. (1992) conducted a study of delayed titanate crosslinked gel with ammonium persulfate breaker stating that a lower concentration of breaker can degrade a fluid based on the fluid viscosity, but higher concentrations of breaker are needed to reduce the damage to the proppant pack.

Brannon and Tjon-Joe-Pin (1994), and, Rae and di Lullo (1996) presented a comprehensive account on the development of fracturing fluids through the years, explaining oxidative and enzymatic breaking systems.

Brannon and Tjon-Joe-Pin (1994), and, DeVine et al. (1998) concluded that guar-linkage specific enzymes (LSE) are the most effective way of reducing the damage caused by polymer degradation. The study claims that enzyme-based fluids provide better degradation compared to oxidative breakers and are also environmentally friendly.

Brannon and Tjon-Joe-Pin (1995) utilized new laboratory procedures to determine breaker efficiency based on the molecular size of broken polymers. The study concluded that a reduction in viscosity does not necessarily mean reduction in molecular weight since a lot of fluids with significantly reduced viscosity contained large polymer fragments with high molecular weights.

Nasr-El-Din et al. (2007) studied the degradation of guar based, borate-crosslinked gels. The work showed that the time required to degrade the gel was a function of breaker type, breaker concentration and the polymer loading. The study also concluded that guar always produced some residue irrespective of the type and concentration of breaker, and this residue can cause formation damage.

1.3 Objectives

The research proposed in this project will use a basic guar gel, prepared by mixing with water at a particular concentration. This gel will then be studied through various experimental procedures using various oxidative and enzymatic breakers to determine breaker activity and breaker efficiency. It will accomplish the following objectives:

1. Identifying the optimum working temperature ranges for each type of breaker studied within the range of 75 °F to 300 °F
2. Determine the effect of increase or decrease in breaker concentrations on the gel-break.
3. Determine the amount of residue generated at for a range of breaker concentrations and working temperatures.
4. Determine the molecular weight distribution/ particle size distribution of the broken gel at different breaker concentrations and working temperatures.
5. Develop breaker-activity curves or “S” curves after achieving the above objectives.

1.4 Thesis Outline

Section 2 presents an introduction to hydraulic fracturing. A brief history of hydraulic fracturing is presented and then the fracturing process itself is discussed.

Section 3 discusses fracturing fluids, particularly guar based fluids. The components of a guar based fracturing fluid and their chemistry is explained. Breakers and their types have been explained in this section.

Section 4 provides a description of the experimental procedures, data and results related to the work done for this project.

Section 5 presents the conclusions based on the experimental work. New developments from this work and their relevance to the field operation are discussed.

2. HYDRAULIC FRACTURING

2.1 Introduction

Hydraulic fracturing is a well stimulation procedure. The reason to stimulate a well is simple, low production rate. Therefore, well stimulation is any procedure done in order to increase the production of a well. There could be a number of reasons that can cause low production rates. These include:

- low permeability
- low reservoir pressure
- high bottomhole pressure
- high fluid viscosity
- high skin

Hydraulic fracturing is an efficient way to counter the problem of low production rates. It creates high permeability zones in the reservoir which connect to the well and cause an increase in well production. Therefore, hydraulic fracturing treatments are applied to tight formations, usually having a permeability of less than 1 md. Hydraulic fracturing treatments are not suited for high permeability reservoirs because the increase in well production is not very significant and is not worth the trouble for high permeability formations, having permeability values larger than 10 md (Economides, 1987).

2.2 History of Hydraulic Fracturing

The earliest efforts made to fracture hydrocarbon formations actually did not use any fluid and therefore were not hydraulic. It is known through documented evidence going back to the 1890s that fracturing was achieved by using explosives. This practice eventually saw its end in the late 1950s and early 1960s, when nuclear devices were used as explosives as an experiment.

Acidizing was the widely accepted method employed for well stimulation till the 1930s. At this time some people started noticing that during the acidizing process, there was a change in the injectivity after a certain point in that it would increase significantly. It was in 1940 that Torrey related this effect to the fracturing of the rock.

The first documented hydraulic fracturing treatment was performed in Kansas at the Hugoton gas field in 1947. The fracturing fluid of choice was oil-based “napalm”. This attempt did not yield very favourable results leading people to believe that hydraulic fracturing was not effective enough to take the place of acidizing. However, it turned out that hydraulic fracturing replaced acidizing in the same Hugoton gas field by 1960s and became the preferred means for stimulation. In these treatments sand was used as proppant.

Nowadays, hydraulic fracturing is a widespread well-established means of well stimulation and thousands of such treatments are performed world over every year. It has become so common that rarely any field is developed these days without fracturing and in some cases it is the only way to make the field productive (Economides, 2007).

2.3 Hydraulic Fracturing Process

In a hydraulic fracturing process, fluid of a certain composition is pumped into the formation at a high injection rate which helps build pressure. Eventually this pressure reaches to a point where the rock cannot bear it and it causes the rock to break or fracture, as shown in Figure 2.1. This breaking of the rock and fracture creation makes way for the fluid to leak-off into the rock formation. Now, in order to keep the fracture growing, the injection rate should be higher than the rate of fluid leaking into the formation. This causes the fracture to grow and penetrate deep into the formation.

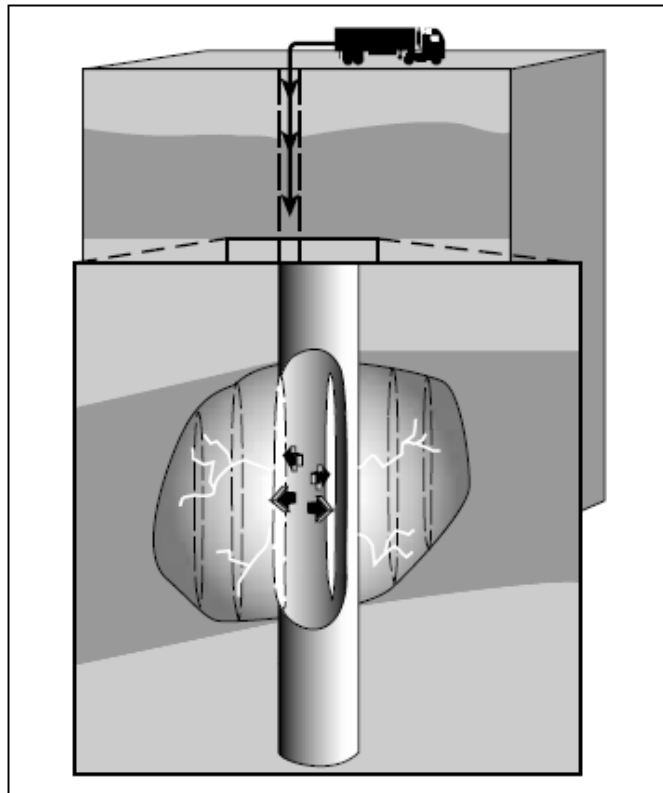


Figure 2.1– Internal pressure breaking the vertical wellbore (Economides and Nolte, 2000)

As long as this injection rate is maintained, the fracture continues to grow. If the pumping is stopped at this point, the fluid inside the fracture will eventually leak-off into the formation and the fracture will close due to the overburden stresses in the rock and this flow channel created to increase the production cannot be utilized. Therefore, in order to stop the fracture from closing, and keep it open, a propping agent or proppant must be injected to the formation with the fracturing fluid. The fluid carries this proppant inside the created fracture and when the fracturing process is complete and the pumping is stopped, the fracturing fluid is recovered from the formation through flowback, leaving this proppant behind.

The proppant prevents the fracture from closing and keeps the flow path open for the formation fluid to flow into the well. This propping agent could be natural, like sand, or synthetic, but it should be able to withstand the forces that cause the fracture to close.

Hydraulic fracturing is achieved in stages. At the start, to initiate the fracture, fluid is pumped without any proppant. The reason is that in the beginning, the fracture length is small and most of the fluid is leaking off into the formation and the fluid loss is maximum at the tip of the fracture. This first stage of pumping only fluid is called the “pad”. Once this stage is completed, then the next stage of fluid carries proppant into the fracture, as shown in Figure 2.2. This mixture of the fracturing fluid and proppant is called slurry. The concentration of proppant in the slurry is increased gradually through the stages as the fracture propagates into the formation. The slurry makes its way to the tip of the fracture, and since the pad stage is lost through leak off at a higher rate, the speed of the slurry is higher than the speed of fracture creation. The slurry eventually

reaches the tip and starts to lose the fluid through leak off too, but the proppant still remains in the fracture. This makes the slurry more concentrated due to the loss of fluid.

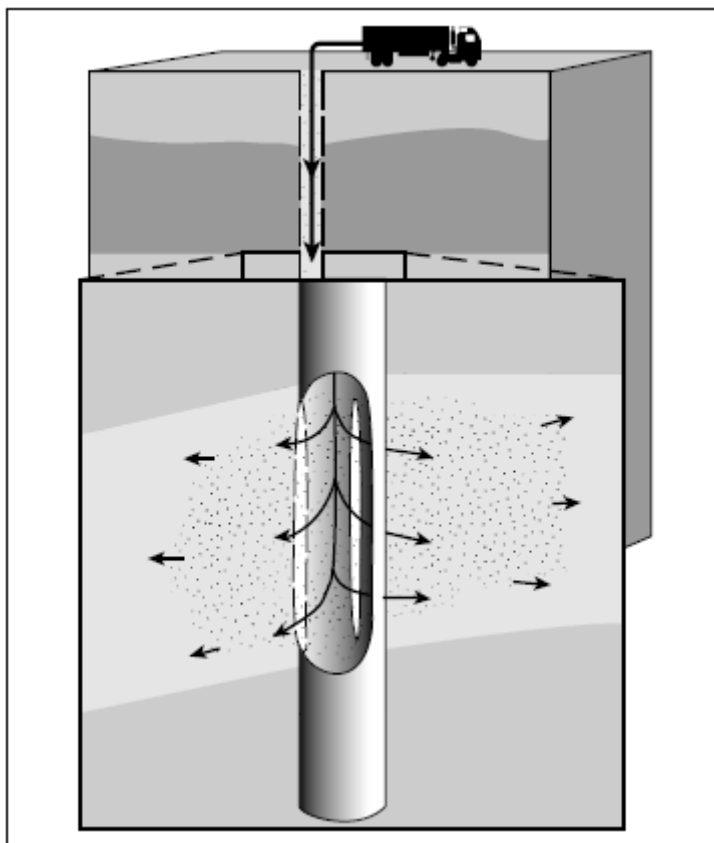


Figure 2.2- Introducing proppant into the fracture (Economides and Nolte, 2000)

The later stages pumped of this slurry, as mentioned earlier, are more concentrated, but they don't stay in the fracture for too long and thus, don't lose as much fluid as the earlier stages with thin concentrations. Eventually, the earlier stages

thorough fluid loss reach a high concentration, same as the later stages which are pumped with higher concentration, which is the desired final concentration the fracturing treatment was designed to achieve. The last stage is pumped to flush the wellbore and remove any proppant left behind.

After the last stage has been pumped, the pumping is stopped and the well is shut-in for a certain amount of time. During this time the fracture closes on the proppant pack. Also, during this time the chemical breakers present in the fluid start working to reduce the viscosity of the fluid so that it can flowback easily (Economides and Nolte, 2000).

Hydraulic fracturing is not a simple procedure by any stretch of imagination. There are a lot of design considerations and every frac-job is designed for the particular formation it is applied to. The fracture design engineer can alter anything from the size of the pad stage to the number of slurry stages, the concentration of proppant in the slurry, injection rate and the type of fluid. All this is designed just right in order to achieve the desired fracture. (Economides, 2007)

Hydraulic fracturing requires a lot of material, from fluids to proppants, mixing trucks and very heavy equipment to pump this fluid at high rates. Dr. Economides in his book *Modern Fracturing* calls it “One of the most energy- and material-intensive industrial activities”. It is said in the book about the power required:

“A typical frac pump will be rated from 700 to 2700 hydraulic horsepower (HHP). To put this into perspective, 1300 HHP is approximately equal to 1 MW, enough electricity to power ~500 homes in Western Europe.” (Economides, 2007)

3. FRACTURING FLUIDS

3.1 Introduction

Fracturing fluid is one of the most important components of a hydraulic fracturing treatment. Fracturing fluids are used for three main purposes:

- creating the fracture
- transporting proppant into the fracture
- placing the proppant inside the fracture

To achieve the above tasks, the fluid has to be designed carefully. The behaviour of a fracturing fluid and its effectiveness in achieving the desired results depends on its chemical composition. The rheological properties, most importantly viscosity, dictate the fluid performance, though, viscosity is not the only rheological property of importance. Other properties like elasticity also play a significant part. The fracturing fluid should be designed in such a way that:

- It is easy to pump offering low friction, and therefore, less wear and tear to the pumping equipment
- maintains sufficient viscosity in the fracture
- exhibits good characteristics for the control of fluid leak-off
- breaks quickly once pumping stops and is easy to flowback
- is cost-effective

(Economides and Nolte, 2000)

Due to this special type of behaviour that is required of the fracturing fluids, i.e., to be thin-enough at the surface to pump easily, then gain viscosity to carry the proppant

and then break and become almost water-like after fracturing is complete for the ease of clean up, Dr. Economides gave them the title

“the ultimate schizophrenic fluids” (Rae and di Lullo, 1996)

3.2 History of Fracturing Fluids

As mentioned in the previous section, the earliest fracturing fluids were oil based, mostly made with “napalm”, which is a hydrocarbon used in warfare. The desired viscosity was achieved by combining it with aluminum soap. The reason behind using oil-based fluids was to avoid any damage to formations that were water-sensitive. Water-sensitive formations have clays which can be mobilized with the introduction of water, causing them to swell or move within the formation and accumulate at pore-throats, causing formation damage. These fluids, though flammable and dangerous and were later substituted with viscous refined oils and gelled crudes. These hydrocarbon-based fluids were in use till the 1960s when the industry shifted towards water-based fluids.

The water-based fluids were safe to use and also more economical. The problem of clay swelling and fines migration in water-sensitive formations was countered by adding salts to these fluids which stabilized the clays. These salts include potassium, sodium and calcium chloride (Rae and di Lullo, 1996).

In order to achieve the required viscosity in water-based fluids to carry the propping agent, the water was combined with naturally occurring gellants like guar gum and locust bean gum, starch and cellulose. Besides these, artificial gellants like polyacrylamide and xanthan gum were developed.

Being abundantly available, cheap and a good viscosifier providing the necessary characteristics required for proppant transport, guar became the gellant of choice for most fracturing operations.

In the beginning, linear guar-based fluids were used and were only effective upto a certain temperature. The reason being the fluid underwent a temperature-thinning or thermal-thinning effect at higher temperatures. This caused a lot of fluid loss through leak off and screening out of the proppant (Economides, 2007).

To remedy the problem of thermal-thinning and make the fluid work effectively at higher temperatures, fluids with very high polymer concentrations were used. The idea was to retain a good viscosity even after the temperature thinning and preventing screen out problems (Alderman, 1970).

This idea brought with it the problem of high friction encountered during pumping, damaging the pumping equipment, and the large size of the polymer fragments causing formation damage and reducing productivity.

This problem led to the use of crosslinkers, which were certain chemical agents used with low polymer concentrations to enhance the viscosity of the fracturing fluid. The first crosslinked guar fluid was used in 1969. The use of crosslinker helped to extend the temperature range for the use of low polymer concentration guar fluids. Thus, the problem of formation damage caused by heavy polymer loadings was reduced considerably.

The quality and performance of crosslinkers and polymers have improved over the years, which have caused more decrease in polymer concentration resulting in cleaner fluids with less flow impairment in the fracture.

The advent of better fluids, capable to withstand higher temperatures, the residual polymer left behind in the formation also became more stable. This gel residue with large molecular fragments is capable of causing considerable formation damage. This problem called for the use of special chemicals called “breakers” to be used as a de-viscosifying tool.

Multiphase-fluids like foams and emulsions have also been used as fracturing fluids. In addition to this, unconventional fluids like viscoelastic surfactants have also been developed which are very efficient, at low viscosities and cause practically zero damage. But they are much more costly compared to the conventional guar fluids. That is why guar-based fluids still remain the most popular and widely used fluids in the industry today (Economides, 2007).

3.3 Types of Fracturing Fluids

As discussed in the previous section, many different types of fracturing fluids have been developed and used over the years starting with oil-based fluids. These types are:

- Oil-based
- Water-based
- Multiphase fluids like foams and emulsions

- Unconventional fluids like Viscoelastic Surfactants (VES)

This project focuses on the most commonly used type of fracturing fluids, i.e, water based fluids, particularly, guar-based fluids. Therefore, a brief discussion follows on water-based fluids and then a detailed account is presented on guar-based fluids, their composition and chemistry.

3.4 Water-Based Fracturing Fluids

As mentioned earlier, water-based fluids are the most commonly used fracturing fluids in the industry and it is not without good reason. These fluids are cheap compared to others, deliver good results and are safe to use. Water is an abundant source, available throughout the world.

Water-based fluids can be linear or crosslinked guar-based fluids. They could be a simple combination of water and a friction reducer like polyacrylamide, or it could be just plain water.

The linear gels, used without crosslinking and water-friction reducer combinations are generally used for shale gas fracturing applications. In this type of fracturing, low viscosity fluid with low proppant loading is pumped into the formation at very high rates to create long fractures or create channels to connect existing natural fractures. This type of fracturing treatment has been given the name “slickwater” fracturing.

The next section presents an account on the different components of guar-based fracturing fluids, their structure and chemistry.

3.5 Guar-Based Fracturing Fluids

Guar-based fluids, which include guar and its derivatives, are the most common type of fracturing fluids used in the industry. They produce good results and are safe to transport and offer good economic value. The guar-based fluid has good proppant transport characteristics, which is one of the most important jobs of a fracturing fluid. They can be used in the form of linear gels, which means only guar and water are mixed together, or crosslinked form, by using special chemicals that alter its structure and increase the viscosity. This makes them versatile fluids, that can be designed and used according to the job requirement. A typical guar-based fluid contains:

- Water
- guar or guar derivative as gelling agent
- crosslinking agent to increase viscosity
- buffer
- breaker to reduce viscosity after pumping stops
- biocide to kill bacteria
- clay stabilizers to prevent clay swelling and fines migration
- surfactant to alter surface tension and wettability

The components named above are the ones most commonly found in guar gels, but it is possible that a gel has some other additive. It is also possible for the fluid to not have one of these components but for water and guar. An example of a typical gel formulation for a 45 lb per 1000 gallon system is provided in Table 3.1.

Table 3.1 - Guar Gel Formulation (45 lb/1000 gal) (Nasr-El-Din et al., 2007)

Component	Amount	Remarks
Polymer	0.54 cm ³	Guar gum
Surfactant	0.2 cm ³	
Gel Breaker (Oxidizer)	0.5 cm ³	Sodium bromate (NaBrO ₃)
Gel Stabilizer	0.29 cm ³	
Bactericide	0.05 cm ³	
KCl	25 g	Clay control
*Crosslinker	0.45 g	Boric acid (H ₃ BO ₃)
HT delay agent	1.5 g	Sodium gluconate (C ₆ H ₁₁ NaO ₇)
Stabilizer	0.1 cm ³	60-100% Alcanolamine
Activator	0.9 g	Sodium hydroxide to control the pH (9-12)
Water	98.32 cm ³	

3.5.1 Guar Gum

Guar gum is the gellant or viscosifying agent in fracturing fluids. It is a polysaccharide produced from guar bean plant. This plant is grown abundantly in Pakistan, India and southern United States. When guar is mixed with water, it swells and forms a viscous gel. This gel has sufficient viscosity and elastic properties to be needed to transport proppants into the fracture and good leak off control. But certain additives can make it even more viscous and, therefore, enhance its performance significantly (Rae and di Lullo, 1996).

3.5.1.1 Structure of Guar

Guar, as mentioned earlier, is a polysaccharide and it is a part of the galactomannan group. It has a linear structure which consists of two different kinds of

sugars, mannose and galactose. There is a long chain or backbone made of mannose units connected to each other by β -1, 4 acetal linkages. This backbone is attached to isolated units of galactose by α -1, 6 acetal linkages. These mannose and galactose units exist in a ratio of 1.5:1 to 2:1. The linear structure of guar polymer is shown in Figure 3.1.

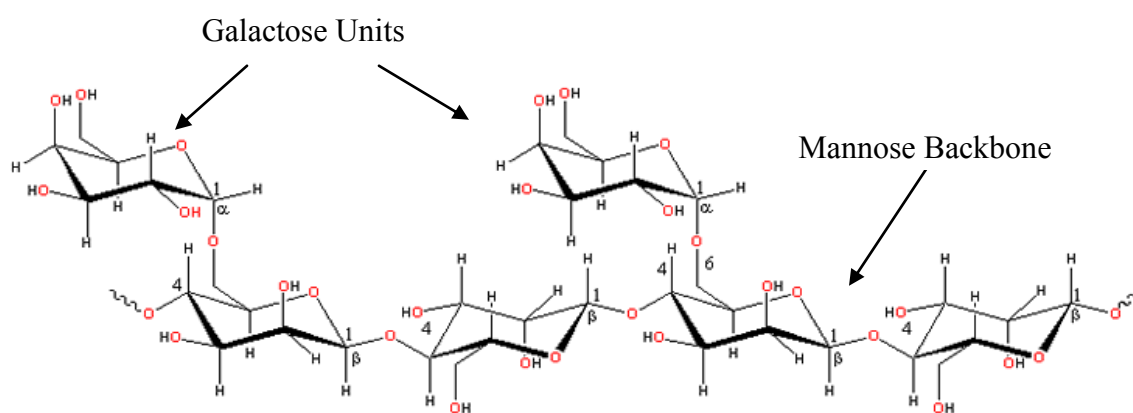


Figure 3.1- Linear structure of guar polymer

The linear structure of guar arises from a single repeating unit made of mannose and galactose. This repeating unit is shown in Figure 3.2. An average guar molecule has approximately 3,700 of these repeating units, which gives guar its long linear structure and makes the guar molecule very heavy having an average molecular weights ranging from 200,000 to 2,000,000 Daltons (Brannon and Tjon-joe-Pin, 1994).

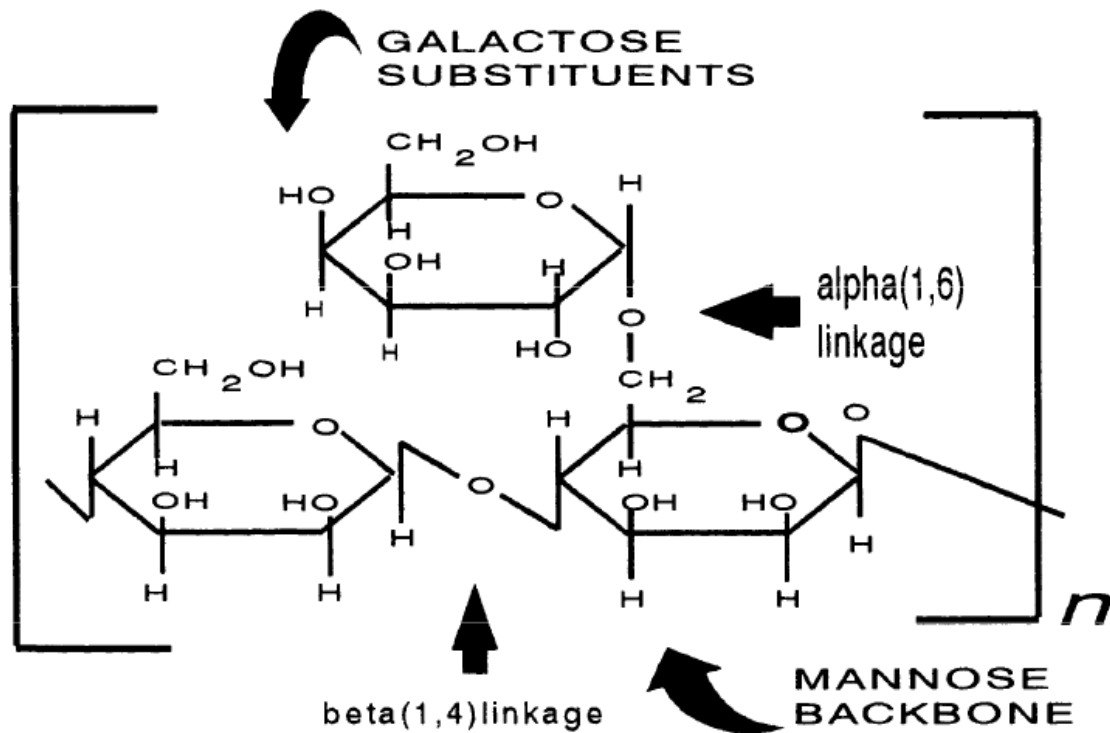


Figure 3.2- A single repeating unit of guar (Brannon and Tjon-joe-Pin, 1994)

3.5.1.2 Guar Derivatives

Guar gum is produced from a plant. There is some natural waster material or residue in this guar, which comes from the plant material. This waste material or residue is of no use and does not help in increasing the viscosity of the guar gel in any way. Natural guar has about 5% to 10% of this residue. When this residue gets pumped along with the guar gel, it causes damage to the formation. In order to avoid the formation damage caused by this residue, guar is chemically treated with certain chemicals to reduce this waste material and clean the guar. This procedure creates guar derviatives,

which contain less amount of the waste material and also increase the working temperature range of guar.

When guar is treated with propylene oxide, it creates hydroxypropyl guar (HPG). HPG contains 2% to 4% residue by mass. A dual treatment, with propylene oxide and chloroacetic acid, creates carboxymethylhydroxypropyl guar (CMHPG), with even lesser amounts of residue, about 1% - 2%. These chemical treatments cost money, and therefore, make these derivatives more expensive compared to the un-derivatized guar.

These derivatised guar were very popular during the 1970s and 80s, but then some new studies and observations shifted the industry back towards the use of natural, un-derviatized guar. Studies showed that the damage caused by HPG and natural guar was not very different (Almond and Bland, 1984, Brannon and Pulsinelli 1992). Another reason was the study showing that although natural guar contains more percentage of residual material by mass, it still compares well with derivatised guar on volume percentage basis, Figure 3.3. Also, the improvement of guar-borate crosslinked systems which increased their working temperature range was also a factor (Rae and di Lullo, 1996). This was achieved by using gel stabilizers like sodium thiosulfate. And the most important reason was cost. Considering all these factors, un-derivatised guar still remains the most popular choice.

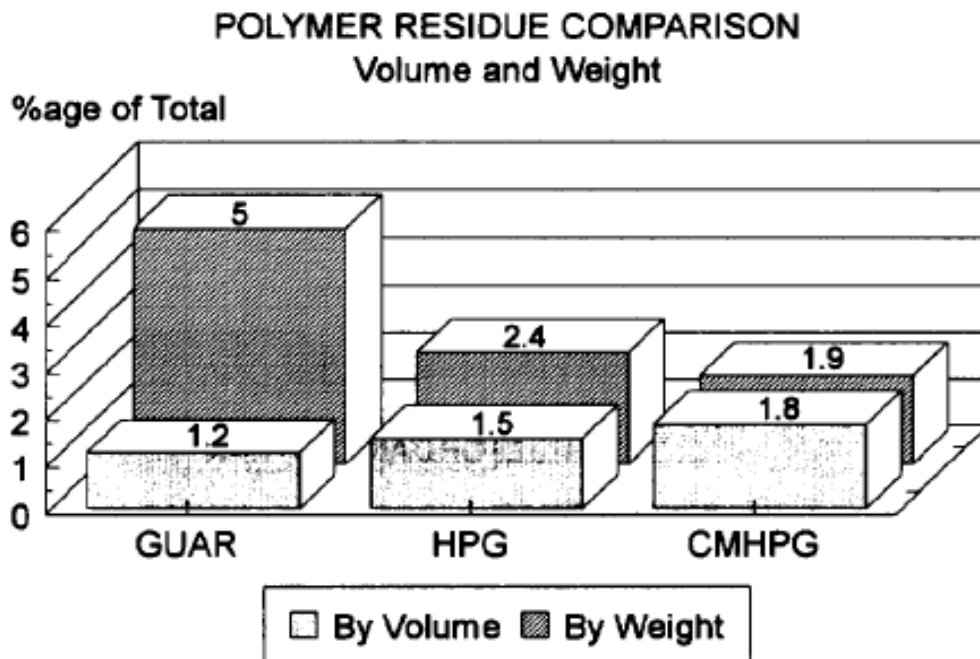


Figure 3.3- A comparison between guar and its derivatives (Rae and di Lullo, 1996)

Over the years, improved techniques have helped produce better quality guar. Natural guar produced these days can have residue amounts as low as 2% or less, with derivatised guar now containing 0.5% (Modern Fracturing, 2007).

3.5.2 Crosslinkers

Crosslinkers are chemical agents used to increase the viscosity of the fracturing fluid. They were developed to reduce the amount of polymer loading in fracturing fluids and still maintain good proppant carrying abilities. There are a lot of different crosslinking agents used in the industry like borates, aluminates, zirconates, organic

titanates etc. Every crosslinker has a particular working range which includes temperature, pH and the type of polymer. The pH ranges for various types of crosslinkers are shown in Figure 3.4., and the temperature ranges are shown in Figure 3.5.

CROSSLINKERS & pH

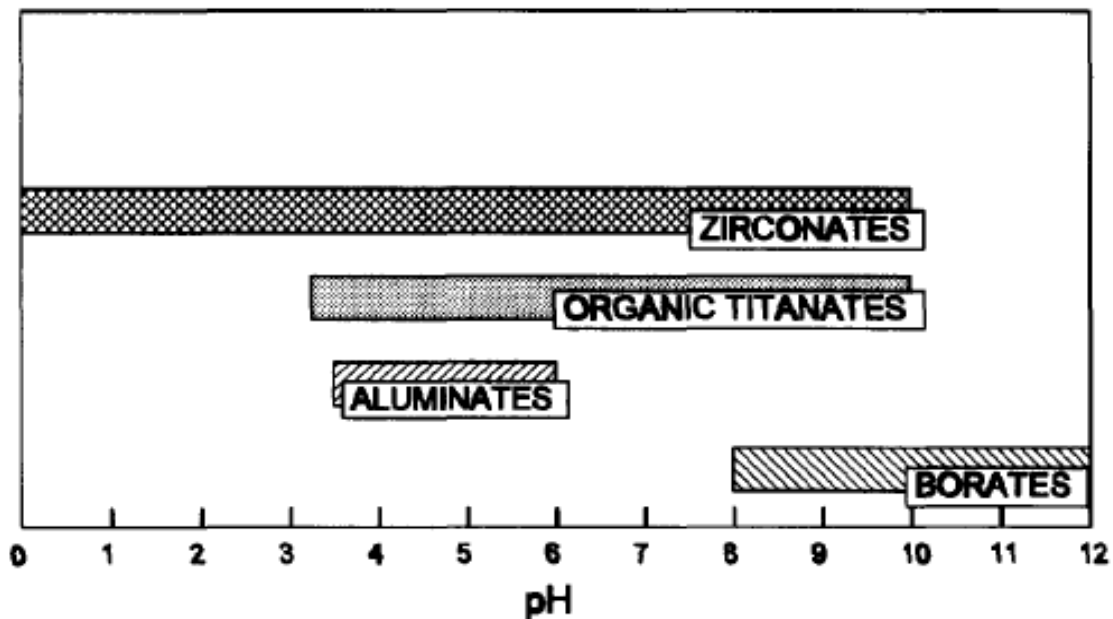


Figure 3.4- pH ranges for various crosslinking agents (Rae and di Lullo, 1996)

Delayed crosslinking systems are used because of the high viscosities of crosslinked fluids. Highly viscosus fluid will create high friction while pumping and increase the pressure and power required to pump it. Therefore, a delayed crosslink can

reduce the pressure and power requirements at the surface making it easier to pump, and then increases the viscosity to provide the necessary proppant carrying ability.

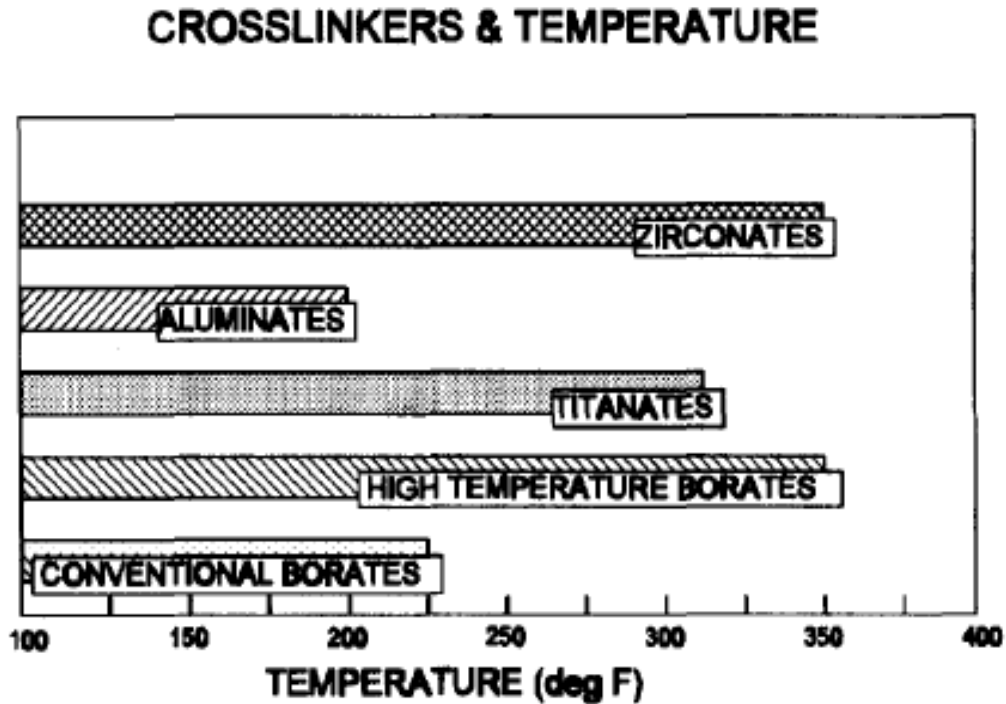
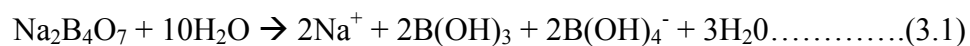
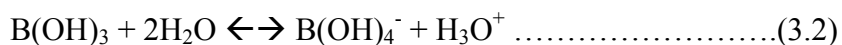


Figure 3.5- Temperature ranges for various crosslinking agents (Rae and di Lullo, 1996)

One of the most widely used crosslinking agents for guar based fluids is borate. Borates are added to the fracturing fluid in the form of borate salts or boric acid. They are basically a source of monoborate ions which are considered to be the crosslinking agents. For example, borax or sodium tetraborate produces monoborate ions in water as shown in Equation 3.1.



Monoborate ion is also produced when boric acid undergoes hydrolysis as shown in Equation 3.2.



At pH values greater than 8.5, this monoborate ion creates complex structures by combining with the cis-hydroxyl groups present in the guar polymer chain (Nasr-El-Din et al. 2007), as shown in Figure 3.6. The generation of monoborate ions is a function of pH and temperature (Harris, 1993). The concentration of monoborate ions increases with increasing pH, which causes more crosslinking to occur. An increase in temperature causes pH to fall, and therefore reduces the crosslink as shown in Figure 3.7.

At higher temperatures, using greater concentration of borates to account for the low pH can cause a phenomenon called ‘syneresis’. Higher concentrations of monoborate ions cause excessive crosslinking or over-crosslinking. The polymer forms a clump and releases the water, making it useless for proppant transport (Harris, 1993). Therefore, the pH of the borate crosslinked fluid should always be maintained at high level, around (10-12). At higher temperatures, using organo borates or low solubility borates (calcium or calcium sodium borate) can prevent syneresis by producing low monoborate ion concentration early and then generating greater concentration at high temperature later.

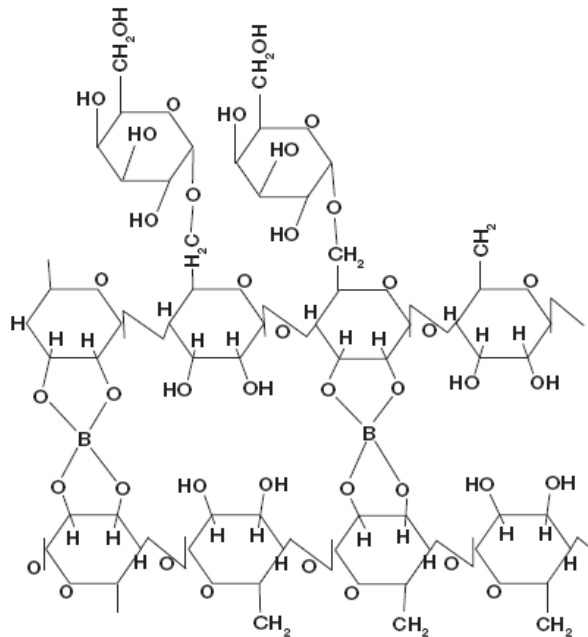


Figure 3.6- Structure of borate crosslinked guar (Modern Fracturing, 2007)

BORATE ION CONCENTRATION 7.2 lb/Mgal BORIC ACID IN 2% KCl

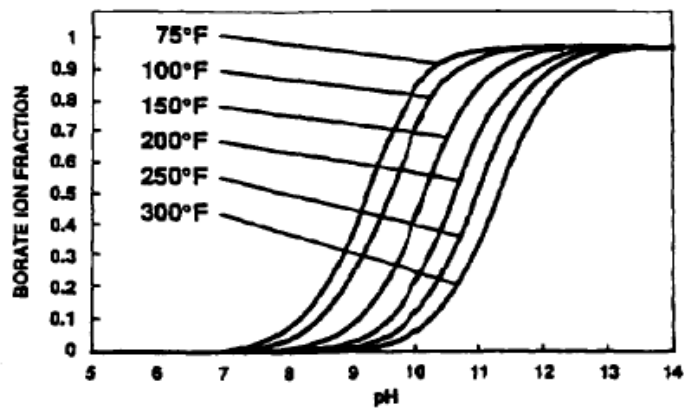


Figure 3.7- Dimensionless monoborate ion concentration vs pH for various temperatures (Haris, 1993)

3.5.3 Buffers

Buffers are used to maintain the pH of the fluid for crosslinking purposes. They are also used as dispersants for polymer particles to prevent the polymer from forming small clumps or 'fish eyes' when mixed with water. They are produced from the reaction of weak acids with strong bases. There are many different buffers used in the industry, depending on the pH requirement. Some examples include sodium acetate, sodium bicarbonate, sodium carbonate, sodium silicate and the same salts for potassium (Rae and di Lullo, 1996).

3.5.4 Breakers

Breakers are the main objects of study in this project. Breakers are chemical agents used to reduce the viscosity of the fracturing fluids after proppant has been delivered inside the fracture. This is required to make it easy to flow the fluid back to the surface and also to prevent the thick fracturing fluid from plugging the formation or reducing the proppant pack permeability. Unbroken gel or residue can be a cause of formation damage and reduced productivity, making the whole fracturing process ineffective or at least significantly decreasing its effectiveness.

Breakers reduce the viscosity of the polymer by breaking the polymer backbone into smaller fragments. This decreases the molecular weight and thus, decreases the viscosity. Breakers can be divided into two main categories

1. Oxidizers
2. Enzymes

3.5.4.1 Oxidizers

Oxidizers or oxidative breakers generate free radicals which react at certain sites on the polymer backbone to break the polymer chain. These radicals which are highly reactive are created through thermal decomposition of the oxidizer. There are 18 places available on a single guar repeating unit where these radicals can react, shown in Figure 3.8.

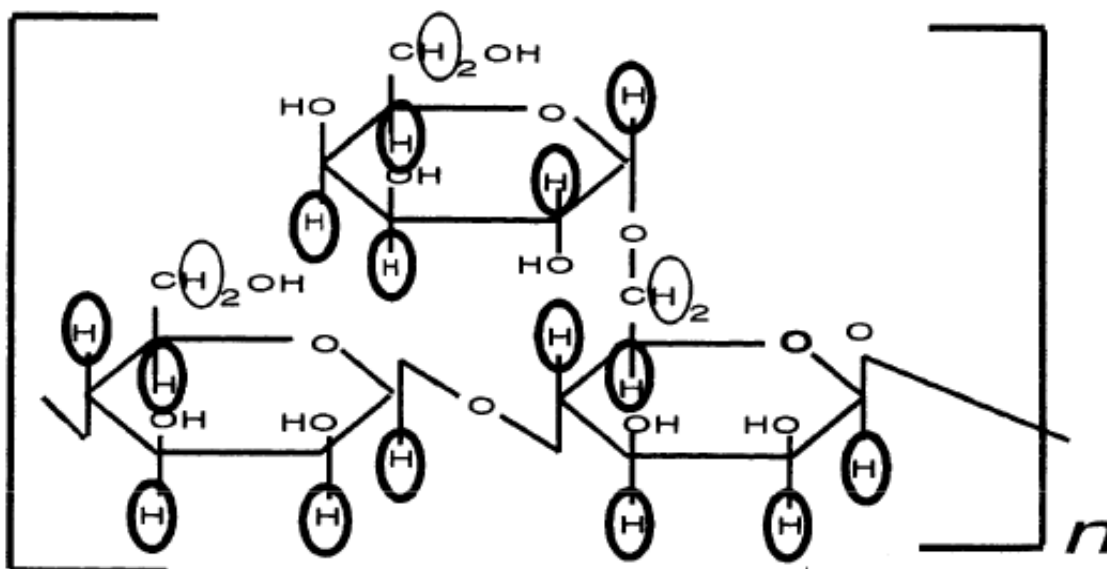
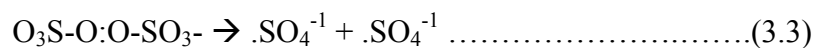


Figure 3.8- Radical reaction sites available on a single repeating unit of guar (Brannon and Tjon-joe-Pin, 1994)

One of the most common types of breakers is persulfate ($S_2O_8^{2-}$) salts of ammonium, sodium and potassium. Persulfate decomposes due to temperature and yields two free radicals as show in Equation 3.3.



These two radicals can attack any of the 18 sites available on the guar repeating unit. Of these 18 sites, the two best sites to degrade the polymer are the β -1, 4 acetal linkages between the mannose units. But these two sites are less acidic than the rest and therefore have lesser affinity toward a reaction with the radicals. The ideal breaking would be if the radicals break the polymer chain at the center creating two equal polymer fragments and then more radicals break these fragments at the center, and so on. If the chain is broken closed to one end instead of the center, it will create a smaller fragment and a larger fragment, and the molecular weight reduction will be less effective.

Oxidizers are highly reactive at high temperatures (>140 °F). As the temperature is increased, they become more and more reactive and the reaction rate between the free radicals and the polymer also increases. They decrease the viscosity of the fracturing fluid very quickly. Persulfate at 200°F has a half-life of about 20 minutes and at 225°F it reduces further to less than five minutes. Therefore, they should be carefully used at high temperatures, increasing the concentration too much can cause fluid to break too soon and lose its proppant carrying ability before the proppant has been transferred into the fracture.

Encapsulated breakers can be used at very high temperatures to delay the break. This helps in using high oxidizer concentrations while preventing the risk of the fluid breaking prematurely, before the pumping is stopped. The encapsulated breaker is the same oxidizer, e.g. persulfate, coated with a synthetic material like PVC, nylon etc.

3.5.4.2 Enzymes

Enzymes or enzymatic breakers are catalysts which accelerate chemical reactions produced from living cells. They are biodegradable and therefore considered environmentally friendly. Enzymes have been in use since 1960s but before 1990s, there were only thought to be effective for low pH (3.5 – 8) and temperatures (<150 °F). Modern day enzymes can go up to 350 °F, thanks to the advancement of biotechnology. Enzymes are reactive at room temperature and therefore they immediately start degrading the polymer as soon as they are introduced.

Enzymes degrade the polymer through a mechanism called the 'lock and key principle'. It means that every enzyme has a particular active site with the ability to attach to a particular substrate site on the polymer and degrade it. This means that if the active site of the enzyme does not match with the substrate site of the polymer, the enzyme will not react with it. This makes the range of application for the enzyme smaller and polymer specific.

Enzymes do not undergo any change in their structure during these reactions and so an enzyme can start another reaction after it breaks the polymer at the first site it attaches itself to. Since the enzyme is not consumed during a reaction, it has the possibility of reacting with infinite number of guar molecules, ideally. In theory, enzymes are supposed to be better breakers than oxidizers because of their ability to start infinite number of reactions, and their polymer specific nature.

Polymer linkage specific enzymes have increased that the range of temperature of enzymes to 350 °F. These enzymes not only attach to a particular polymer, but also

are specific to the types of linkage they attack, which makes them more effective. Once this polymer linkage specific enzyme attached itself to the polymer, it stays put until it degrades the polymer. This means that it will go wherever the polymer goes and thus creates a homogeneous distribution of breaker throughout the fluid (Brannon and Tjon-Joe-Pin, 1994).

3.5.5 Biocides

Biocides are used to kill bacteria. Bacteria like to eat the natural polymers present in the fracturing fluids. Therefore they can reduce the viscosity of the fracturing fluid and make it lose its proppant carrying ability. In addition to this, bacteria can also make the reservoir fluids produce hydrogen sulfide and turn sour, which can be a huge problem. Therefore biocides are added to the mixing tanks of fracturing fluids. One of the most common examples of biocides is Gluteraldehyde which provides very good protection against sulfate reducing bacteria (SRB) (Modern Fracturing, 2007).

3.5.6 Clay Stabilizers

Clay stabilizers are salts like ammonium chloride or potassium chloride, added to water-based fracturing fluids to prevent the swelling of clays in water-sensitive formations, i.e, formations that contain clays that can be mobilized when introduced to water (Modern Fracturing, 2007).

3.5.7 Surfactants

Surfactants are used to reduce surface and interfacial tensions, and change the wettability of the fluids for easier recovery from the formation. Reduction of surface tension can make the recovery of the fluid easy after the fracturing process is completed. Reducing the interfacial tension between reservoir fluids and water protects from emulsions forming and reducing permeability. Changing the wettability of the fracturing fluid by changing its contact angle of leak-off into the formation makes it easier to flowback (Modern Fracturing, 2007).

3.6 Formation Damage Caused by Fracturing Fluids

Fracturing fluids can cause damage to the formation. Unbroken gel or polymer can cause severe reduction in proppant pack permeability and has adverse effect on fracture conductivity. Fracturing fluid leaking-off into the formation can cause damage to the fracture face. This decreases the permeability of the formation outside the fracture.

A lot of research has been conducted and is still going on to improve the fracturing fluids so that it does not cause formation damage. This research project is also a part of this effort, in order to study the breaking system to provide maximum degradation and minimize the amount of unbroken gel in the fracture.

3.7 Rheological Properties of Fracturing Fluids

Mostly, the fracturing fluids are non-Newtonian fluids, which means that their viscosity depends on the shear rate. The rheology of fracturing fluids is defined by the

power law model, shown in Equation 3.4.

$$\tau = K \gamma^n \dots\dots\dots(3.4)$$

where τ is the shear stress having units of lbf/ft², γ is the shear rate in sec⁻¹, K is the consistency index having units of lbf-secⁿ/ft² and n is the dimensionless flow behavior index.

The values of n and K are calculated by plotting a log-log chart of shear stress against shea rate. The slope of the straight-line part of this plot gives n and K is the value of the shear stress at shear rate of 1 s⁻¹.

The fluid properties are generally measured using rotational viscometers with cylindrical geometries. Thus, the parameters obtained are geometry dependent and are represented as n' and Kv. These parameters have been calculated for all the viscosity tests conducted in this study.

4. EXPERIMENTAL PROCEDURES, RESULTS AND DISCUSSION

4.1 Materials

All materials used for this research project were provided by the BJ services company. These are actual products used in hydraulic fracturing treatments in the field.

The materials used in the laboratory testing were:

- Tap water (tomball)
- Guar polymer: dry powder form and slurry form.
- Oxidative breaker: Ammonium persulfate, sodium persulfate, magnesium peroxide, sodium bromate.
- Enzymatic breaker: Galactomannanase

4.2 Experimental Procedures

There were three different experimental procedures used in this study. The goal was to measure the viscosity of the gels with and without breakers, the amount of unbroken gel and residue generated and the molecular weight distribution of the broken polymer. The step by step procedure to perform these tests follows starting with the mixing procedure to make the gel.

4.2.1 Preparing the Gel

All the testing was conducted on 30 ppt gels first, and then some higher polymer loadings of 60 ppt, were also tested. For the 30 ppt loading, dry polymer was used to make the gel, because the amount of gel used is not that large. For the higher loadings,

polymer slurry was used, which contains 4 ppg guar, mineral oil, an organophilic clay and a surfactant that activates the clay. It is easier to mix in water. This is required because the dry polymer has a tendency to clump together when mixed with water, if it is not added properly, and form 'fish-eyes'. These fish-eyes are small clumps that have dry polymer at the center with hydrated polymer forming a coating over them, thus making it impossible for the dry polymer to come into contact with water.

The gel was mixed using overhead mixers. For 30 ppt gels, which were used for the majority of tests, a JANKE & KUNKEL mixer was used which had a maximum speed of 2000 rpm, as shown in Figure 4.1. Since the maximum speed on this mixer is not high enough for mixing heavier polymer loadings, a Servodyne high efficiency mixer was used for the 60 ppt gels. The Servodyne mixer used had a maximum speed of 2300 rpm.

Mixing Procedure for 30 ppt Gels

1. Weigh 1000 gm of tap water in a plastic beaker.
2. Weigh 3.6 gm (for 30 ppt) of dry polymer in a weigh bowl.
3. Put the beaker under the overhead mixer and start the mixer.
4. Set the mixer speed high enough (~500 rpm) so that a big vortex is created, but make sure the water does not make a splashing sound else it will trap air bubbles.
5. Start adding the dry polymer slowly, dumping it too quickly can cause the formation of clumps or 'fish-eyes'.

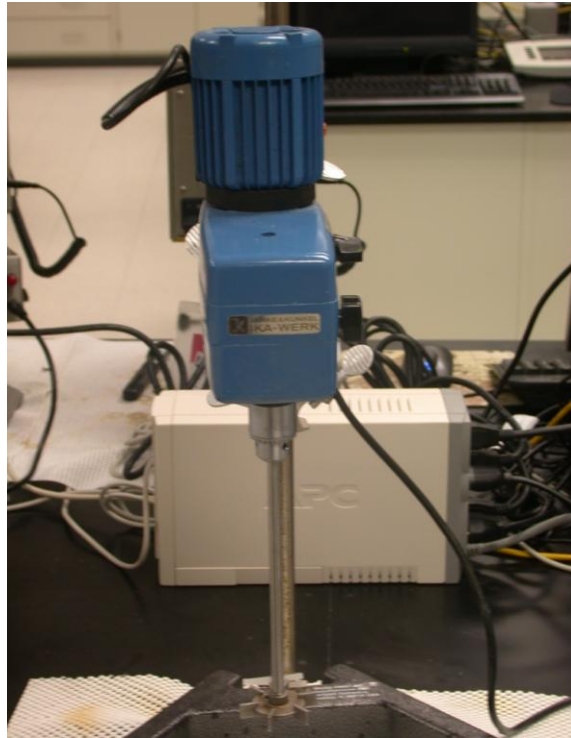


Figure 4.1- JANKE & KUNKEL overhead mixer

6. Keep increasing the rpm with the addition of polymer until a speed of 1800 rpm is reached.
7. After all the dry polymer has been added, start a stop-watch.
8. Let the gel hydrate for thirty minutes.
9. Stop the mixer.
10. Measure the apparent viscosity of the gel on a viscometer at a shear rate 511 s^{-1} .
It should be around 28 – 30 cp.

Mixing Procedure for 60 ppt Gels

As mentioned earlier, polymer slurry was used to make the 60 ppt gels. A different mixer, with high speed, and bigger mixing paddle was used. To prepare the 60 ppt gel, 15 ml of slurry was injected into the water. The gels were injected using syringes with their tips cut off to make it easier to suck in and discharge the thick slurry.

The rest of mixing procedure was the same as for dry polymer. The maximum speed of 2300 rpm was maintained for 30 minutes of hydration time. After mixing, the gel was left to hydrate overnight because of the high polymer concentration. This gives the polymer time to hydrate completely.

4.2.2 Viscosity Measurement

The major part of this research concentrated around generating viscosity profiles for the guar gels. The viscosity of these gels was measured at temperatures ranging from 75 °F to 300 °F, with 25 °F increments. Various concentrations of breakers were added to the prepared samples and then put on a viscometer to generate 'break profiles'. There were two kinds of viscometers used. For low temperatures, OFITE M900 viscometers as shown in Figure 4.2 were used. The tests for temperatures ranging from 75 °F to 175 °F were conducted on these viscometers. For temperatures ranging from 200 °F to 300 °F, Chandler 5550 HPHT viscometers were used, shown in Figure 4.3. Both viscometers had an R1-B1, rotor-bob configuration.

The break profiles generated are a measure of viscosity with time, over a range of shear rates, showing the loss in fluid viscosity as it is degraded by the breaker over time.



Figure 4.2– OFITE M900 viscometer

OFITE M900 Viscosmeter

The tests on the OFITE viscometer were conducted for 6 hr break time per test. A test sequence was written in the software program for the viscometer to shear the fluid at 100 s^{-1} for around 10 minutes and then perform a shear rate sweep of 17 s^{-1} , 40 s^{-1} , 50 s^{-1} , 60 s^{-1} , 75 s^{-1} , 100 s^{-1} , 511 s^{-1} , 1020 s^{-1} , 511 s^{-1} , 100 s^{-1} , 75 s^{-1} , 60 s^{-1} , 50 s^{-1} , 40 s^{-1} , and 17 s^{-1} , for a total of 5 minutes approximately. This makes a cycle of around 15 minutes total, 10 minutes constant shear rate and 5 minutes shear rate sweep. This cycle was set to repeat for the whole test length of 6 hr. The required temperature was also controlled and maintained using the software program.



Figure 4.3– CHANDLER 5550 HPHT viscometer

Procedure for OFITE M900

Prepared gel sample was taken in a plastic beaker and then the appropriate amount of breaker was added according to the breaker concentration required. The breaker was mixed in the gel using the overhead mixer vigorously at 1000 rpm for 1 minute. After mixing the gel was immediately put on the viscometer and the test was started. For the enzymatic breakers, the breaker was injected just after starting the test because enzymes become active as soon as they are added. The instructions follow:

1. Pour the sample into the steel container (>160 ml) used with the viscometer.
2. Put the steel contained inside the heating cup

3. Lift the heating cup so that the rotor is immersed into the gel sample till the line maked on the rotor.
4. Load the appropriate sequence on the software program with required temperature and shear rates.
5. If the test temperature is above 100 °F, i.e 125 °F to 175 °F, cover the container with an aluminum foil wrapping it around the rotor to prevent fluid loss through evaporation.
6. Start the test. Monitor it from time to time to see that it runs smoothly.
7. The viscometer will stop automatically once the sequence is completed and the corresponding data file can be saved on the computer.

Using the data generated, the break profile charts for each concentration and temperaturea are created. Baseline viscosity tests were also conducted with gels without any breaker added.

CHANDLER 5550 HPHT Viscometer

The Chandler 5550 HPHT viscometer was used for testing the fluid at higher temperatures (200 °F to 300 °F). This is required to prevent evaporation of the fluid at high temperatures by applying pressure on it throughout the test. This viscometer has a temperature limit of 500 °F and can maintain a maximum pressure of 2000 psi. The cup used with this viscometer is small (~50 ml), and it has pressure seal. The fluids were tested under a pressure of about 500 psi. Initially, a similar sequence (6 hr test) to that of the OFITE M900 was written on the software program for this viscometer, and a number

of tests were conducted with this sequence. But later it was found that the high shear rates of 511 s^{-1} and 1020 s^{-1} cause damage to the pressure seal, which shreds while rotating and is expensive to replace, so these high rates were omitted from the sequence in the later part of the testing. Also, in the later part of testing for high temperatures, an additional 2 hr test time was added to the sequence, during which the gel was allowed to cool while the viscosity was measured to see the effects of temperature thinning and observe the amount of viscosity regained by the gel.

The sample was prepared in the same way as for OFITE M900. The amount was smaller (50 ml) and appropriate amount of breaker concentration was added and mixed for 1 minute at 1000 rpm. The instructions follow:

1. Pour the sample ($50 \text{ ml} \pm 2\text{ml}$) in the viscometer cup.
2. Tare the measured parameters using the software, after mounting the separator and bob on the viscometer.
3. Tighten the cup on the viscometer.
4. Pressurize the cup by turning the pressure knob on the visometer.
5. Start the test sequence on the software program and monitor it from time to time.
6. After the test is finished, allow the gel to cool until the temperature falls below $100 \text{ }^{\circ}\text{F}$ atleast.
7. Relieve the pressure by turning the pressure knob to 'vent' and unscrew the cup.
8. The results are recored ans a saved automatically in a MS Excel file.

The viscosity break profile charts are generated for each breaker and oncentration tested. Baseline viscosity tests were also conducted with gels without any breaker added.

4.2.3 Residue-After-Break (RAB) Test/ Water Bath – Filtration Test

The residue after break test is designed to determine the amount of unbroken gel and residue generated after the gel has been broken. Prepared gel samples of 200 ml were put in water bath, shown in Figure 4.4, heated to desired temperature (125 °F and 150 °F). The samples are left overnight in the bath to allow for maximum break time. The next day, each sample is taken out and allowed to cool. It is then filtered under pressure in an OFITE filter press, shown in Figure 4.5. The filter paper is weighed before and after to calculate the amount of unbroken gel and residue generated for each concentration of breaker at a particular temperature. Barroid specially hardened filter papers, Catalog no. 988, diameter 2.5 inches, were used for this test. This filter paper has a pore size of 2 – 5 microns. The instructions for the test follow:

1. Weigh the dry filter paper in a weigh bowl.
2. Put the O-ring, metal spacer and filter paper in the bottom side of the cell. Close the bottom and tighten it.
3. Turn the cell over and pour the gel sample inside. Put an O-ring in the groove provided, close the top and tighten it.
4. Put the cell inside the chamber on the filter press.
5. Attach the pressure line to the top valve and secure it.
6. Put an empty jar under the bottom valve.
7. Apply 500 psi pressure using the pressure regulator and open the top valve slightly (rotate 90 degrees).



Figure 4.4– Temperature controlled waterbath

8. Open the bottom valve to allow the filtration to start.
9. After the filtration is complete, the filter paper is kept in an oven to be dried overnight. The oven is set to a temperature of around 150 °F – 160 °F. Higher temperatures can burn the filter paper.
10. The weight of the dried filter paper is measured the next day.

The difference in before and after weights gives the amount of unbroken gel and residue that could not pass through the paper and therefore, can plug the formation and cause formation damage.

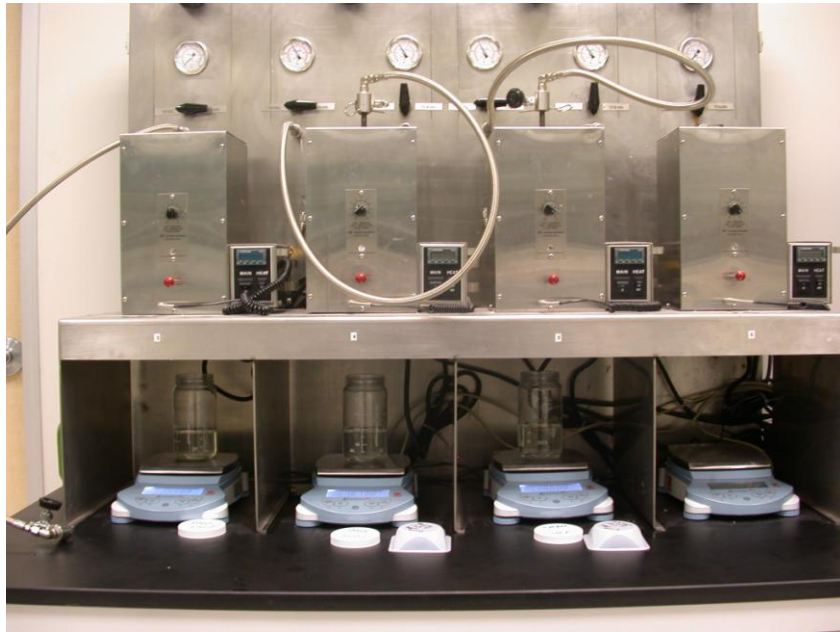


Figure 4.5– Filtration process going on in fluid loss cells

Care should be taken as to not expose the filter paper too much to the atmosphere after it is taken out of the oven. Guar polymer has the tendency to absorb moisture, which will change the final weight of the paper. Therefore, the papers should be taken straight to the balance and weighed immediately.

This filtration is a very slow process. The thicker the fluid, the more time it will take to filter. Blank gel samples, having no breaker added, took even 3 days to filter. In some cases (thicker or less broken fluids), the pressure was increased to 1000 psi to expedite the filtration process.

4.2.4 Molecular Weight Cut Off Procedure

This procedure was intended to be used to determine the molecular weight distribution. The procedure utilizes specially made molecular weight cut-off tubes and a high speed centrifuge, shown in Figure 4.6. The tubes, shown in Figure 4.7, consist of two parts; top part, which contains membranes of different sizes ranging from 5000 MW to 1,000,000 MW units, and bottom/collection part, that collects the fluid that passes through the membrane during centrifugation. The broken gel sample of known volume is placed into one tube of each size (one set of tubes) and then centrifuged at high RPM (2500-4000 RPM) for 30 minutes to 1 hour. The bottom/collection part is weighed before and after the centrifugation to determine the amount of sample that passed through each membrane and then the molecular weight distribution is calculated.

Due to some inexplicable reasons, this part of experimentation was not successful. The gels samples did not pass through the membranes within the test time. The samples that were forced to pass through prolonged centrifugation yielded absurd results with negative distributions etc. The reasons could be related to the material of the membrane. It was concluded that the membrane breaks or gets worn off during the test. Whatever the reasons maybe, unfortunately, these tests were unsuccessful.

Work is still being carried out to determine the reasons of failure and make this procedure workable for guar fluids. This method, potentially, could be very easy and useful to determine the molecular weight distribution of the broken fluids. The effort goes on.

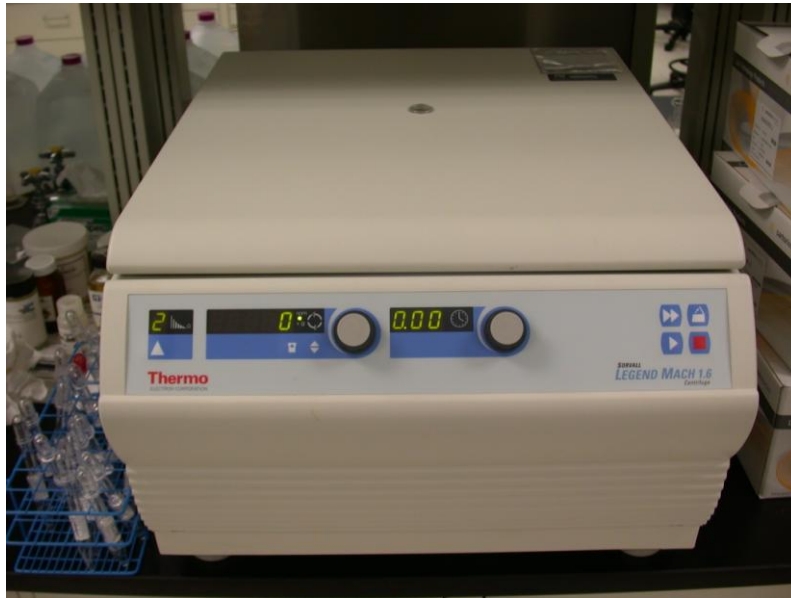


Figure 4.6– Thermo scientific high speed centrifuge

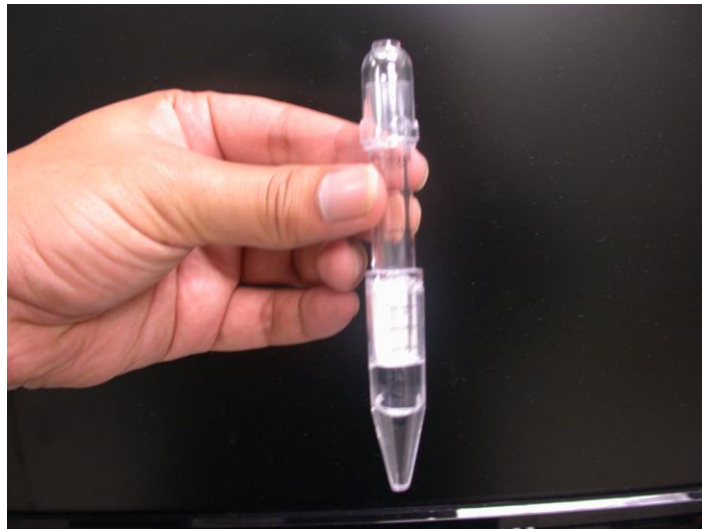


Figure 4.7– Special molecular weight cut off tube

4.3 Results and Discussion

4.3.1 Viscosity Measurement

4.3.1.1 Ammonium Persulfate

Ammonium persulfate is used in the field for a temperature range of 130 °F to 200 °F. The concentrations tested for the viscosity profile tests were 0.25 ppt, 0.5 ppt and 1 ppt. The temperatures at which these concentrations were tested ranged from 75 °F – 250 °F. The curves were generated on the basis on temperature and concentration both. The charts are presented in the following figures. The semi-log charts were created to see the small differences in viscosity, where the curves were too close to each other. Figures 4.8 – 4.14 present the charts developed based on the concentration of ammonium persulfate, while Figures 4.15 – 4.22 are developed based on the temperature of the fluid.

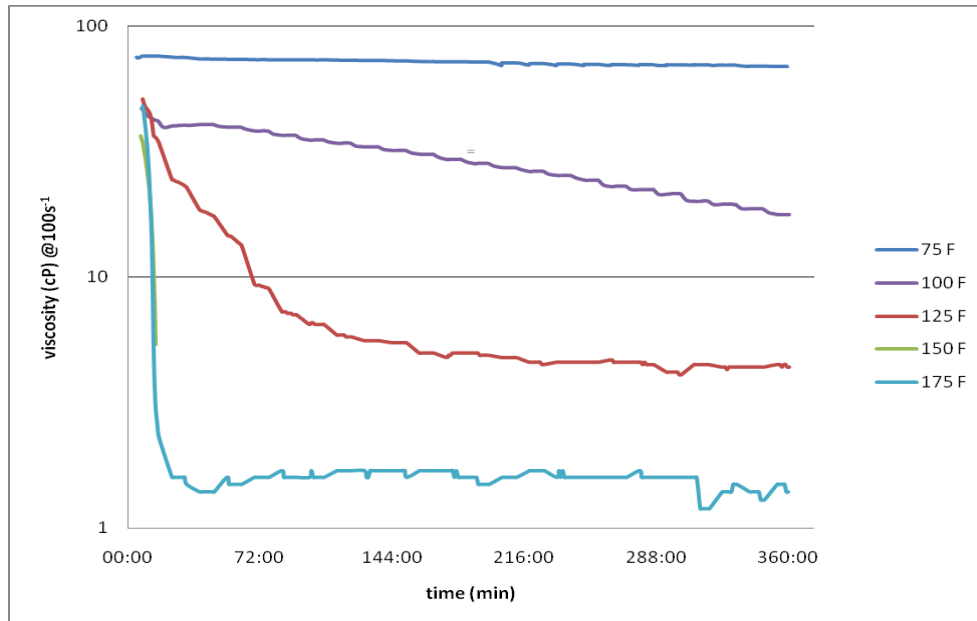


Figure 4.8– Viscosity profile of 30 ppt guar gel with 0.25 ppt ammonium persulfate (75 °F – 175 °F)

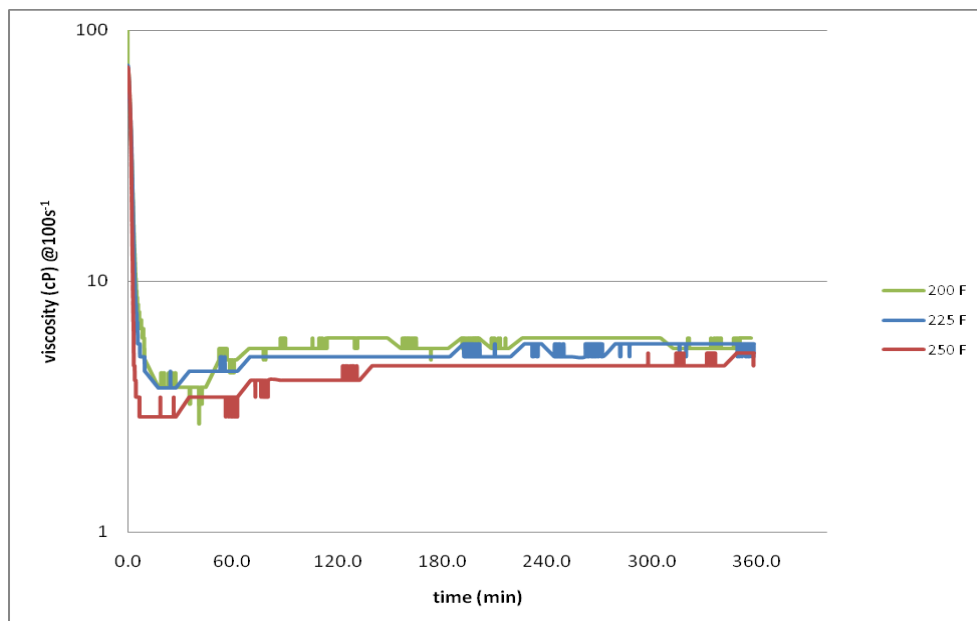


Figure 4.9- Viscosity profile of 30 ppt guar gel with 0.25 ppt ammonium persulfate (200 °F – 250 °F)

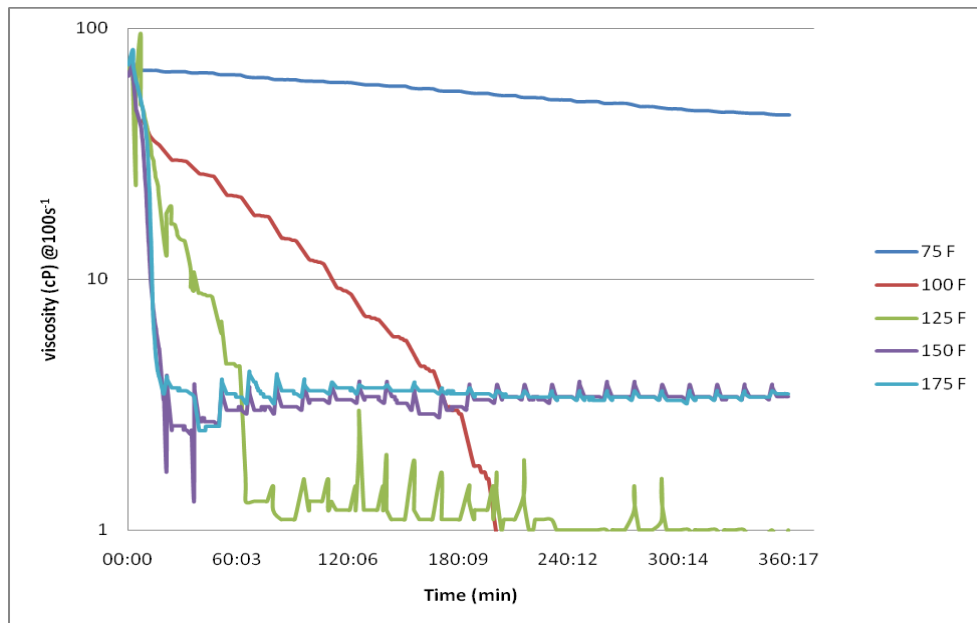


Figure 4.10– Viscosity profile of 30 ppt guar gel with 0.5 ppt ammonium persulfate (75 °F – 175 °F)

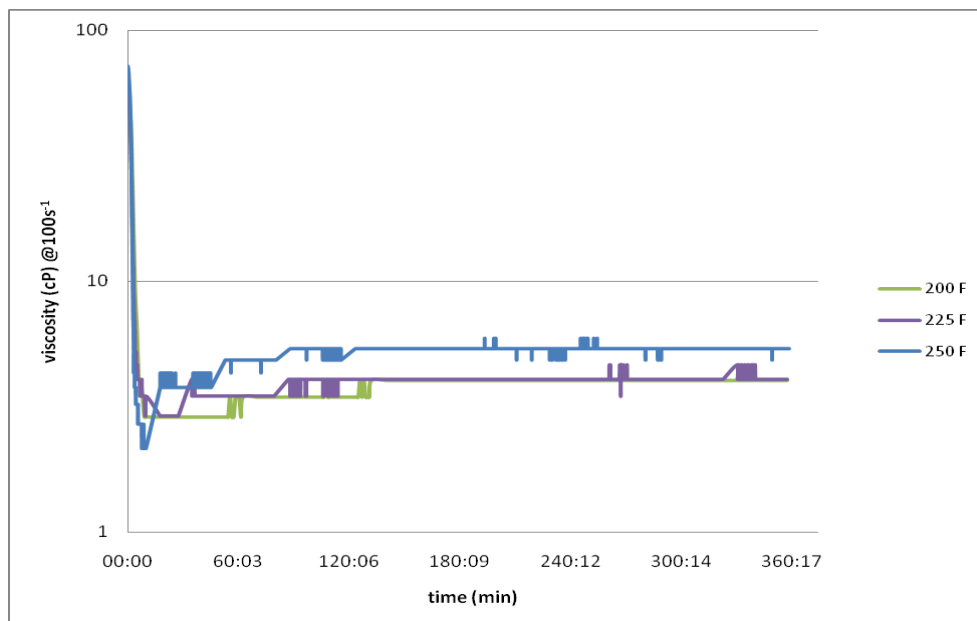


Figure 4.11- Viscosity profile of 30 ppt guar gel with 0.5 ppt ammonium persulfate (200 °F – 250 °F)

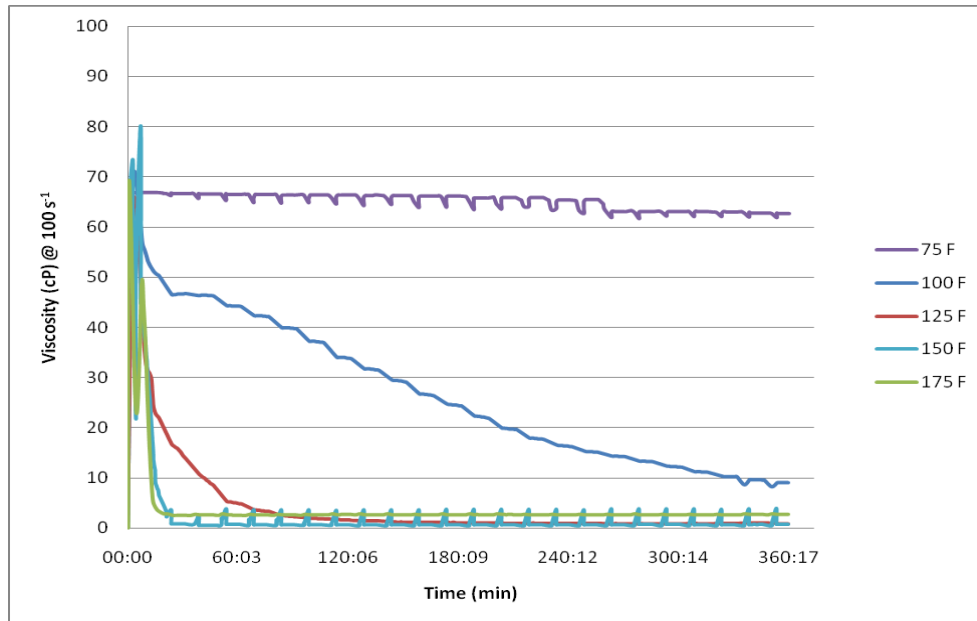


Figure 4.12- Viscosity profile of 30 ppt guar gel with 1 ppt ammonium persulfate (75 °F – 175 °F)

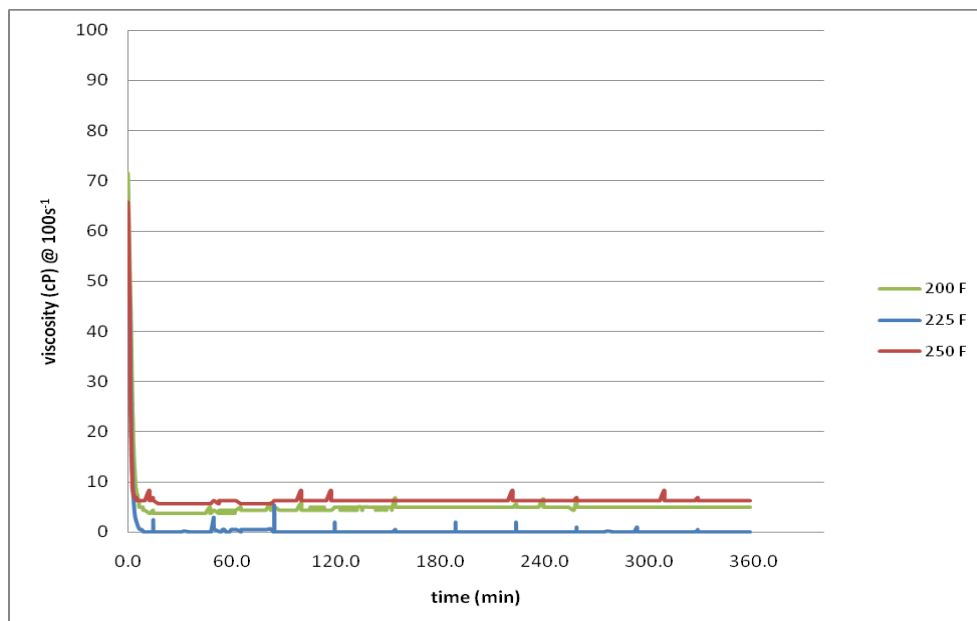


Figure 4.13- Viscosity profile of 30 ppt guar gel with 1 ppt ammonium persulfate (200 °F – 250 °F)

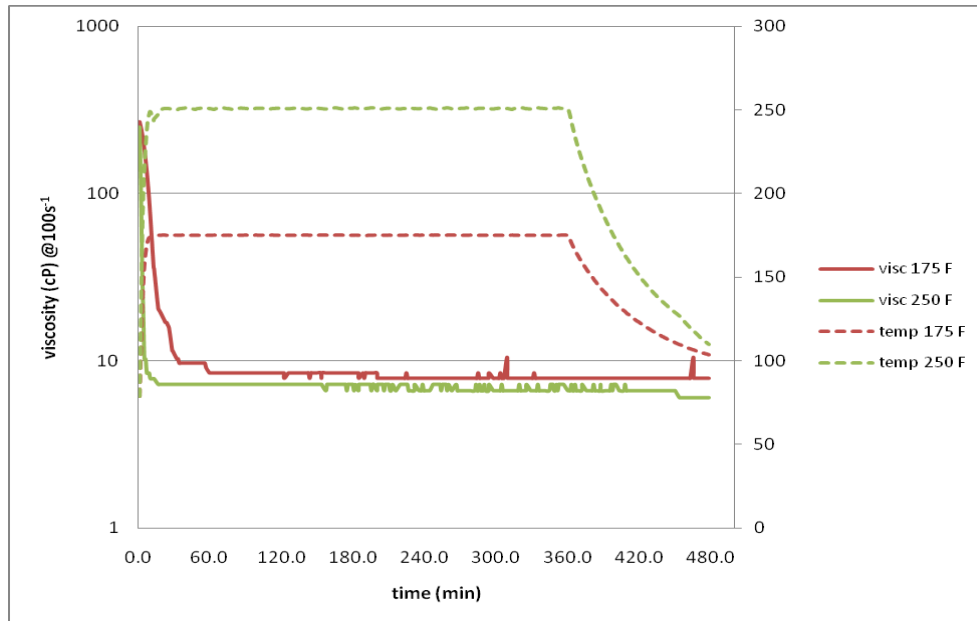


Figure 4.14- Viscosity profile of 60 ppt guar gel with 1 ppt ammonium persulfate

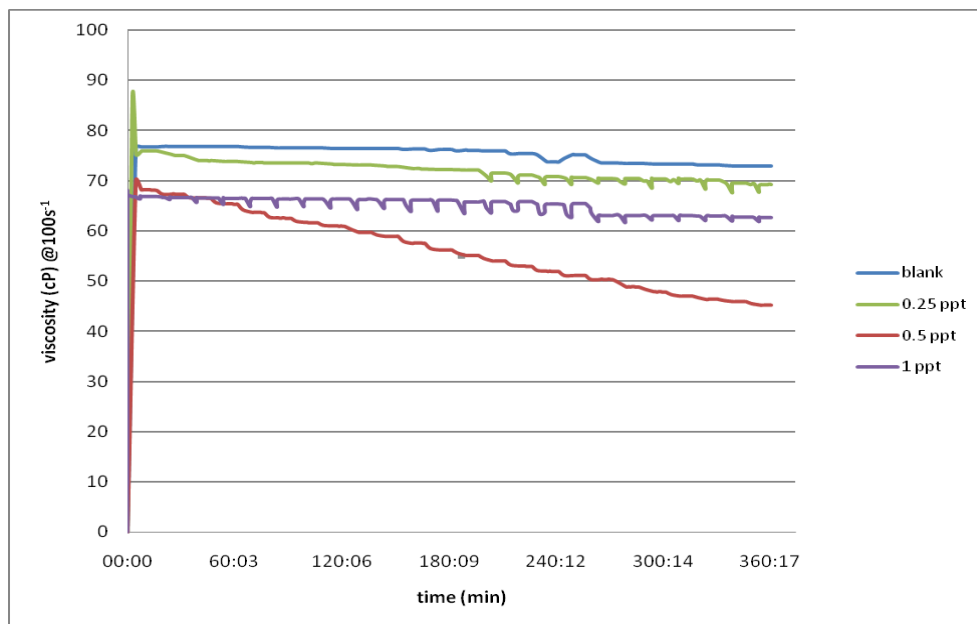


Figure 4.15- Viscosity profile of 30 ppt guar gel with ammonium persulfate at 75 °F

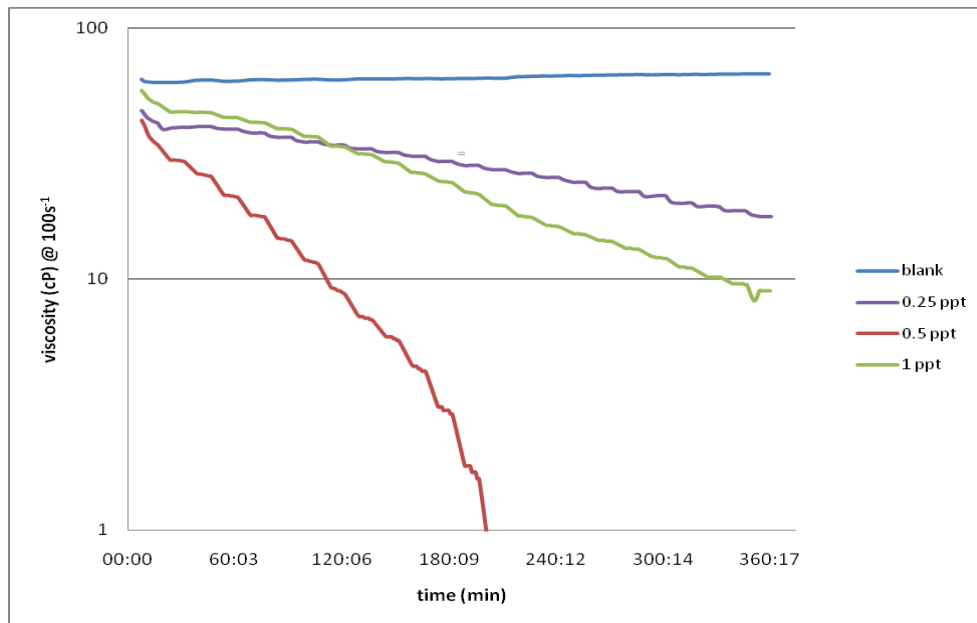


Figure 4.16- Viscosity profile of 30 ppt guar gel with ammonium persulfate at 100 °F

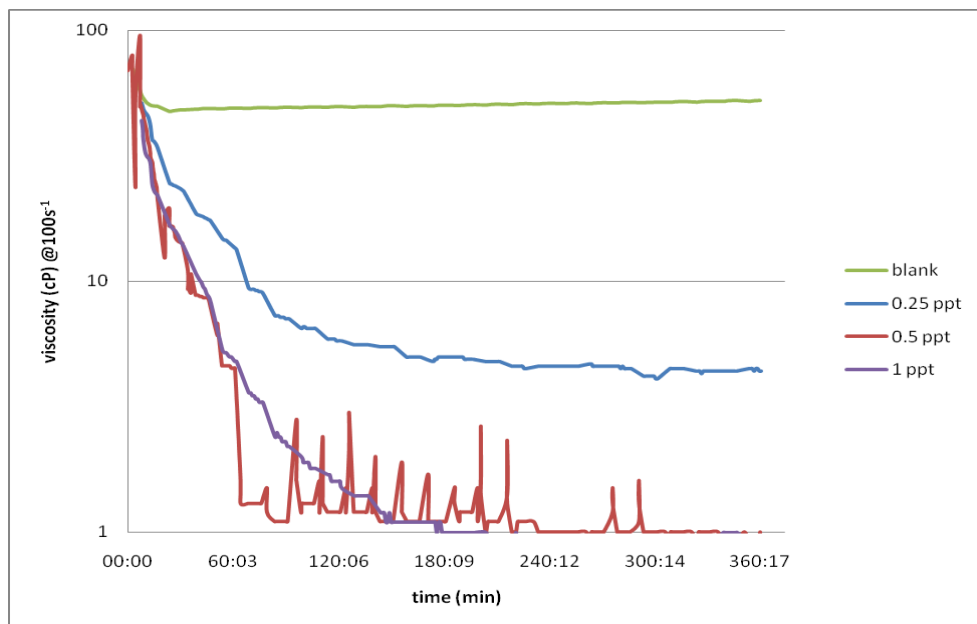


Figure 4.17- Viscosity profile of 30 ppt guar gel with ammonium persulfate at 125 °F

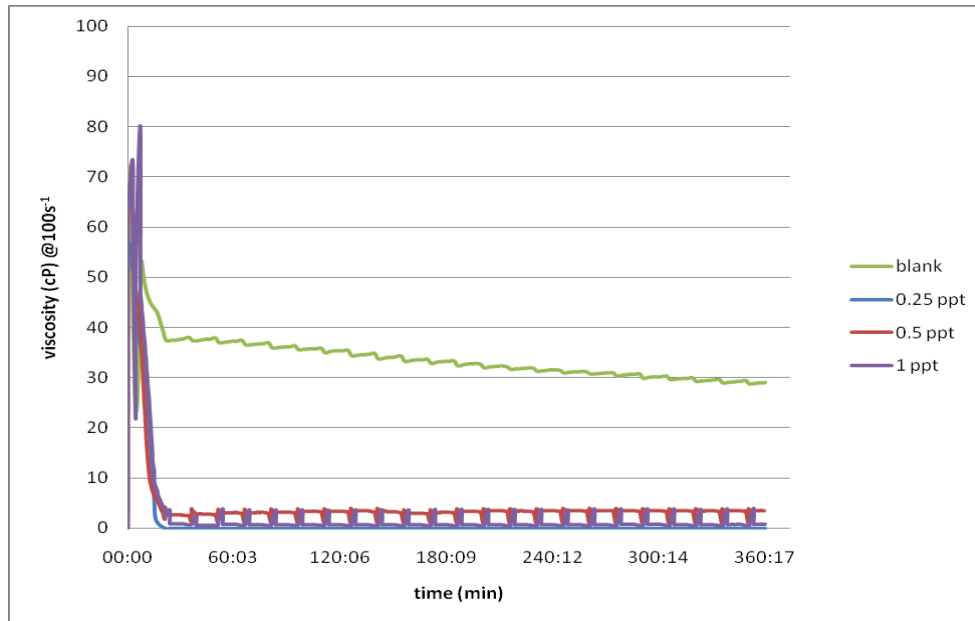


Figure 4.18- Viscosity profile of 30 ppt guar gel with ammonium persulfate at 150 °F

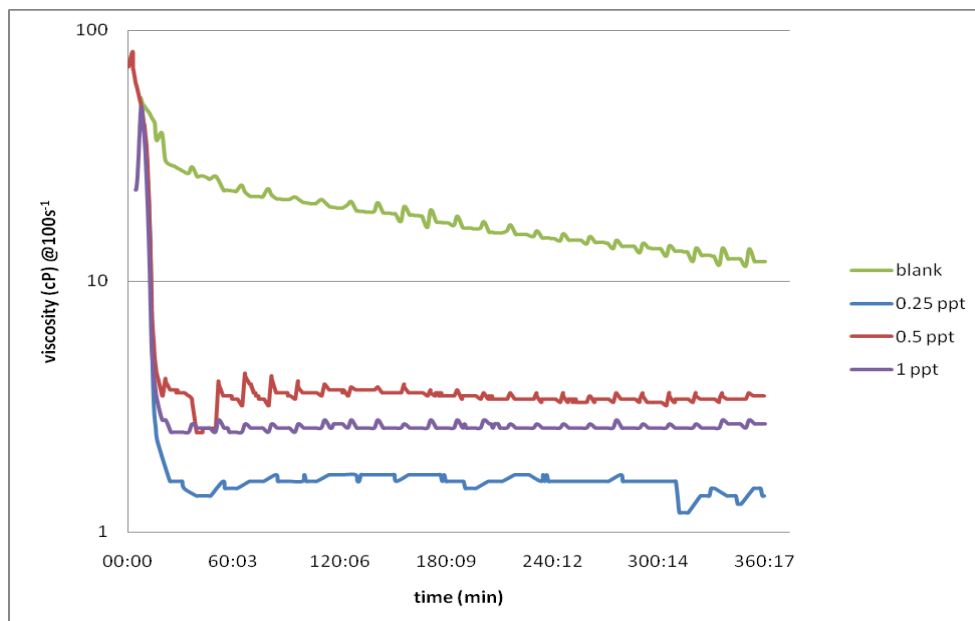


Figure 4.19- Viscosity profile of 30 ppt guar gel with ammonium persulfate at 175 °F

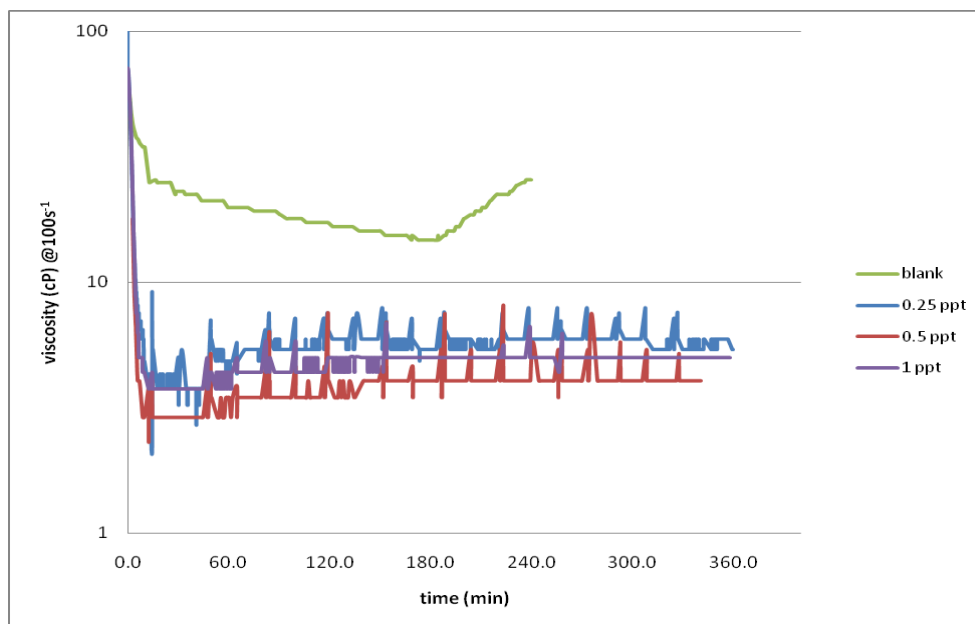


Figure 4.20- Viscosity profile of 30 ppt guar gel with ammonium persulfate at 200 °F

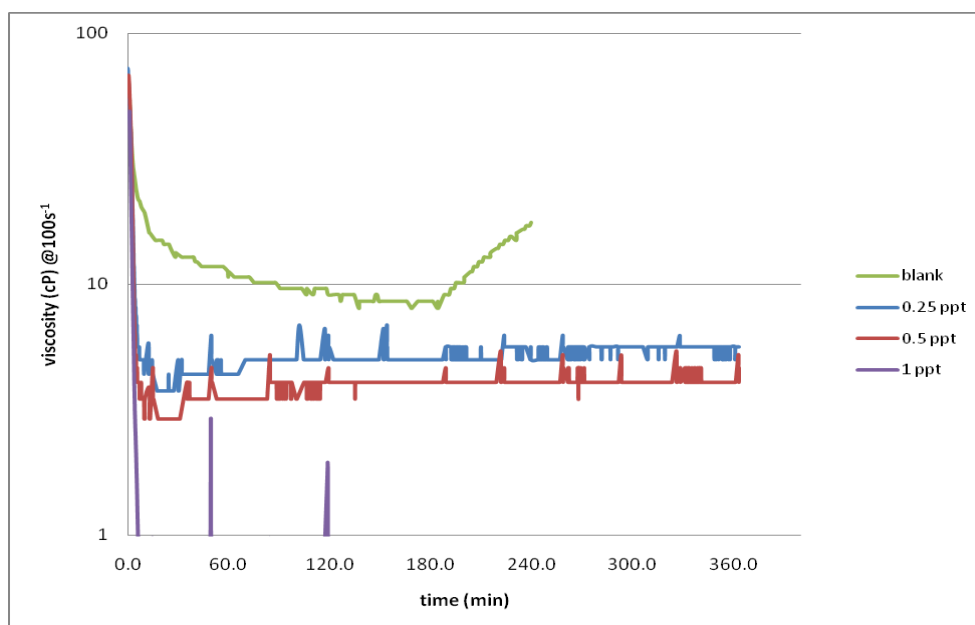


Figure 4.21- Viscosity profile of 30 ppt guar gel with ammonium persulfate at 225 °F

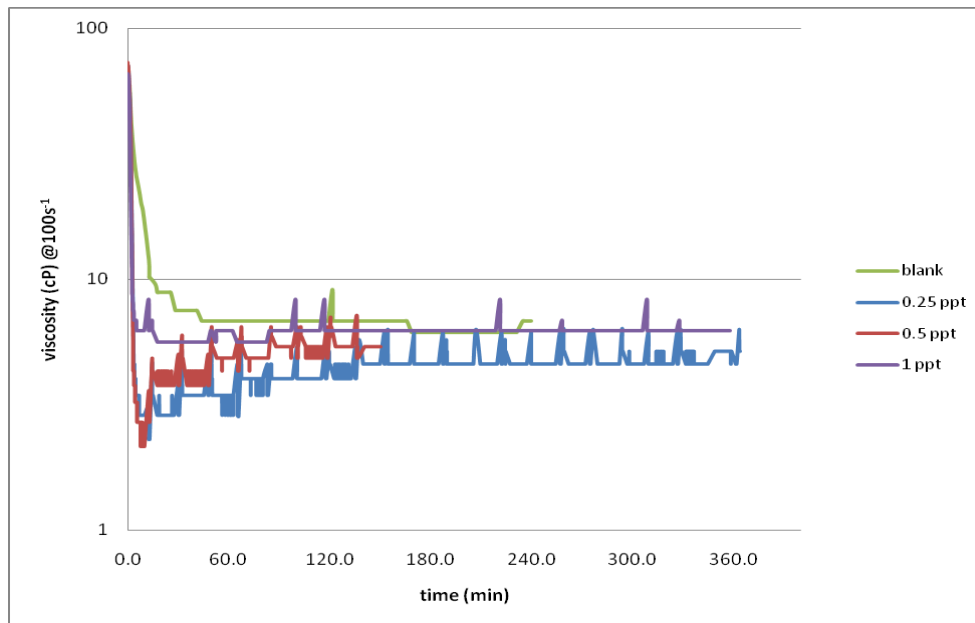


Figure 4.22- Viscosity profile of 30 ppt guar gel with ammonium persulfate at 250 °F

4.3.1.2 Magnesium Peroxide

Magnesium peroxide is used in the field for a higher range than ammonium persulfate. Its working temperature range is from 225 °F to 275 °F. The concentrations tested were 1 ppt, 5 ppt and 10 ppt for a temperature range of 175 °F to 250 °F. The curves were generated in the same way as the ammonium persulfate curves, based on concentration and temperature both. Figure 4.23 – 4.26 show the charts developed on the basis of concentration and 4. 27 – 4. 30 are developed on the basis of tmeperature.

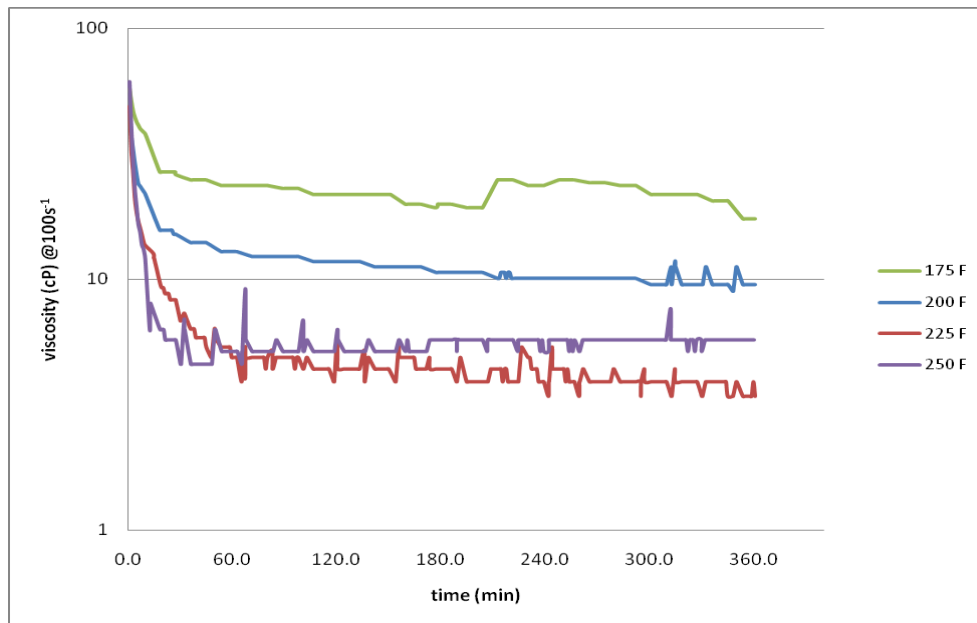


Figure 4.23- Viscosity profile of 30 ppt guar gel with 1 ppt magnesium peroxide

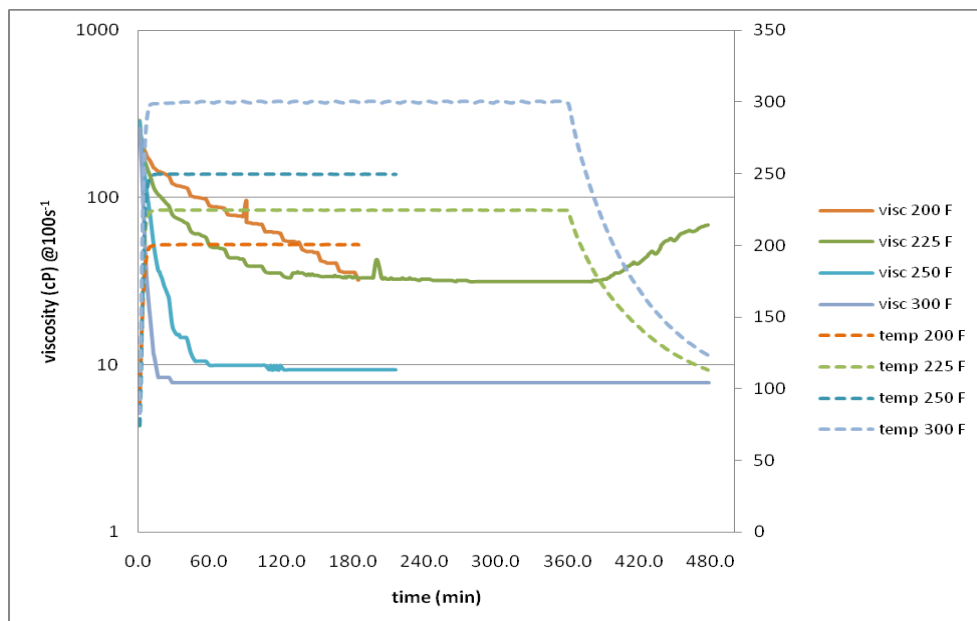


Figure 4.24- Viscosity profile of 60 ppt guar gel with 1 ppt magnesium peroxide

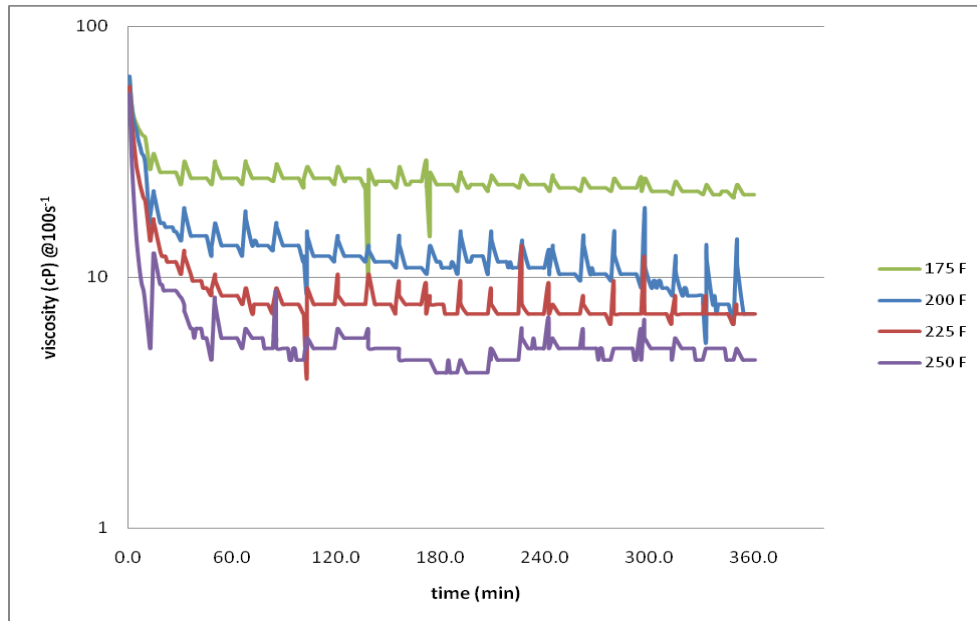


Figure 4.25- Viscosity profile of 30 ppt guar gel with 5 ppt magnesium peroxide

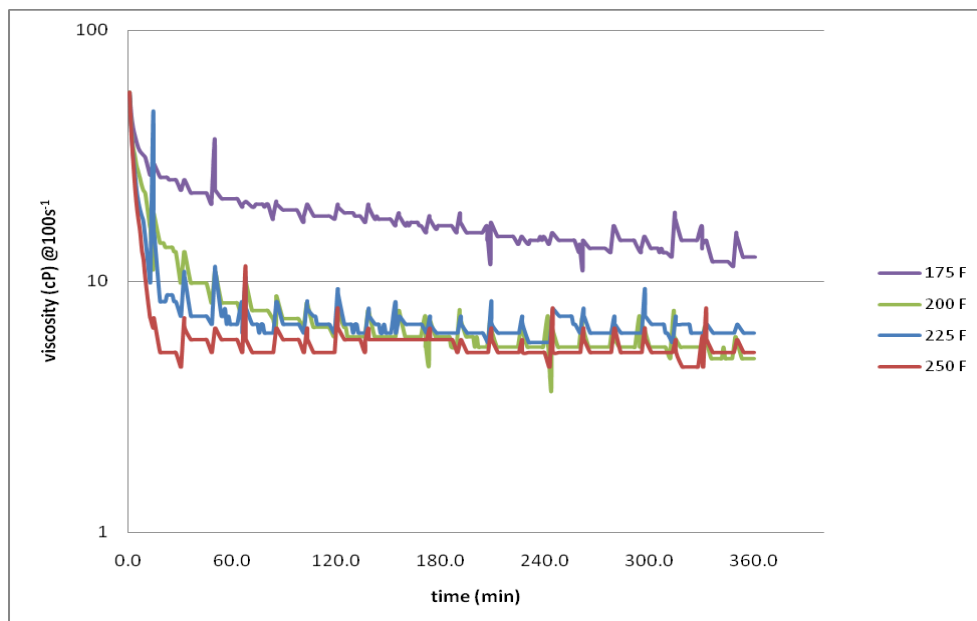


Figure 4.26- Viscosity profile of 30 ppt guar gel with 10 ppt magnesium peroxide

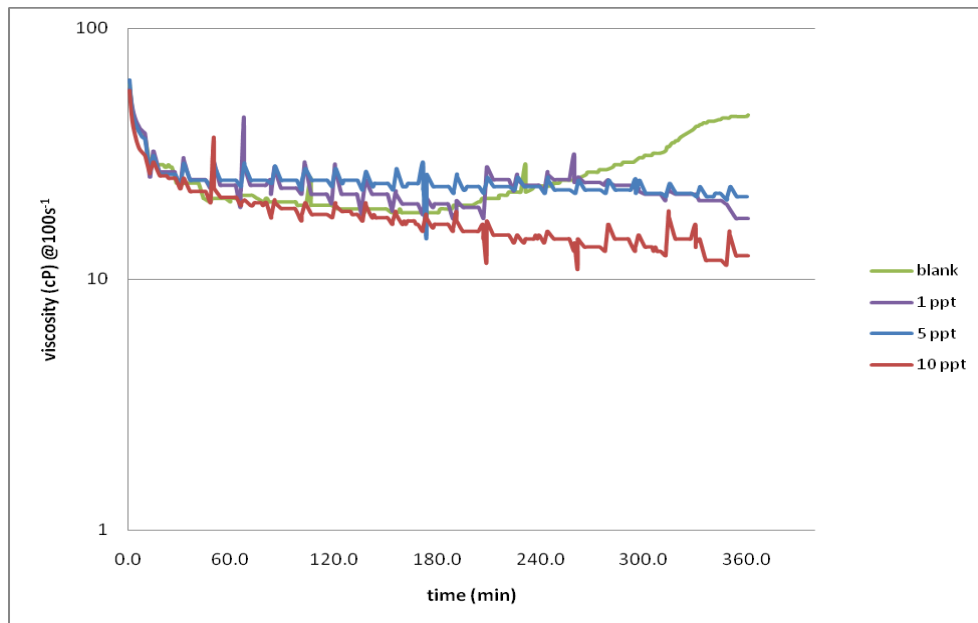


Figure 4.27- Viscosity profile of 30 ppt guar gel with magnesium peroxide at 175 °F

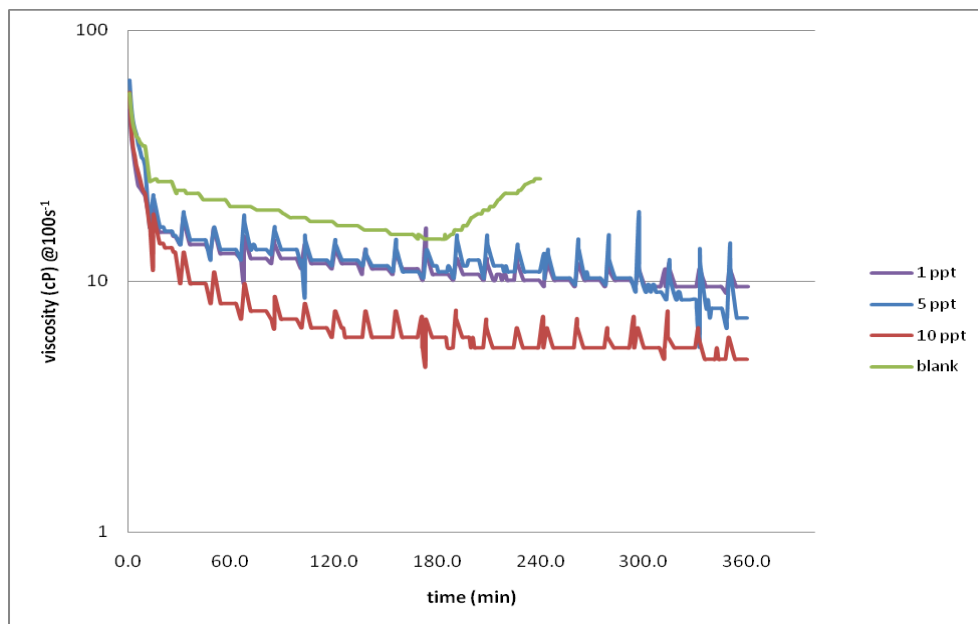


Figure 4.28- Viscosity profile of 30 ppt guar gel with magnesium peroxide at 200 °F

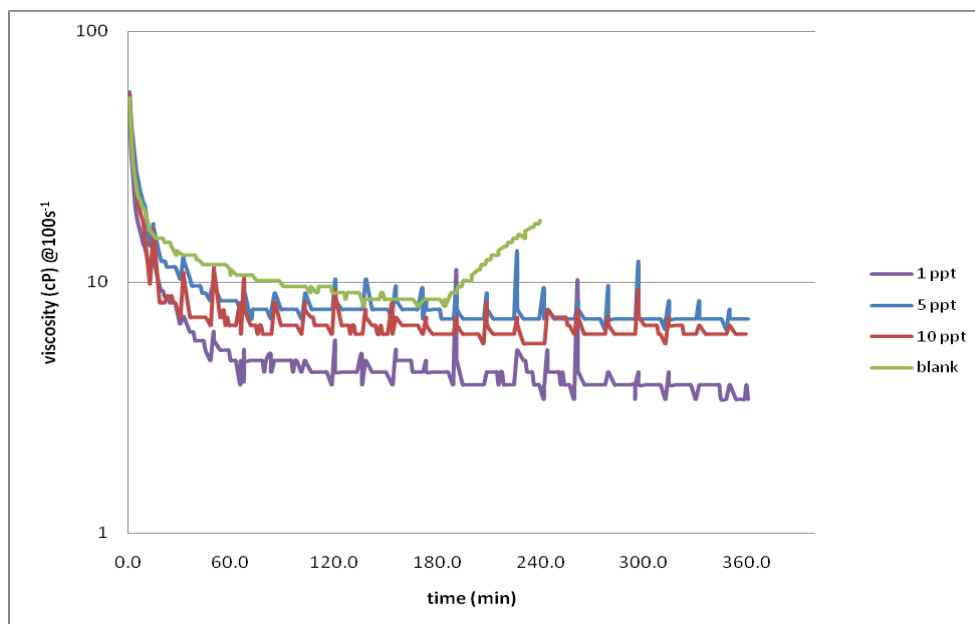


Figure 4.29- Viscosity profile of 30 ppt guar gel with magnesium peroxide at 225 °F

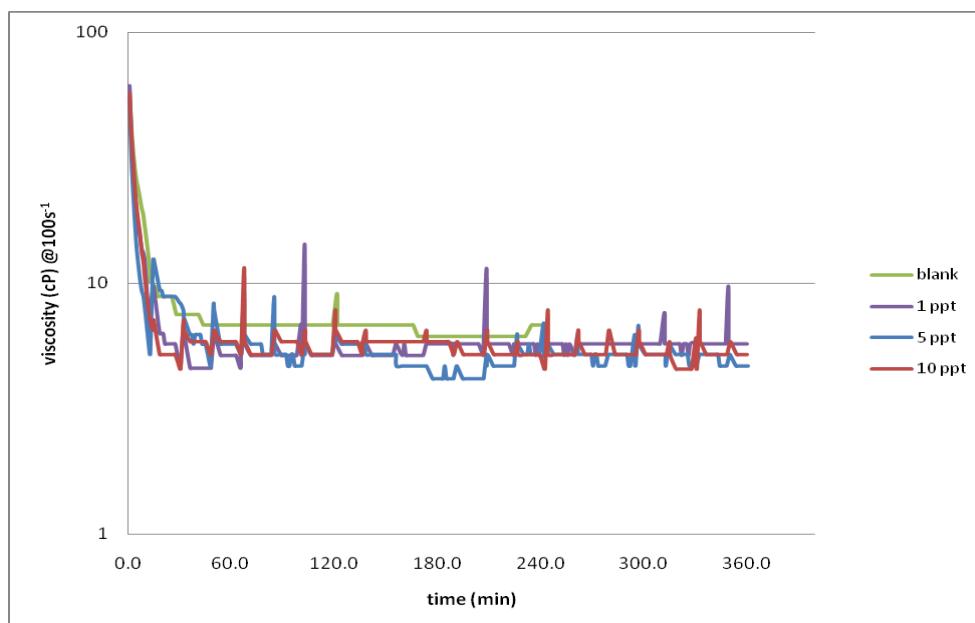


Figure 4.30- Viscosity profile of 30 ppt guar gel with magnesium peroxide at 250 °F

4.3.1.3 Sodium Bromate

Sodium bromate is used for a range of 275 °F to 450 °F in the field, although it can work at 260 °F with higher loading. The concentrations tested were 1 ppt, 5 ppt and 10 ppt over a temperature range of 150 °F to 300 °F. The tests were run for additional 1 – 2 hr while the fluid cooled down to see the regain in viscosity which was lost due to temperature thinning. The curves were generated on the basis of concentration and temperature. Temperature profiles are also shown for cool down time. Figure 4.31 – 4.34 are based on concentration while Figure 4.35 – 4.40 are based on temperature.

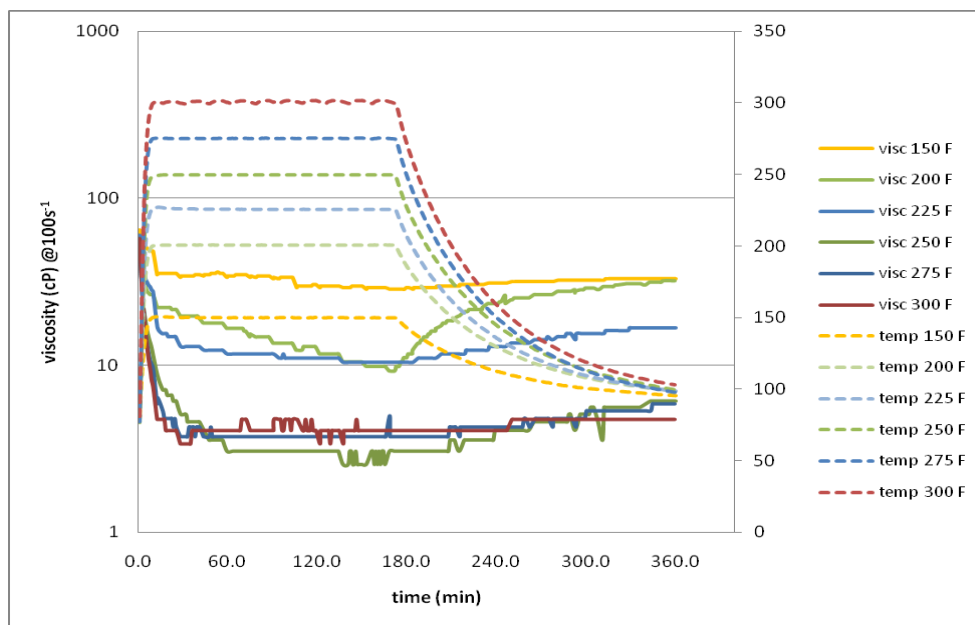


Figure 4.31- Viscosity profile of 30 ppt guar gel with 1 ppt sodium bromate

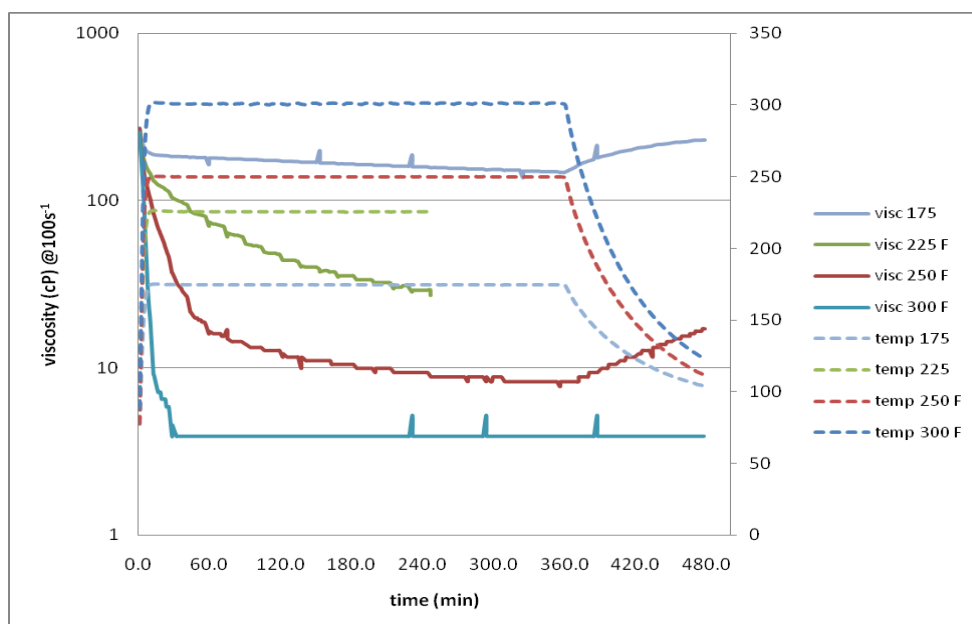


Figure 4.32- Viscosity profile of 60 ppt guar gel with 1 ppt sodium bromate

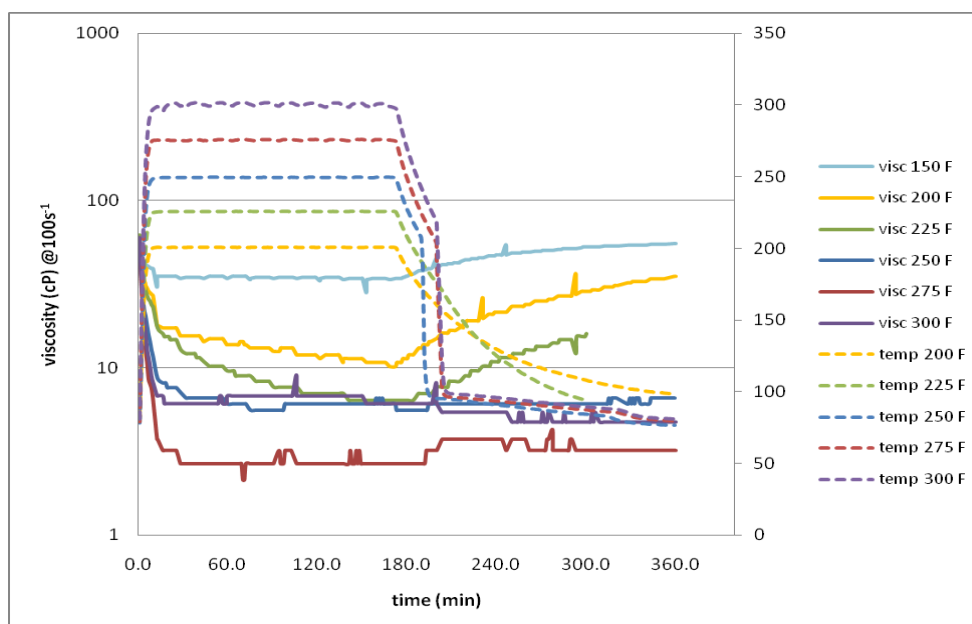


Figure 4.33- Viscosity profile of 30 ppt guar gel with 5 ppt sodium bromate

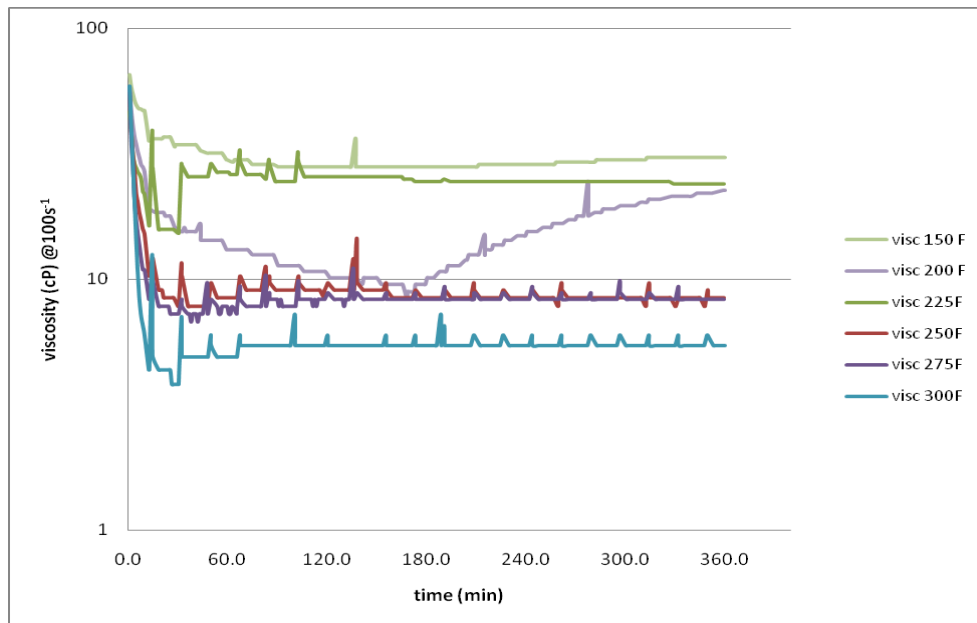


Figure 4.34- Viscosity profile of 30 ppt guar gel with 10 ppt sodium bromate

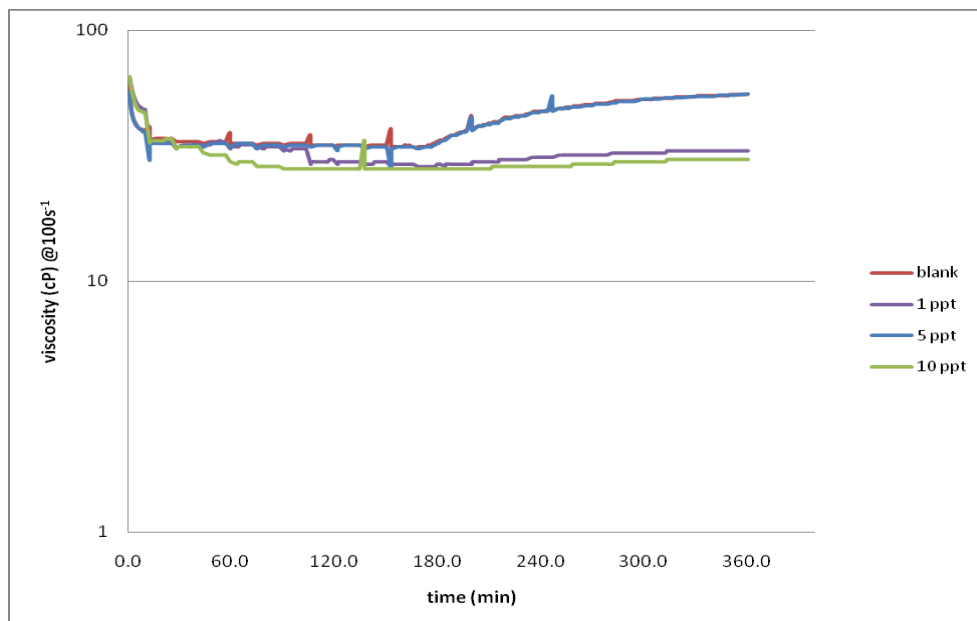


Figure 4.35- Viscosity profile of 30 ppt guar gel with sodium bromate at 150 °F

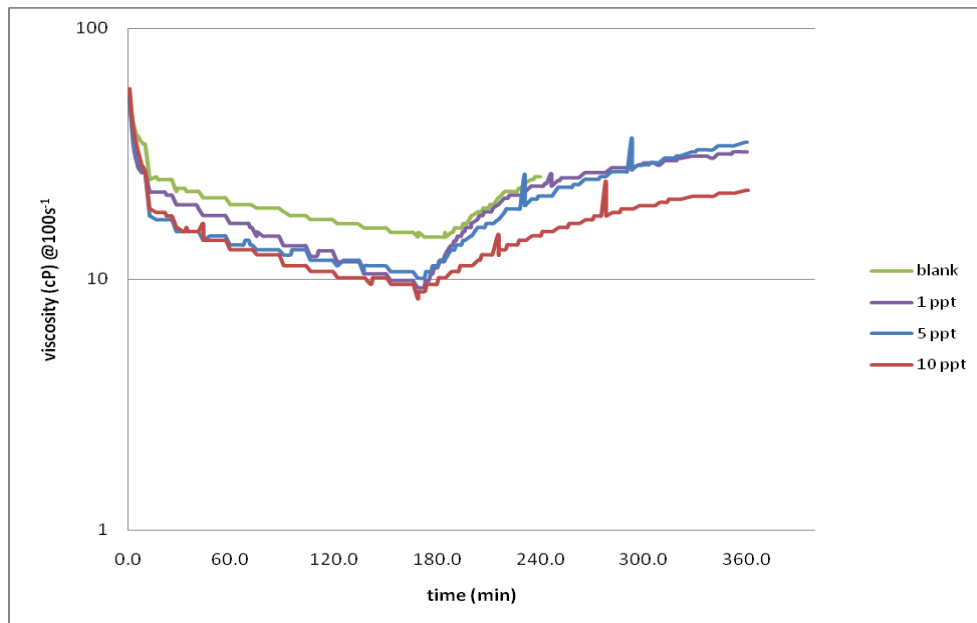


Figure 4.36- Viscosity profile of 30 ppt guar gel with sodium bromate at 200 °F

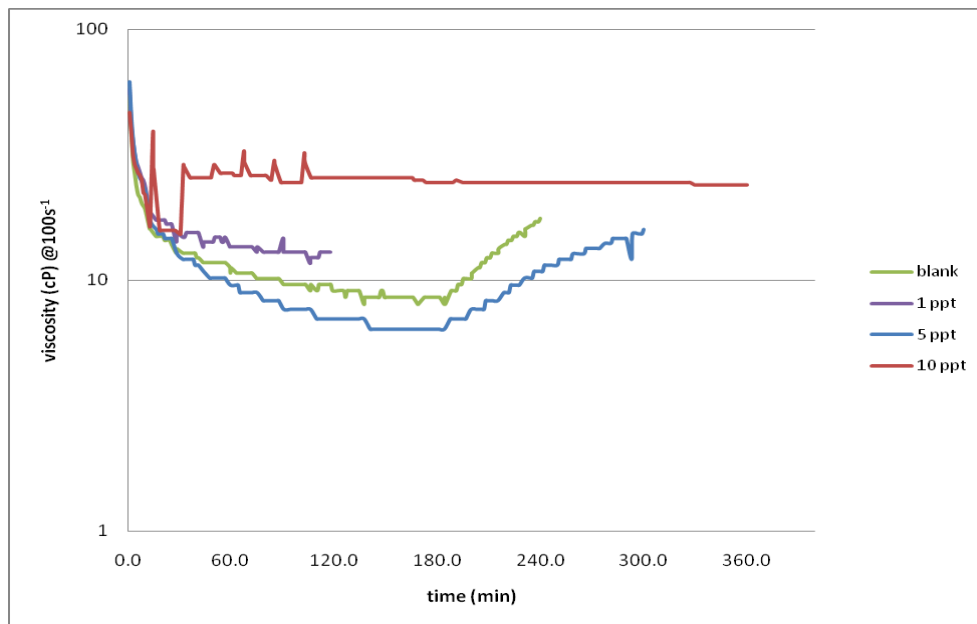


Figure 4.37- Viscosity profile of 30 ppt guar gel with sodium bromate at 225 °F

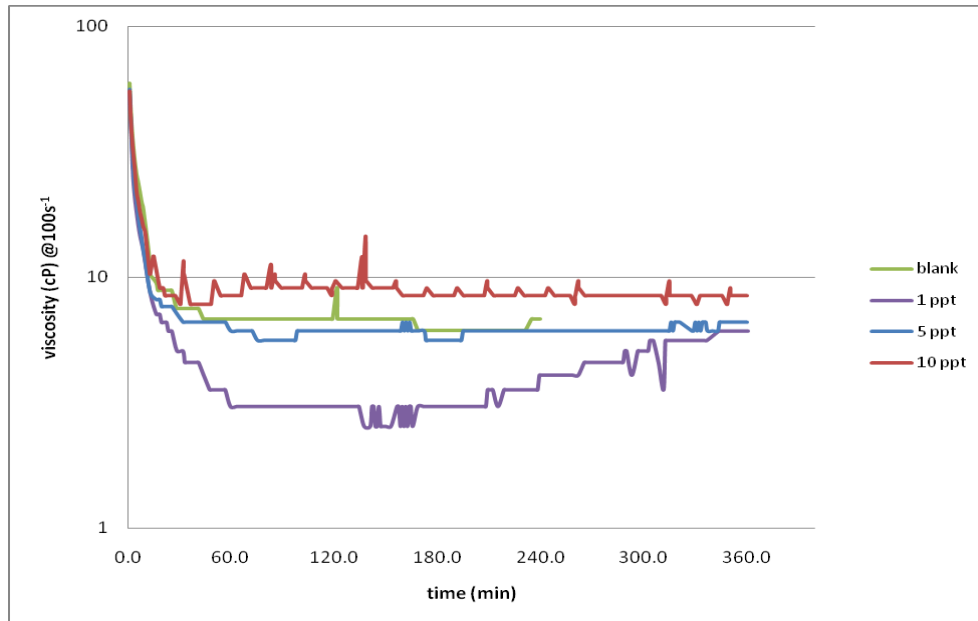


Figure 4.38- Viscosity profile of 30 ppt guar gel with sodium bromate at 250 °F

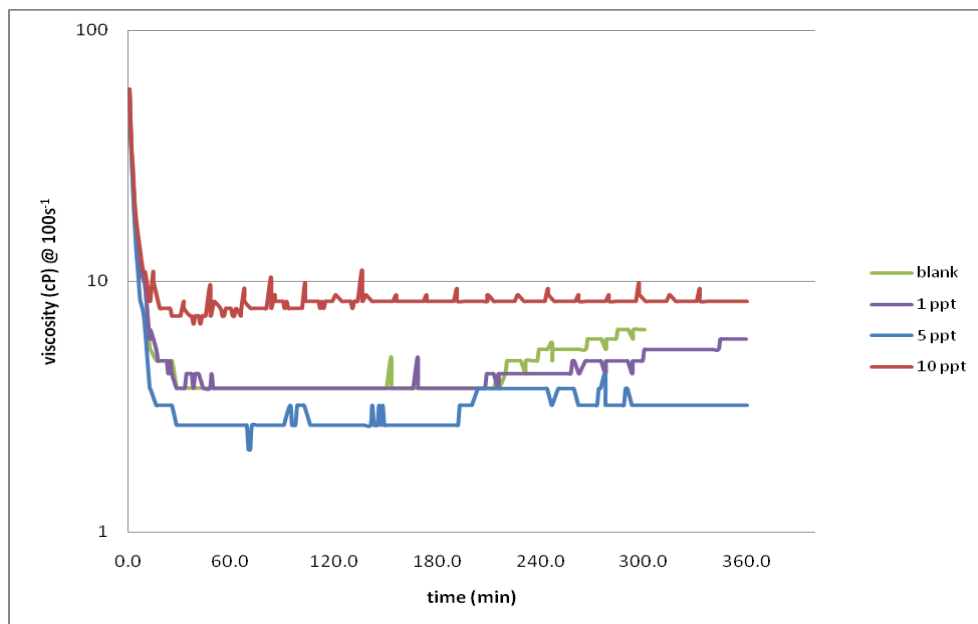


Figure 4.39- Viscosity profile of 30 ppt guar gel with sodium bromate at 275 °F

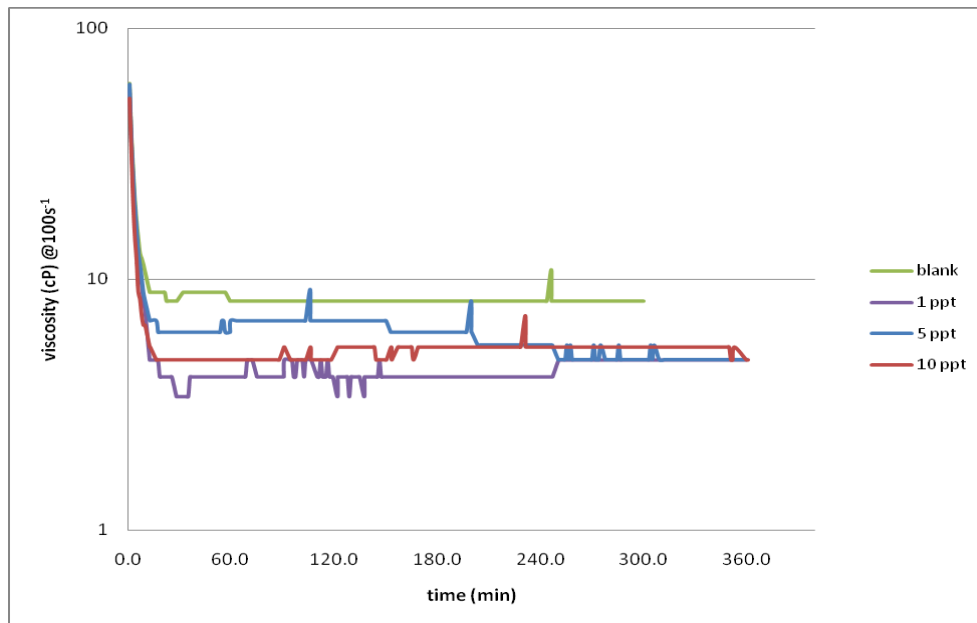


Figure 4.40- Viscosity profile of 30 ppt guar gel with sodium bromate at 300 °F

4.3.1.4 Galactomannanase Enzyme

Galactomannanase was the only enzyme tested in this study. It was tested to see the comparison between the performance of oxidative and enzymatic breakers. This enzyme is used in the field for a temperature range of 70 °F to 300 °F. Though in this study, it was only tested for a range of 75 oF to 175 oF, to compare its effectiveness against ammonium persulfate. The concentrations tested were 0.5 gpt and 1 gpt. Figure 4.41 – 4.42 are based on concentration while Figure 4.43 – 4.47 are based on temperature.

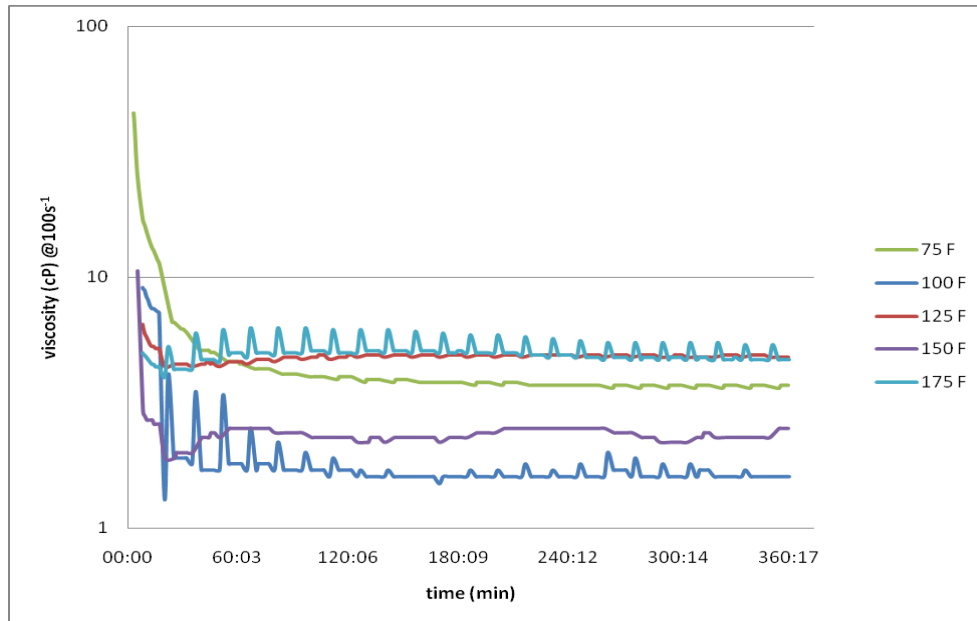


Figure 4.41- Viscosity profile of 30 ppt guar gel with 0.5 gpt galactomannanase

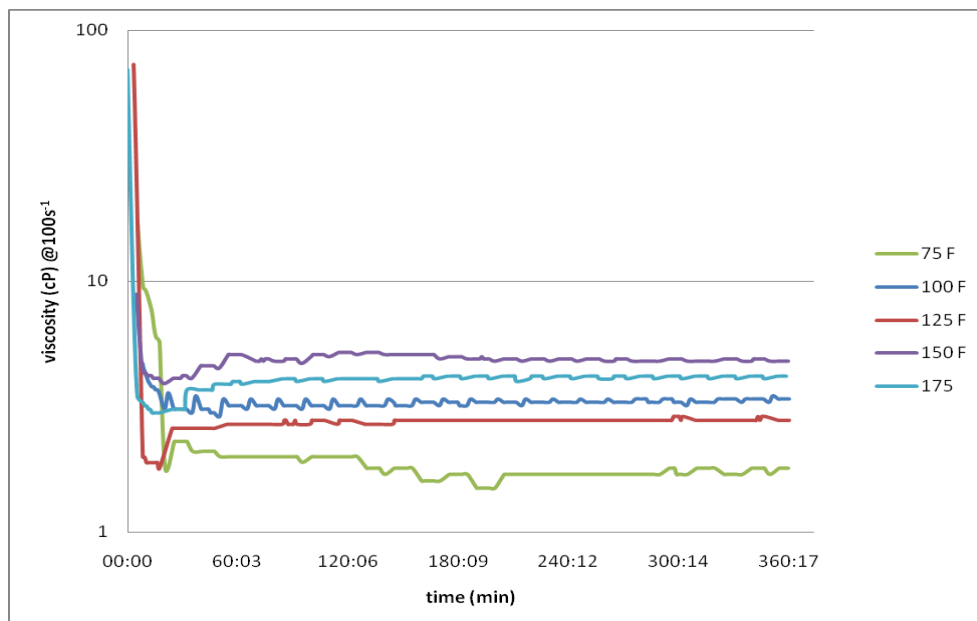


Figure 4.42- Viscosity profile of 30 ppt guar gel with 1 gpt galactomannanase

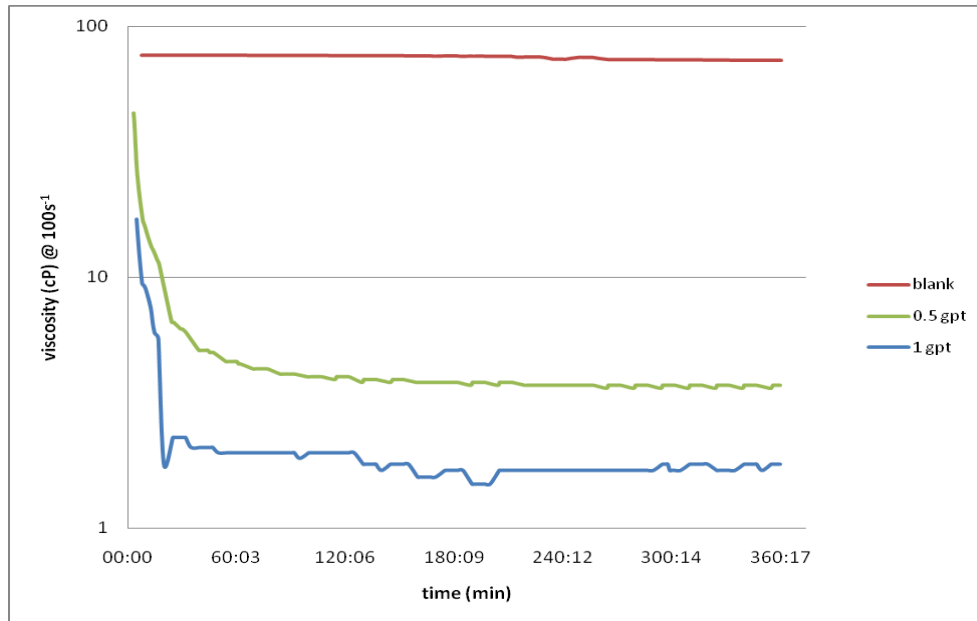


Figure 4.43- Viscosity profile of 30 ppt guar gel with galactomannanase at 75 °F

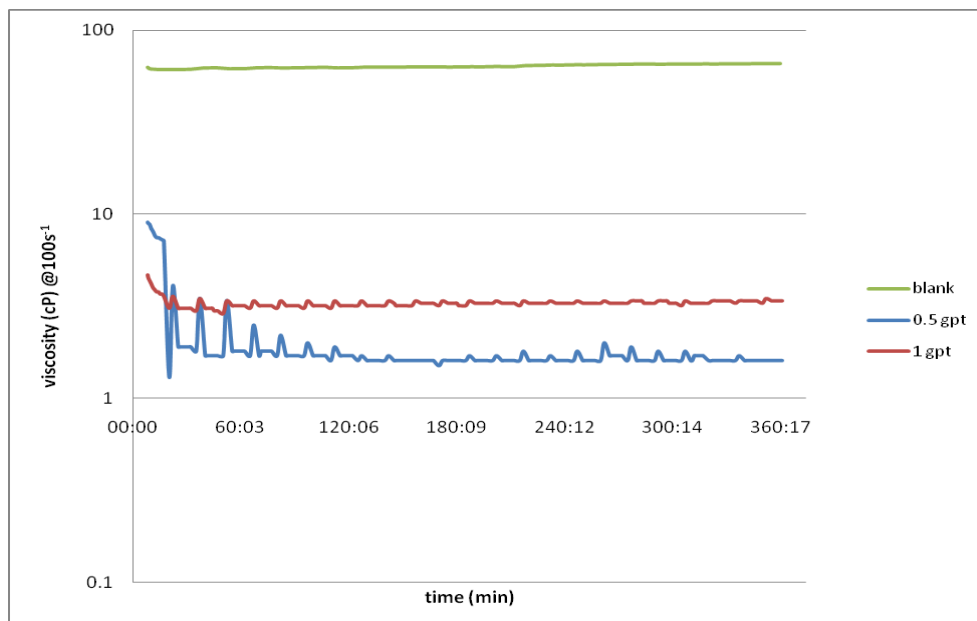


Figure 4.44- Viscosity profile of 30 ppt guar gel with galactomannanase at 100 °F

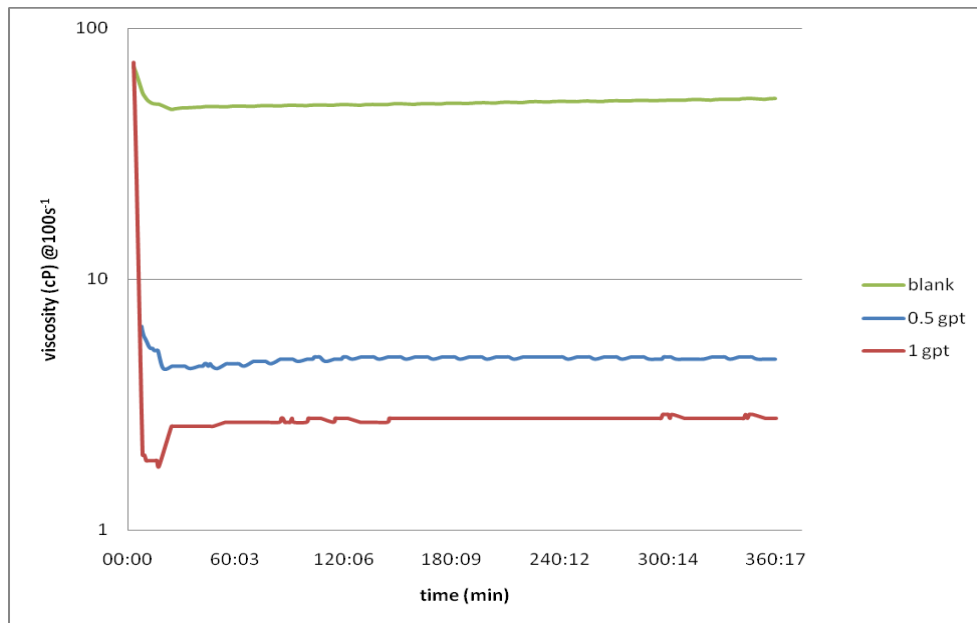


Figure 4.45- Viscosity profile of 30 ppt guar gel with galactomannanase at 125 °F

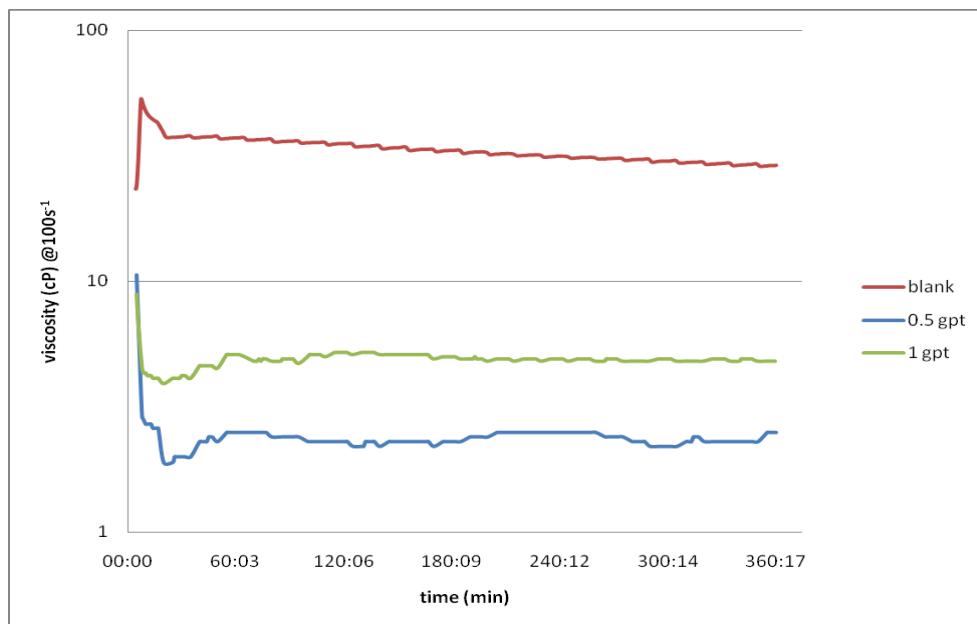


Figure 4.46- Viscosity profile of 30 ppt guar gel with galactomannanase at 150 °F

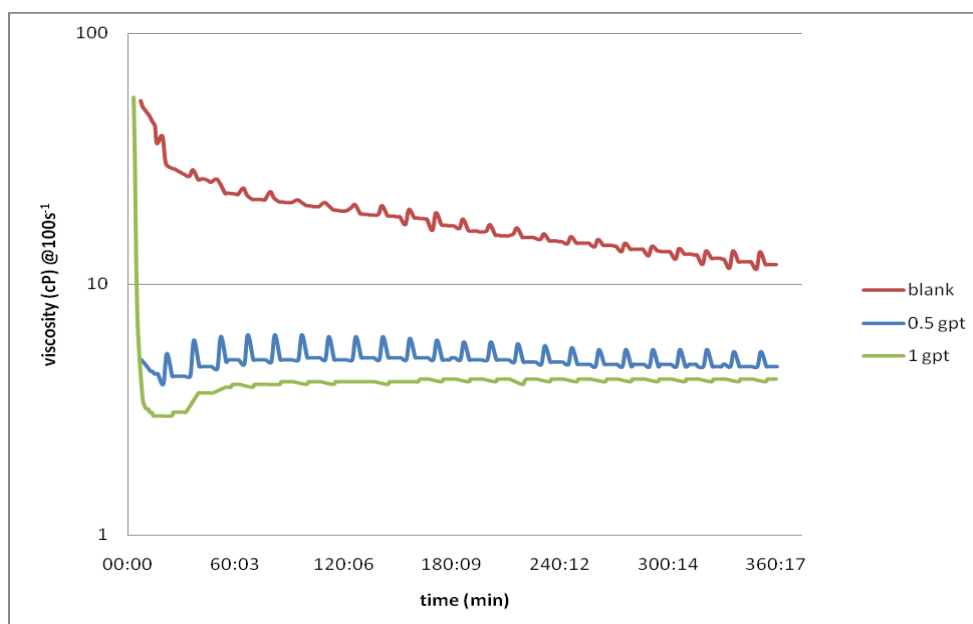


Figure 4.47- Viscosity profile of 30 ppt guar gel with galactomannanase at 175 °F

4.3.1.5 Flow Parameters n' and K

The flow behavior index, n' , and consistency index, K , were calculated using the ramp data from the viscometer tests. Some examples of the flow parameters values calculated from the viscometer test data are shown in Tables 4.1 – 4.4. The flow parameters for the rest of the tests are provided in Appendix A.

Table 4.1– Flow parameters n' and K for 30 ppt guar gel with 1 ppt ammonium persulfate at 125 °F

Elapsed Time (h:mm)	n'	K (lbf-s ^{n'} /ft ²)
0:00	0.4773	0.0132
0:17	0.8433	0.0007
0:32	0.9610	0.0003
0:47	0.9904	0.0001
1:02	0.9471	0.0001
1:17	0.8937	0.0001
1:32	0.8636	0.0001
1:47	0.8223	0.0001
2:02	0.8220	0.0001
2:17	0.8100	0.0001
2:32	0.7688	0.0001
2:47	0.7327	0.0001
3:02	0.7103	0.0001
3:17	0.6985	0.0001
3:32	0.6935	0.0001
3:47	0.6744	0.0001
4:02	0.6586	0.0001
4:17	0.6468	0.0001
4:32	0.6409	0.0001
4:47	0.6221	0.0002
5:02	0.5951	0.0002
5:17	0.5795	0.0002
5:32	0.5292	0.0003
5:47	0.5369	0.0002
6:02	0.5682	0.0002

Table 4.2– Flow parameters n' and K for 60 ppt guar gel with 1 ppt magnesium peroxide at 225 °F

Elapsed Time (h:mm)	n'	K (lbf-s ⁿ /ft ²)
0:15	0.5877	0.0168
0:31	0.6585	0.0082
0:46	0.6696	0.0060
1:02	0.6434	0.0055
1:17	0.6178	0.0053
1:33	0.5934	0.0052
1:48	0.5631	0.0054
2:04	0.5174	0.0061
2:20	0.0489	0.0578
2:35	0.0574	0.0538
2:51	0.0576	0.0530
3:06	0.0536	0.0537
3:22	0.0496	0.0541
3:38	0.0423	0.0556
3:54	0.0346	0.0572
4:09	0.0297	0.0584
4:25	0.0175	0.0613
4:40	0.0132	0.0622
4:56	0.0128	0.0623
5:11	0.0125	0.0625
5:27	0.0127	0.0625
5:43	0.0131	0.0624
5:58	0.0124	0.0624
6:14	0.0125	0.0626
6:29	0.0248	0.0596
6:45	0.0743	0.0508
7:00	0.1632	0.0380
7:16	0.3015	0.0237
7:32	0.4500	0.0143
7:47	0.5105	0.0122
8:03	0.5357	0.0119

Table 4.3– Flow parameters n' and K for 30 ppt guar gel with 1 gpt galactomannanase at 175 °F

Elapsed Time	n'	K
(h:mm)		(lbf-s ⁿ /ft ²)
0:01	0.5235	0.0038
0:17	0.4248	0.0012
0:32	0.4118	0.0015
0:47	0.3738	0.0019
1:02	0.3599	0.0021
1:17	0.3519	0.0022
1:32	0.3446	0.0023
1:47	0.3447	0.0023
2:02	0.3414	0.0023
2:17	0.3390	0.0023
2:32	0.3354	0.0024
2:47	0.3324	0.0024
3:02	0.3289	0.0025
3:17	0.3235	0.0025
3:32	0.3243	0.0025
3:47	0.3200	0.0025
4:02	0.3190	0.0026
4:17	0.3180	0.0025
4:32	0.3171	0.0026
4:47	0.3112	0.0026
5:02	0.3098	0.0027
5:17	0.3072	0.0027
5:32	0.3046	0.0027
5:47	0.3018	0.0027
6:02	0.2949	0.0028

Table 4.4– Flow parameters n' and K for 30 ppt guar gel with 1 ppt sodium bromate at 250 °F

Elapsed Time (h:mm)	n'	K (lbf-s ⁿ /ft ²)
0:15	0.5232	0.0015
0:31	0.3678	0.0018
0:46	0.2261	0.0027
1:02	0.1366	0.0033
1:17	0.1011	0.0037
1:33	0.0855	0.0039
1:48	0.0661	0.0042
2:04	0.0145	0.0050
2:19	0.0058	0.0052
2:35	0.0000	0.0053
2:51	0.0460	0.0045
3:06	0.1065	0.0038
3:22	0.0622	0.0049
3:37	0.1193	0.0040
3:53	0.1115	0.0043
4:08	0.1370	0.0042
4:24	0.1549	0.0041
4:39	0.2086	0.0035
4:55	0.1759	0.0042

4.3.2 Early Time Data

Early time data was also plotted from the viscosity break profile tests. This data shows the reduction in viscosity for the first 10 minutes of the test. It is evident from the results shown earlier, that the major drop in the viscosity of the fluid happens in the first few minutes. The early time data helps in identifying the effectiveness of the breakers for shorter breaking times.

In certain fracturing applications, for tight formations, it is required to have a thick fluid at the surface to reduce the wear and tear of the pumping equipment, yet have a low viscosity downhole when it enters the formation. The early time data is basically the pipe-time data when the fluid travels through the length of the well towards the bottom. The breaker should break the fluid during this pipe-time and make it almost water-like before it enters the formation. This is the reason why early time data is required, to see which breaker type and concentration is best suited for a particular fracturing treatment.

Results also show that it is possible at any tested temperature, a particular concentration of breaker may be slow in the first few minutes in bringing down the viscosity compared to another concentration, but in the long run it causes more reduction in viscosity and vice versa. Some examples of the early time charts produced from the full-length viscosity profiles are presented in Figures 4.48 – 4.55. The remaining plots can be found in Appendix B.

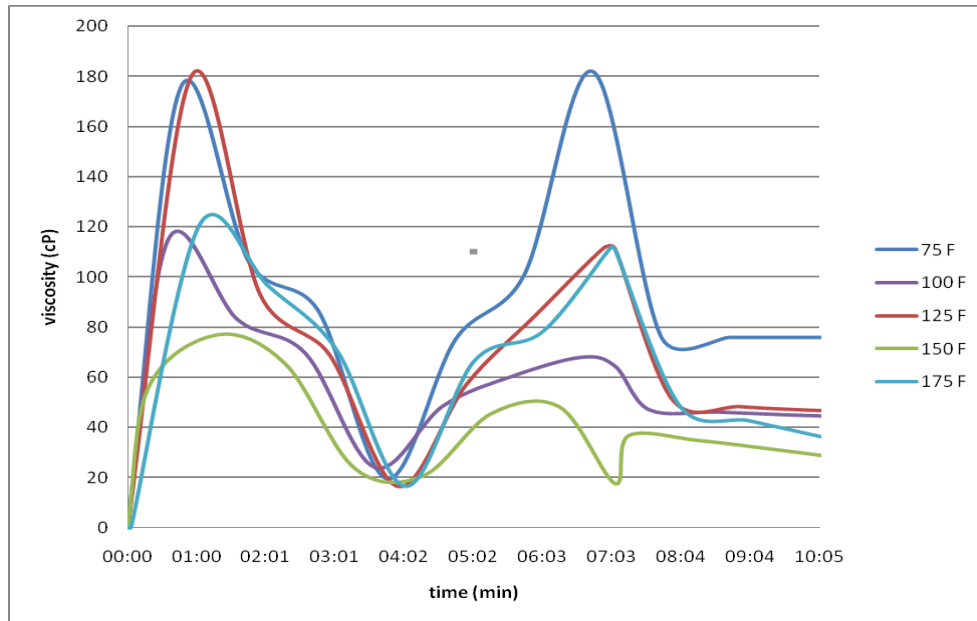


Figure 4.48– Early time viscosity of 30 ppt guar gel with 0.25 ppt ammonium persulfate (75 °F – 175 °F)

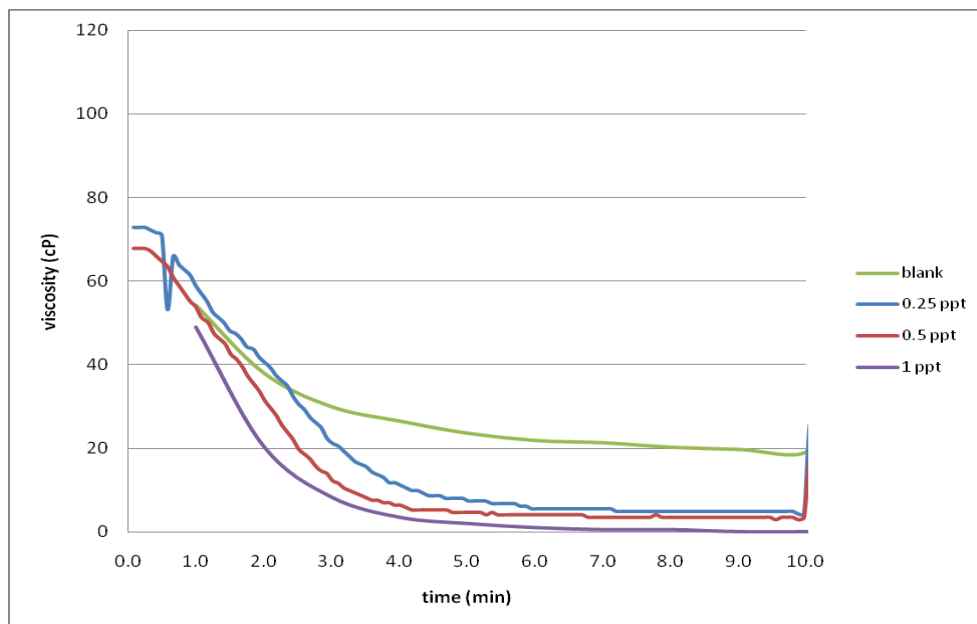


Figure 4.49– Early time viscosity of 30 ppt guar gel with ammonium persulfate at 225 °F

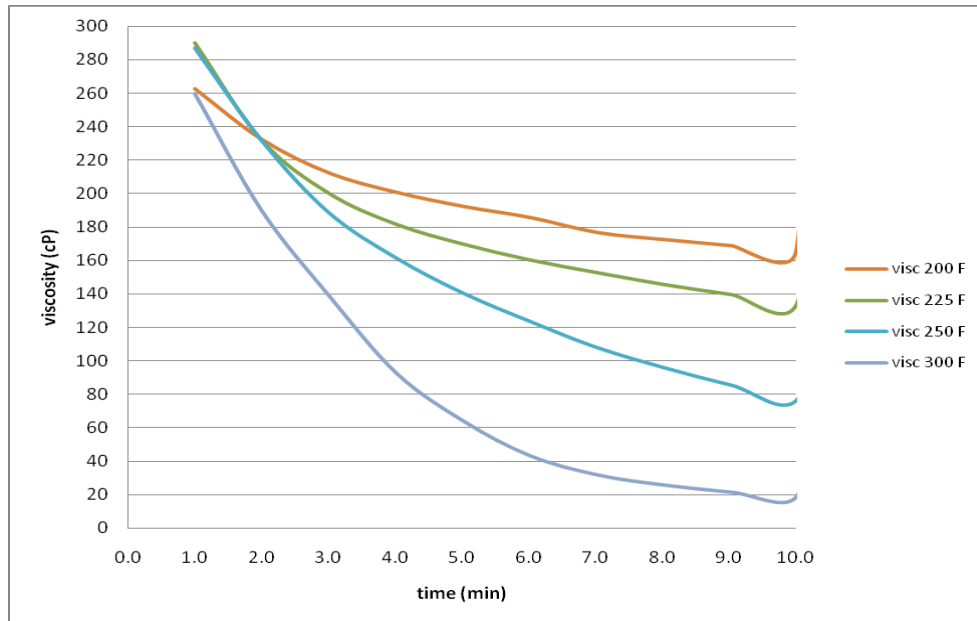


Figure 4.50– Early time viscosity of 60 ppt guar gel with 1 ppt magnesium peroxide

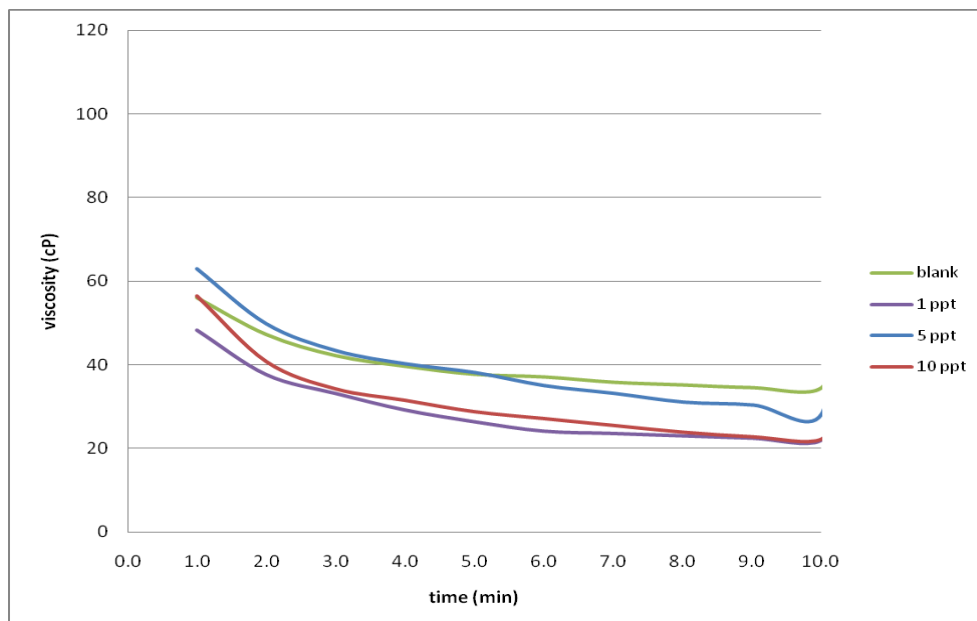


Figure 4.51– Early time viscosity of 30 ppt guar gel with magnesium peroxide at 200 °F

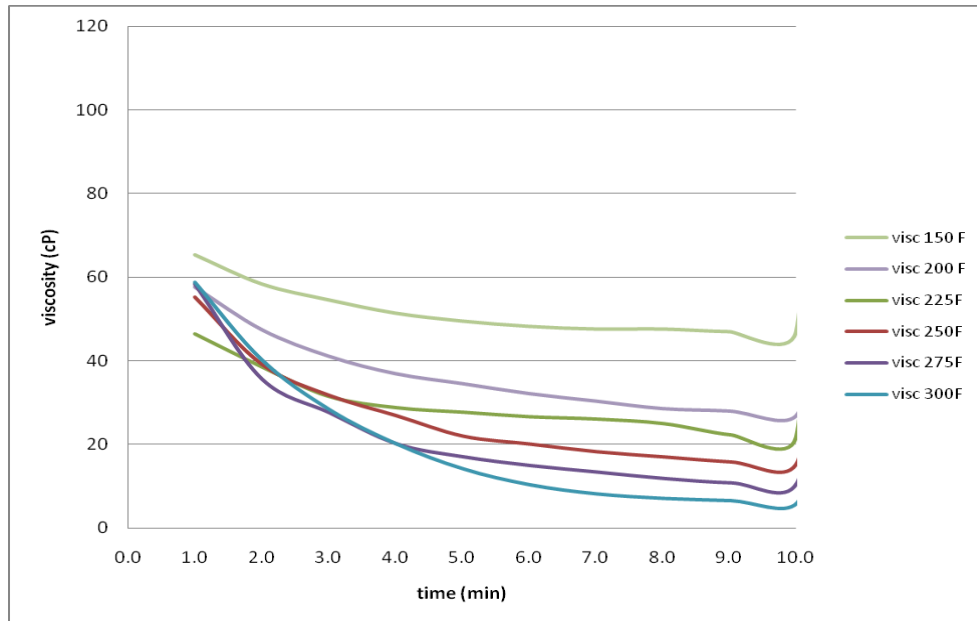


Figure 4.52– Early time viscosity of 30 ppt guar gel with 10 ppt sodium bromate

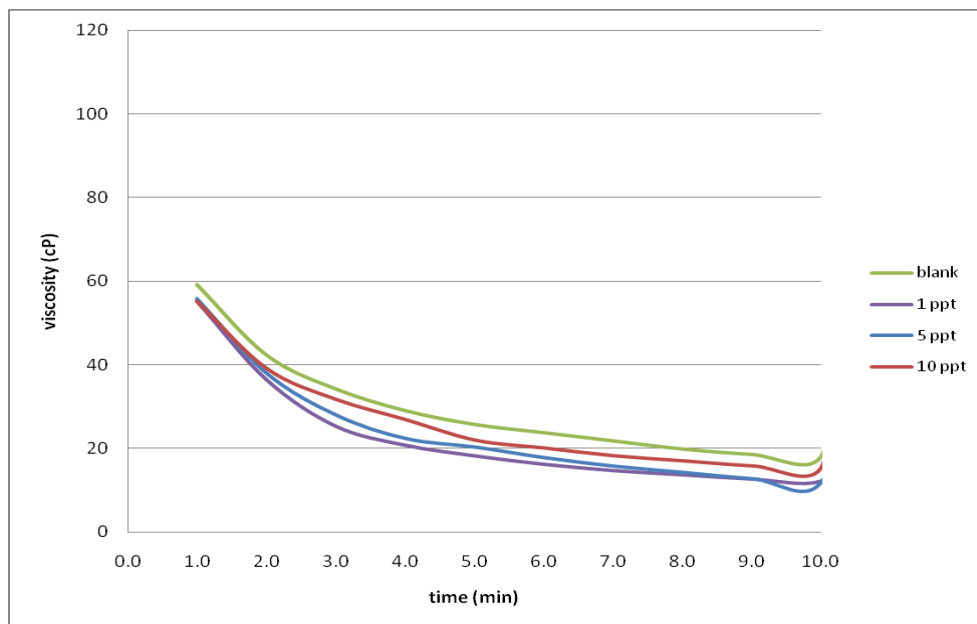


Figure 4.53– Early time viscosity of 30 ppt guar gel with sodium bromate at 250 °F

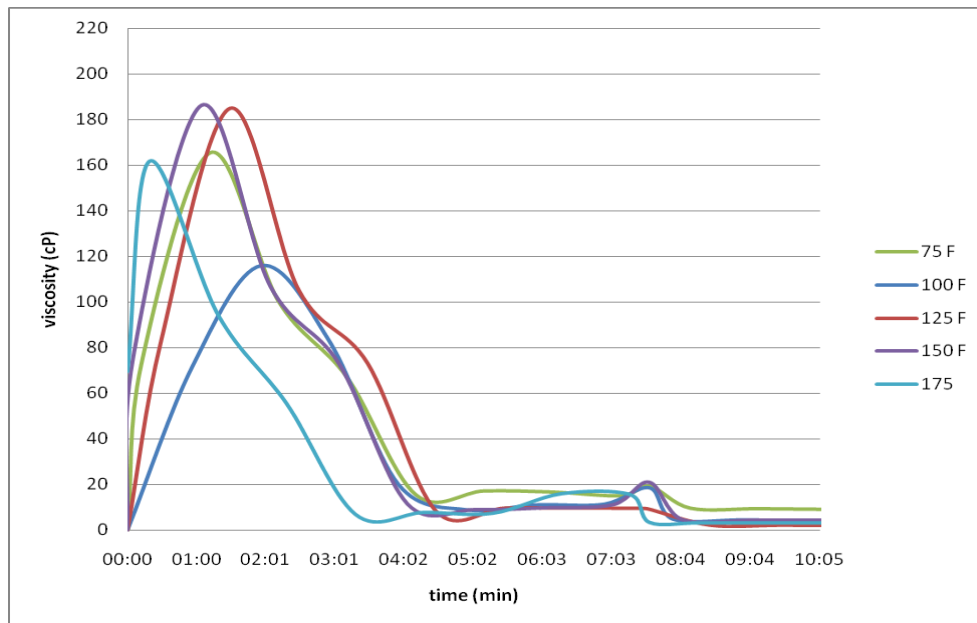


Figure 4.54– Early time viscosity of 30 ppt guar gel with 1 gpt galactomannanase

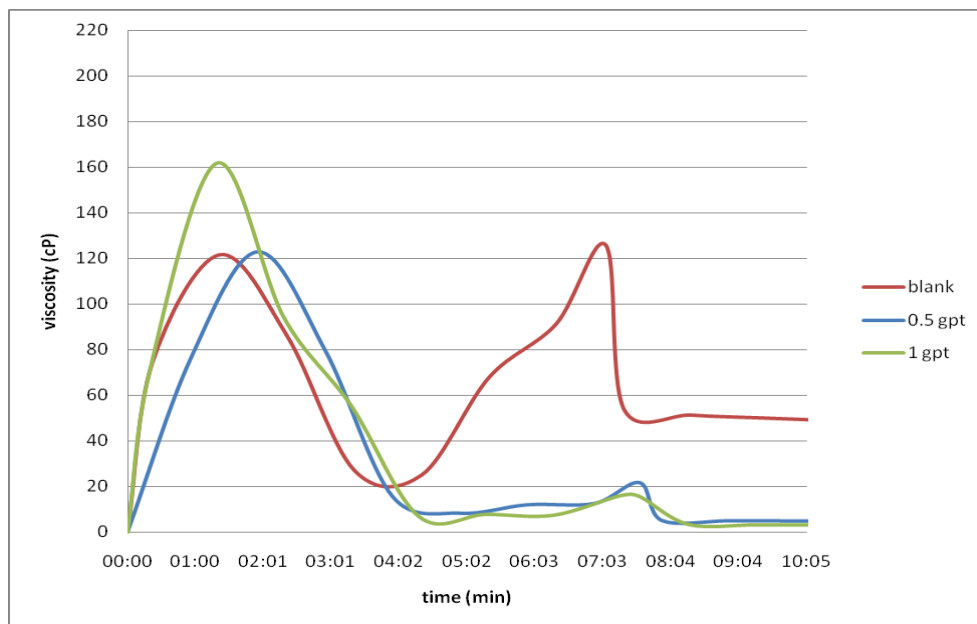


Figure 4.55– Early time viscosity of 30 ppt guar gel with galactomannanase at 175 °F

4.4 Breaker Activity Curves (S-Curves)

The breaker activity or S - curves were developed using the viscosity data for each breaker. The idea is simple; from every test data, where a particular coccentration of breaker was tested at a particular temperature, the lowest viscosity at 100 s^{-1} was chosen. This does not include the sweep data, the viscosity is chosen from the constant shear data which is the 10 min (approx.) intervals between the sweeps.

After choosing the lowest viscosity data points for each breaker at each concentration and temperature, the breaker activity curves are plotted. As with the viscosity profile data, the curves are plotted both on the basis of concentration and temperature.

4.4.1 Ammonium Persulfate

The lowest viscosity points at 100 s^{-1} taken from the test data are shown in the Table 4.5. Based on the values in the table, breaker activity curves are presented in Figure 4.56 and 4.57.

Table 4.5– Lowest viscosity values from ammonium persulfate tests with 30 ppt gel

Temperature (°F)	Concentration			
	0 ppt	0.25 ppt	0.5 ppt	1 ppt
	Viscosity (cP)			
75	73	70	45	63
100	66	18	0.1	9
125	52.5	4.4	0.8	0.8
150	29	0.1	3.4	0.7
175	12	1.4	3.5	2.7
200	15	6	4	5
225	9	5	4	0.1
250	6	4.5	5.3	6

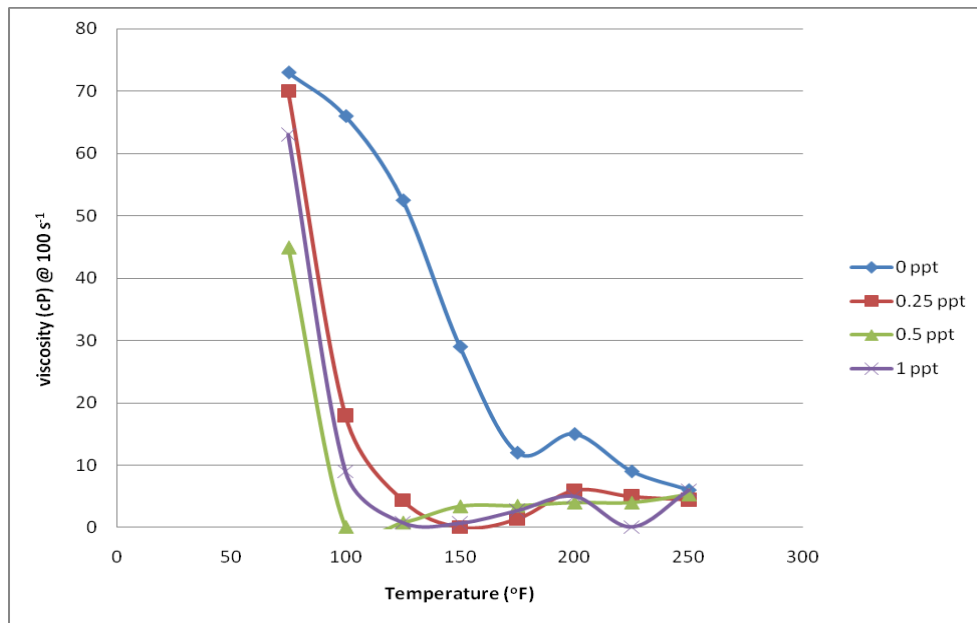


Figure 4.56– Breaker activity curves 30 ppt gel with ammonium persulfate based on temperature

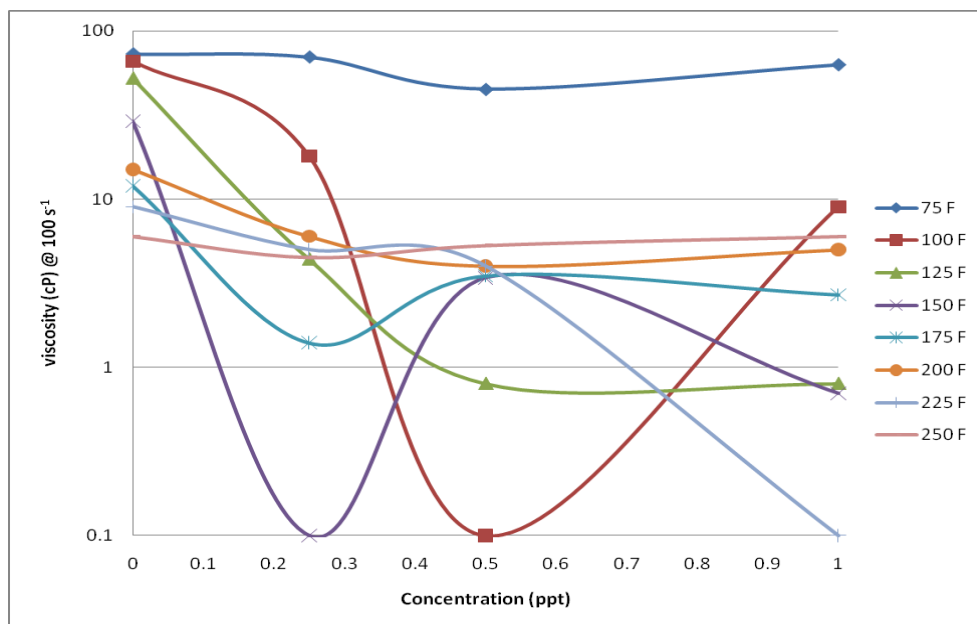


Figure 4.57– Breaker activity curves for 30 ppt gel with ammonium persulfate based on concentration

4.4.2 Magnesium Peroxide

The lowest viscosity values at 100 s^{-1} , taken from the test data, are shown in the Table 4.6. Based on the values in the table, breaker activity curves are presented in Figures 4.58 and 4.59.

Table 4.6- Lowest viscosity values from magnesium peroxide tests with 30 ppt gel

Temperature (°F)	Concentration			
	0 ppt	1 ppt	5 ppt	10 ppt
	Viscosity (cP)			
175	23.5	21	21	12.5
200	15	9.5	7	5.5
225	8.5	3.4	7	6.2
250	6	5.7	4.6	5.2

There was only one concentration of magnesium peroxide tested with the 60 ppt gel, i.e. 1 ppt. The same concentration was also tested for sodium bromate for comparison between the performances of the two breakers. Table 4.7 shows the lowest viscosity values reached in these tests at 100 s^{-1} and Figure 4.60 presents its activity curves.

Table 4.7-Lowest viscosity values from magnesium peroxide tests with 60 ppt gel

Temperature (°F)	Concentration	
	0 ppt	1 ppt
	Viscosity (cP)	
175		145.4
200	73.7	35.6
225	33.1	31.6
250	11	9.3
300	5.2	7.8

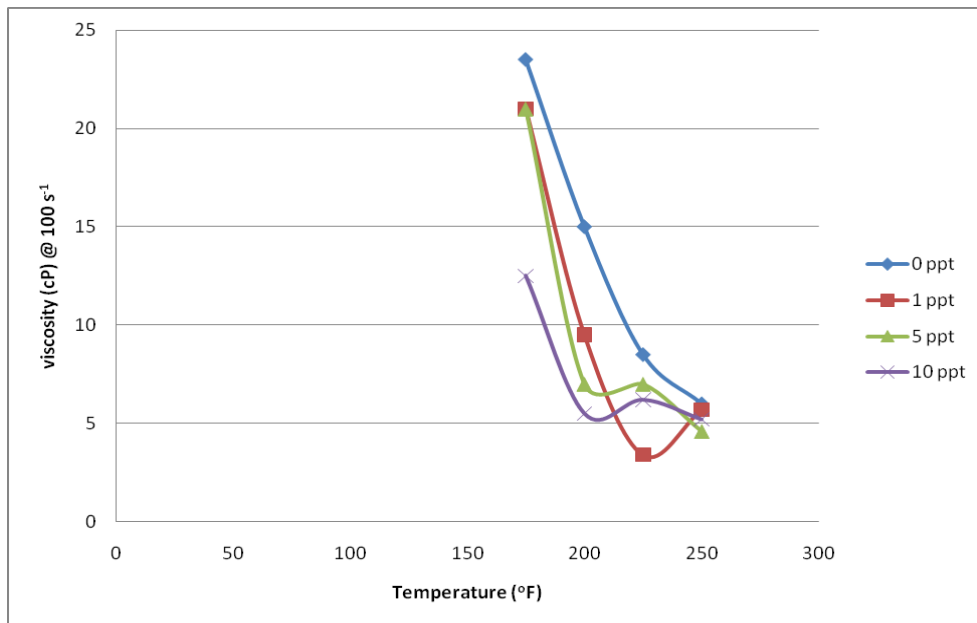


Figure 4.58– Breaker activity curves 30 ppt gel with magnesium peroxide based on temperature

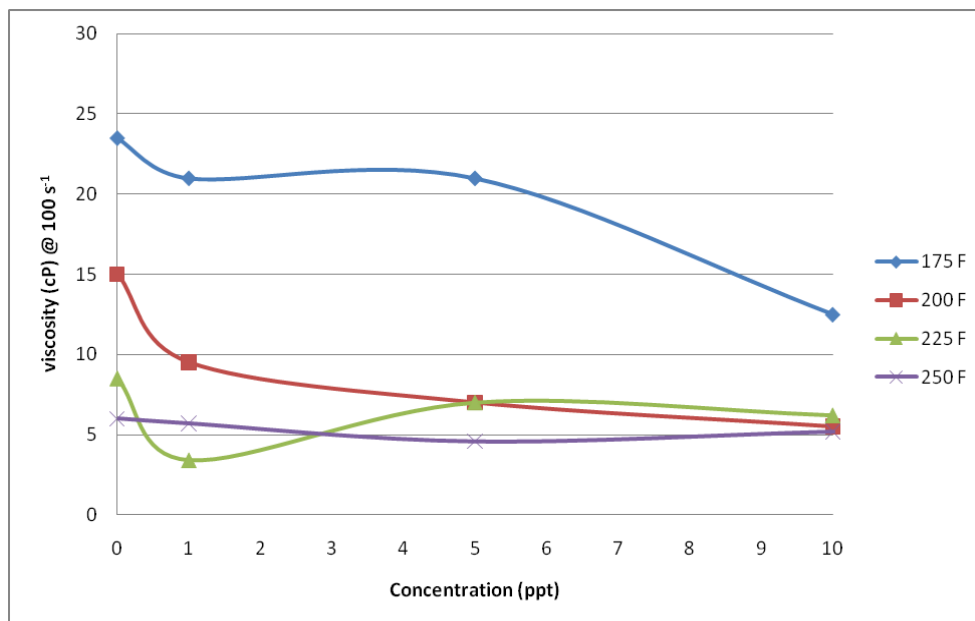


Figure 4.59– Breaker activity curves 30 ppt gel with magnesium peroxide based on concentration

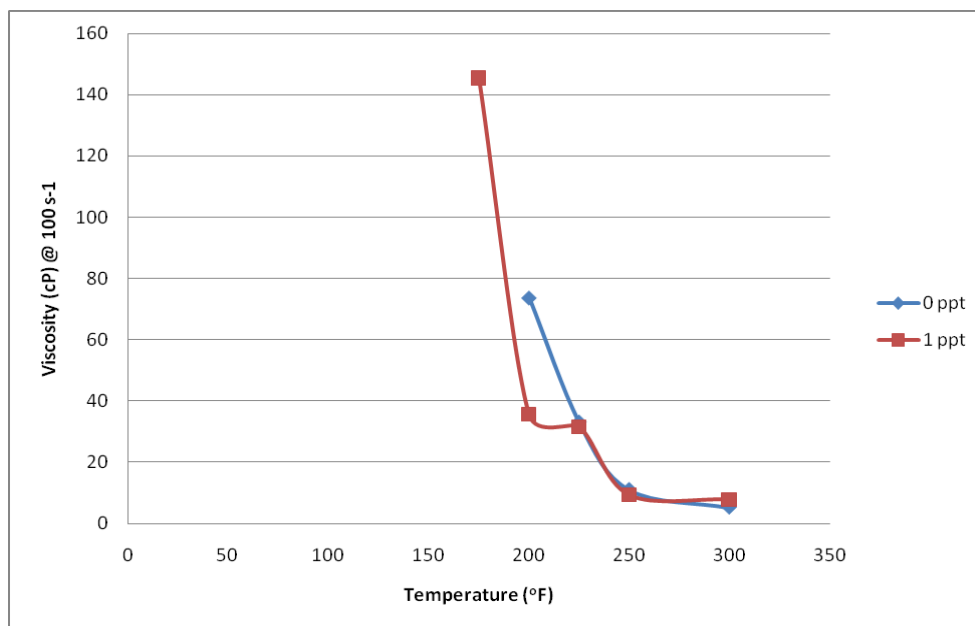


Figure 4.60– Breaker activity curves for 60 ppt gel with magnesium peroxide based on temperature

4.4.3 Sodium Bromate

The lowest viscosity values at 100 s^{-1} , taken from the test data for 30 ppt gels, are shown in the Table 4.8. Based on the values in the table, breaker activity curves are presented in Figure 4.61 and 4.62.

Table 4.8- Lowest viscosity values from sodium bromate tests with 30 ppt gel

Temperature (°F)	Concentration			
	0 ppt	1 ppt	5 ppt	10 ppt
	Viscosity (cp)			
150	33.5	29.2	33.5	27.9
200	14.7	10.7	9.9	9.5
225	8.5	12.9	6.4	23.9
250	6	3	5.6	8.4
275	3.7	3.7	2.6	8.2
300	8	4	4.7	5.4

As mentioned earlier, there was only one concentration of sodium bromate tested with the 60 ppt gel, i.e. 1 ppt. The comparison with magnesium peroxide will be presented later. Table 4.9 below shows the lowest viscosity values reached in these tests with 60 ppt gel and Figure 4.63 presents the activity curves.

Table 4.9- Lowest viscosity values from sodium bromate tests with 60 ppt gel

Temperature (°F)	Concentration	
	0 ppt	1 ppt
	Viscosity (cP)	
200	73.7	62.2
225	33.1	29.2
250	11	8.3
300	5.2	3.9

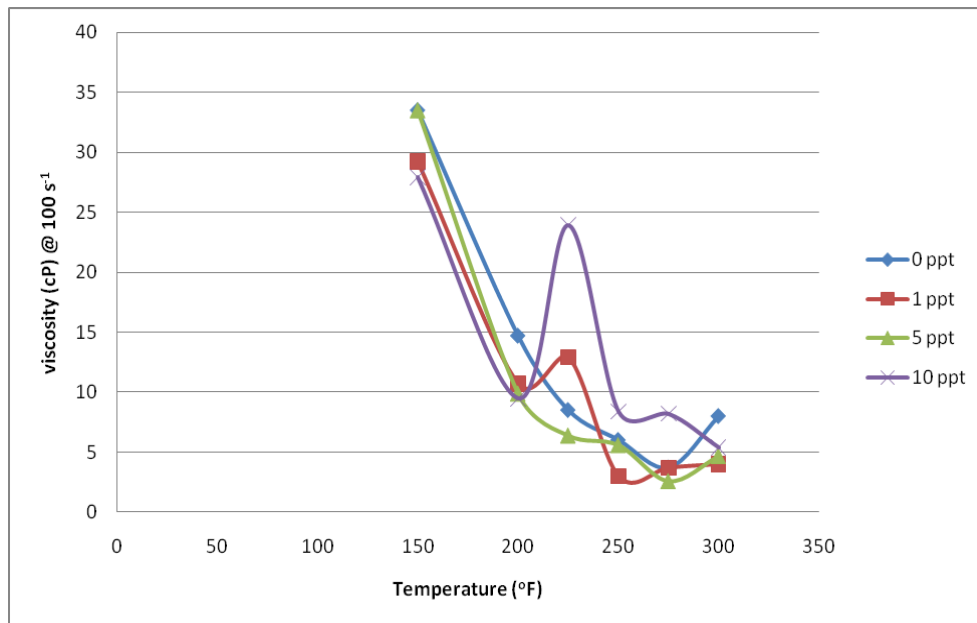


Figure 4.61– Breaker activity curves 30 ppt gel with sodium bromate based on temperature

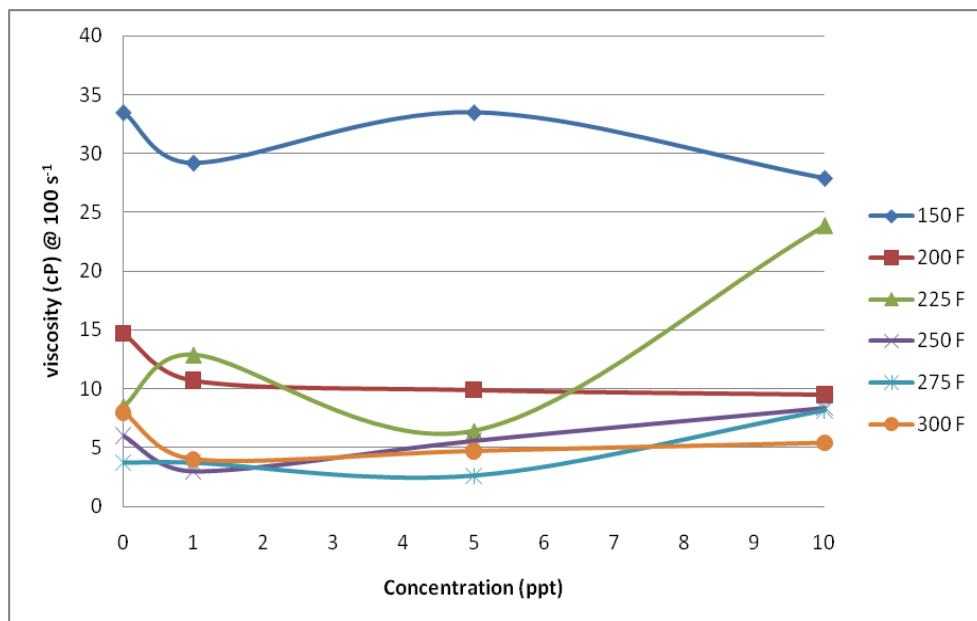


Figure 4.62– Breaker activity curves 30 ppt gel with sodium bromate based on concentration

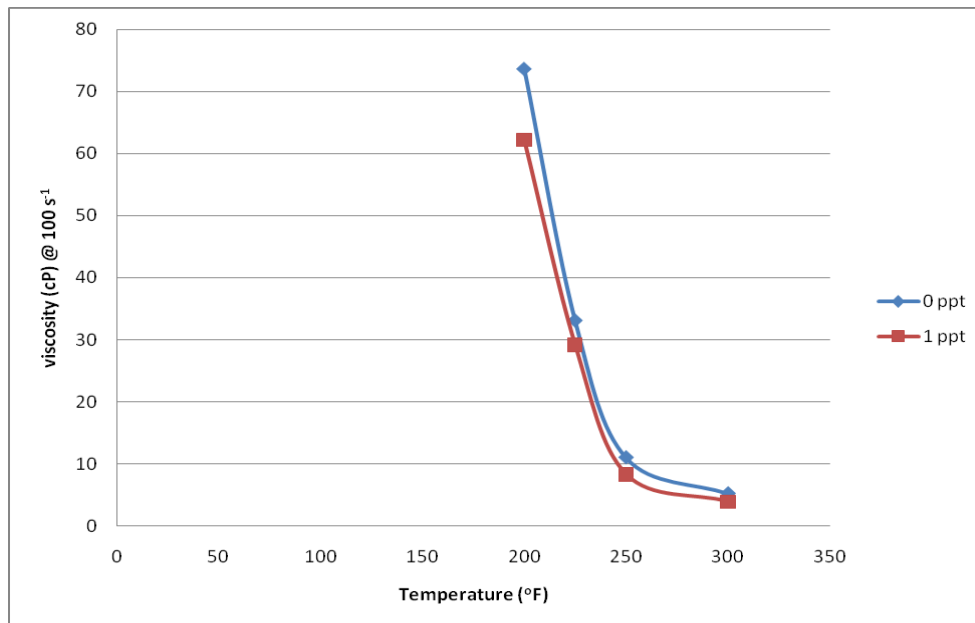


Figure 4.63– Breaker activity curves for 60 ppt gel with sodium bromate based on temperature

4.4.4 Galactomannanase Enzyme

The lowest viscosity values for galactomannanase at 100 s^{-1} , taken from the test data for 30 ppt gels, are shown in the Table 4.10. Based on the values in the table, breaker activity curves are presented in Figure 4.64 and 4.65.

Table 4.10- Lowest viscosity values from galactomannanase tests with 30 ppt gel

Temperature (°F)	Concentration		
	0 ppt	0.5 ppt	1 ppt
	Viscosity (cp)		
75	73	3.7	1.8
100	66	1.6	3.4
125	52.5	4.8	2.8
150	29	2.5	4.8
175	12	4.7	4.2

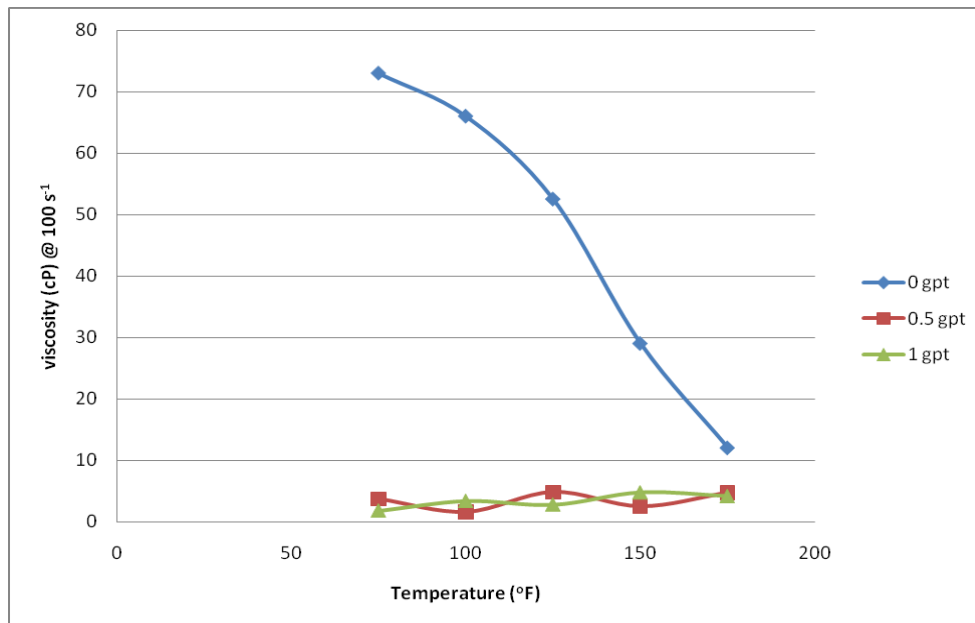


Figure 4.64– Breaker activity curves for 30 ppt gel with galactomannanase based on temperature

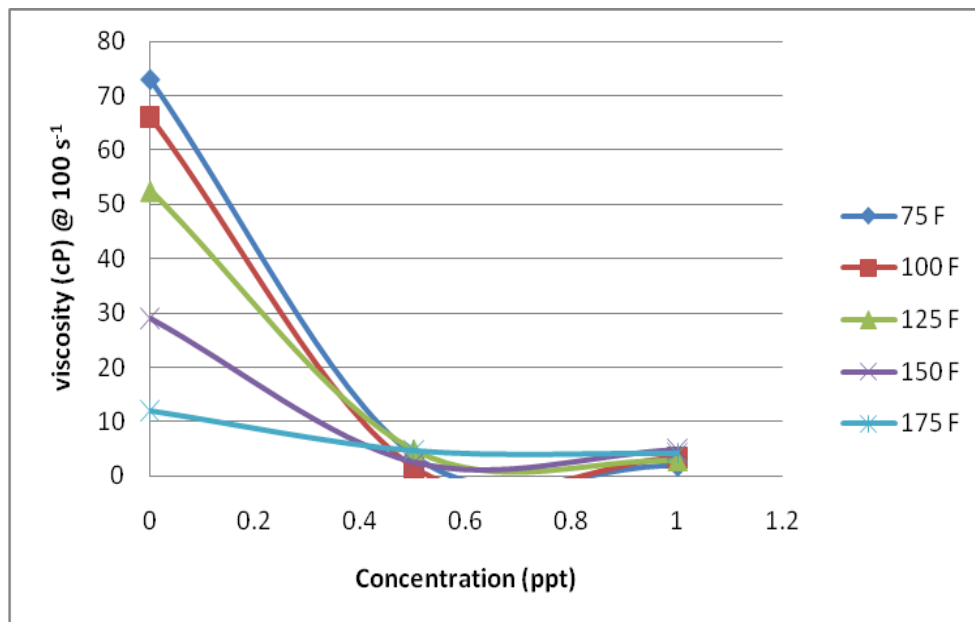


Figure 4.65– Breaker activity curves for 30 ppt gel with galactomannanase based on concentration

4.5 Comparison of Breaker Activity Curves

In this section, breaker activities are compared with each other by means of the breaker activity or ‘S’ curves. Activity curves for breakers tested, at the same concentration, are plotted against each other on a chart. The activity curves for 1 ppt breaker concentration with 30 ppt gel are shown in Figure 4.66.

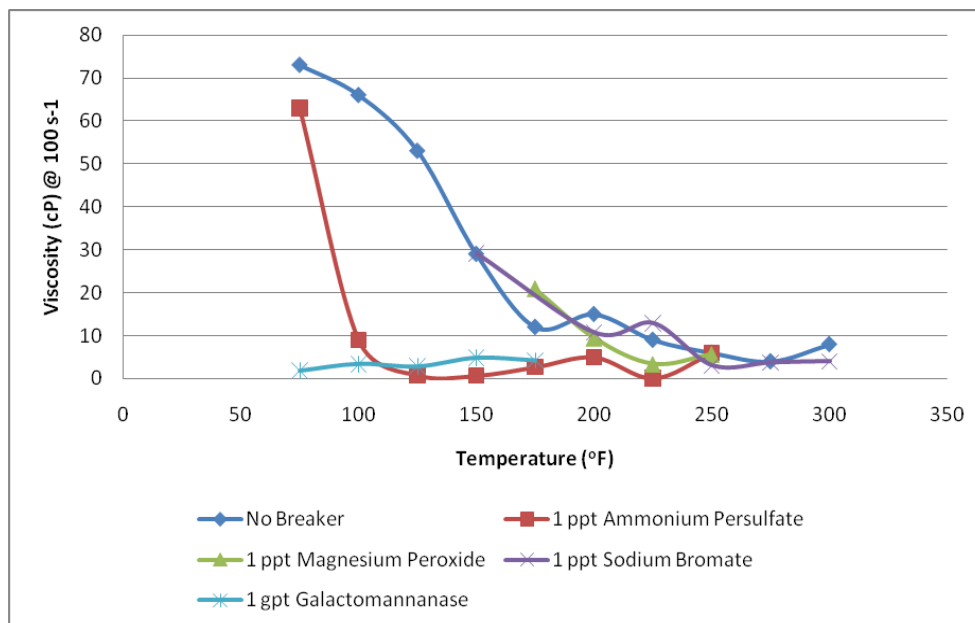


Figure 4.66- Breaker activity curves for different breakers at 1 ppt concentration tested with 30 ppt gels

Similarly, the activity curves for 1 ppt breaker concentration with 60 ppt gel are shown in Figure 4.67

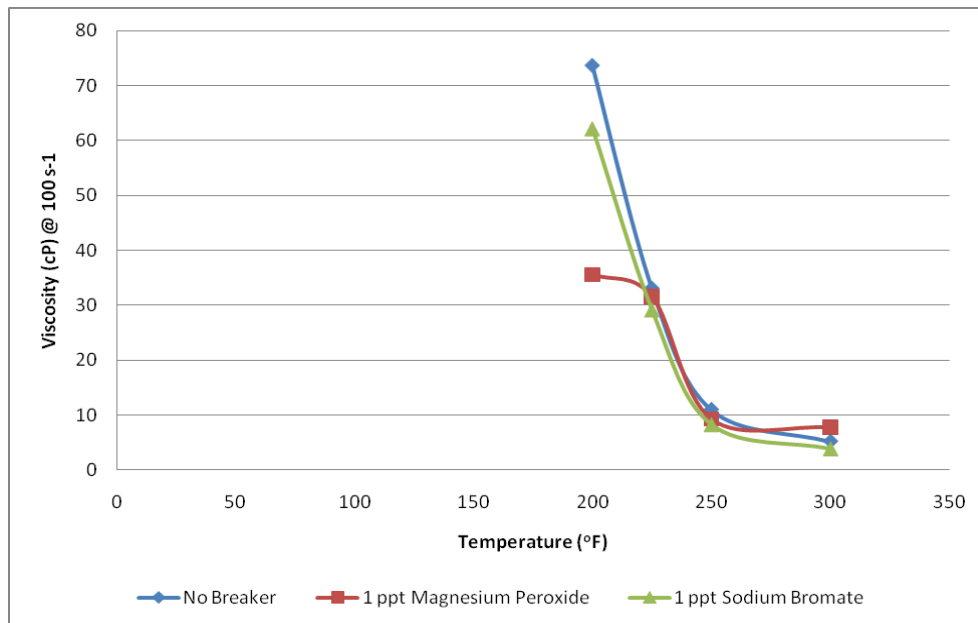


Figure 4.67- Breaker activity curves for different breakers at 1 ppt concentration tested with 60 ppt gels

4.6 Ammonium Persulfate - 24 hour Break Tests

While conducting the room temperature test for ammonium persulfate for the S – curve development, something very interesting was noted. It has been established that breakers are activated by temperature and each breaker has its own working temperature range. The working range for ammonium persulfate is 130 °F – 200 °F. It has been found during literature survey that if the temperature is lower than 125 °F, a breaker catalyst is required to activate ammonium persulfate (Brannon and Tjon-Joe-Pin, 1995). But oddly, during the course of this research, it was found that ammonium persulfate was working at room temperature and degraded the fluid considerably. The tests were repeated and the concentration of ammonium persulfate was also changed, and it was found to be active at room temperature. The figures that follow are the results of 24 hr break tests without breaker, and with various concentrations of ammonium persulfate, Figures 4.68 – 4.73. The shear rate sequence is the same as described earlier, with approximately 10 minutes of constant shear at 100 s^{-1} and then a 5 minute sweep of various shear rates ranging from 17 s^{-1} to 1020 s^{-1} and then back to 17 s^{-1} . This constant shear and sweep cycle keeps on repeating.

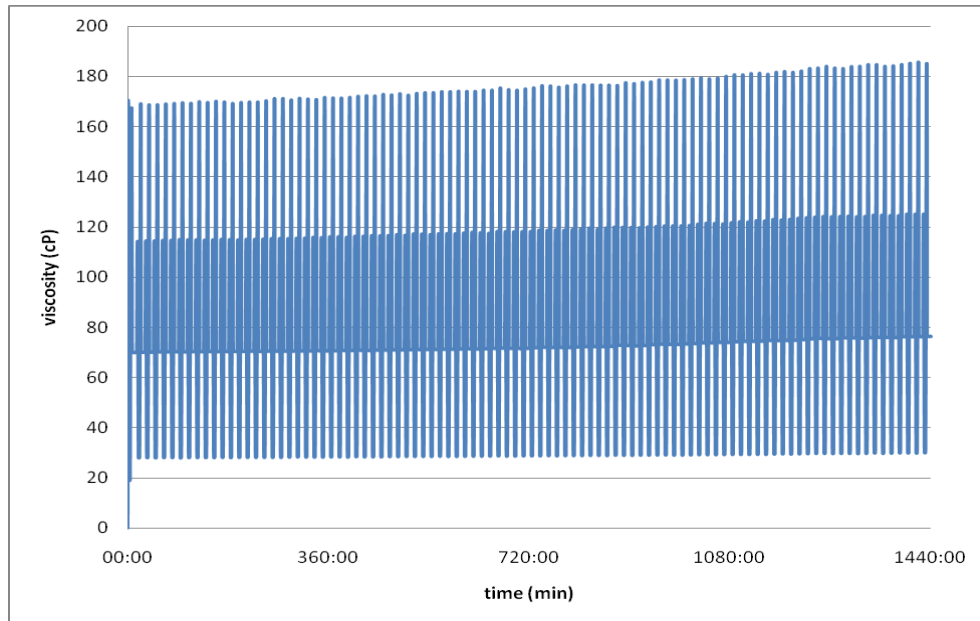


Figure 4.68- 24 hr viscosity profile of 30 ppt gel without any breaker added at room temperature

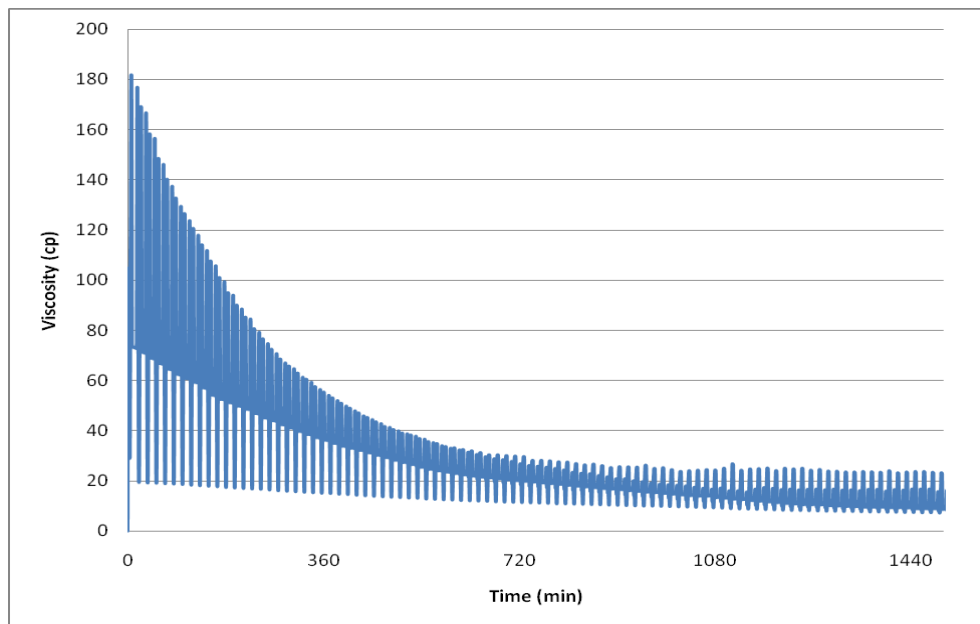


Figure 4.69- 24 hr viscosity profile of 30 ppt gel with 0.25 ppt ammonium persulfate at room temperature

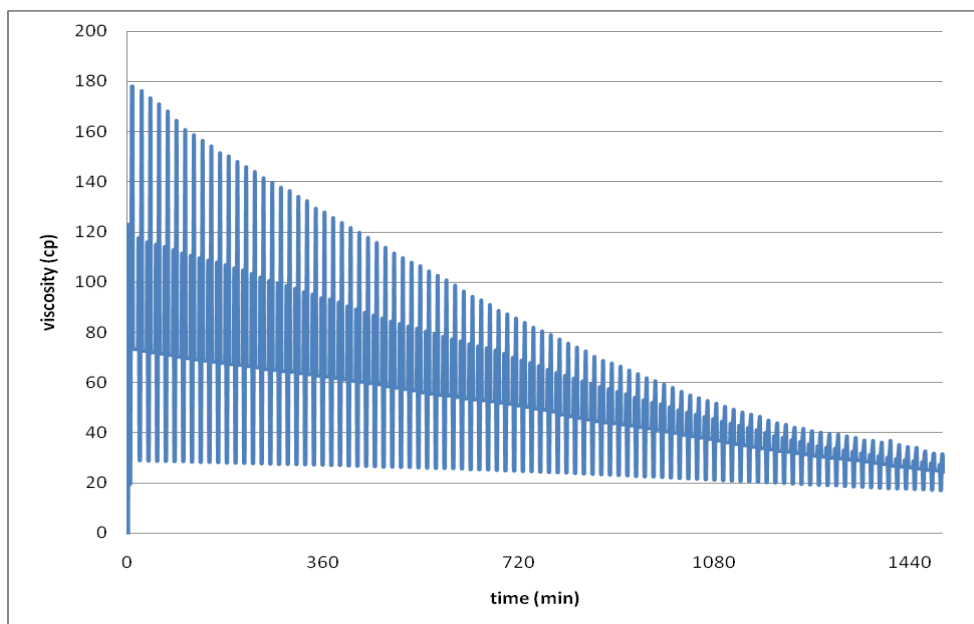


Figure 4.70- 24 hr viscosity profile of 30 ppt gel with 0.5 ppt ammonium persulfate at room temperature

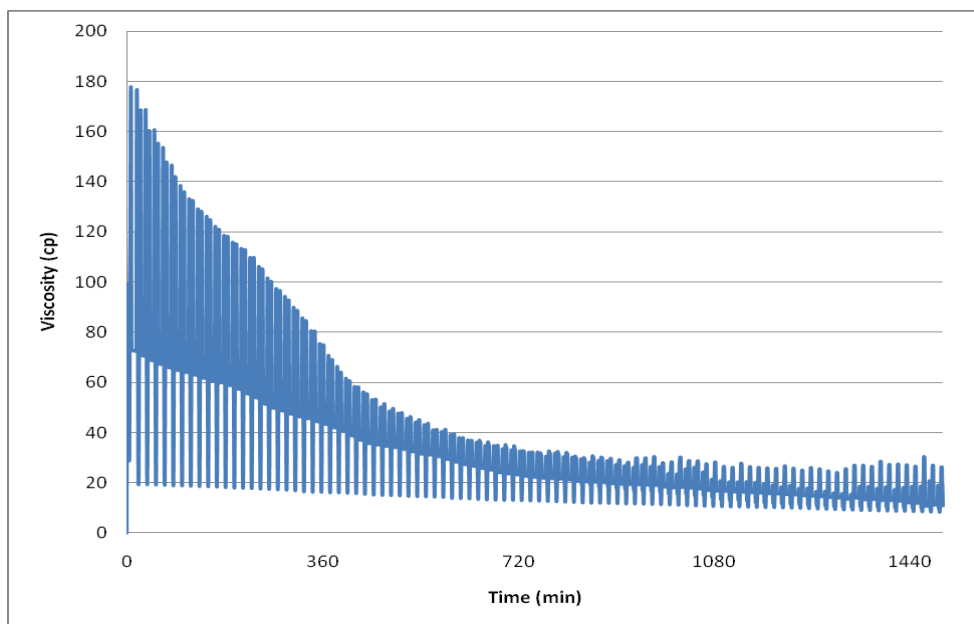


Figure 4.71- 24 hr viscosity profile of 30 ppt gel with 1 ppt ammonium persulfate at room temperature

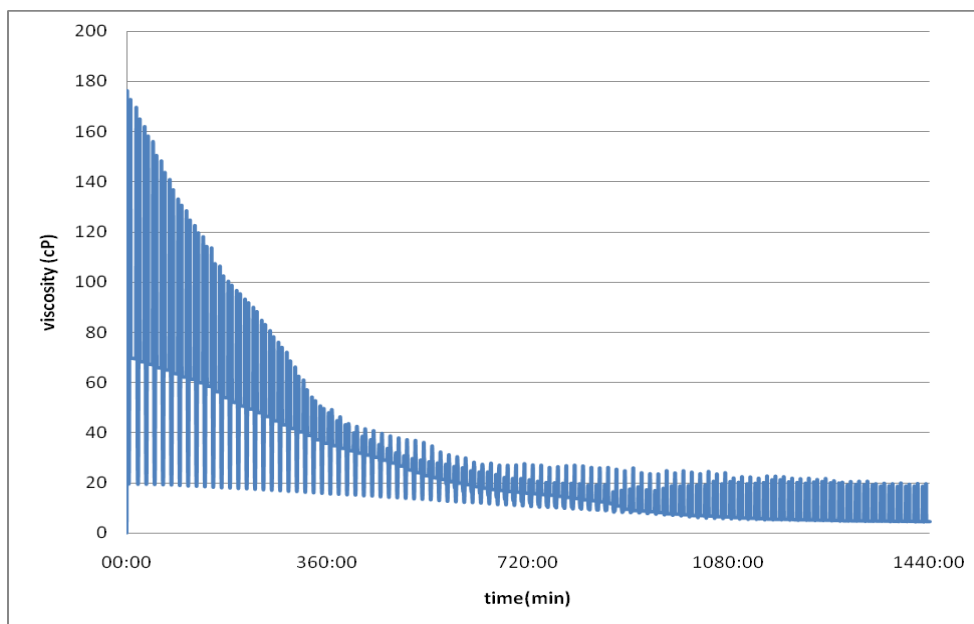


Figure 4.72- 24 hr viscosity profile of 30 ppt gel with 5 ppt ammonium persulfate at room temperature

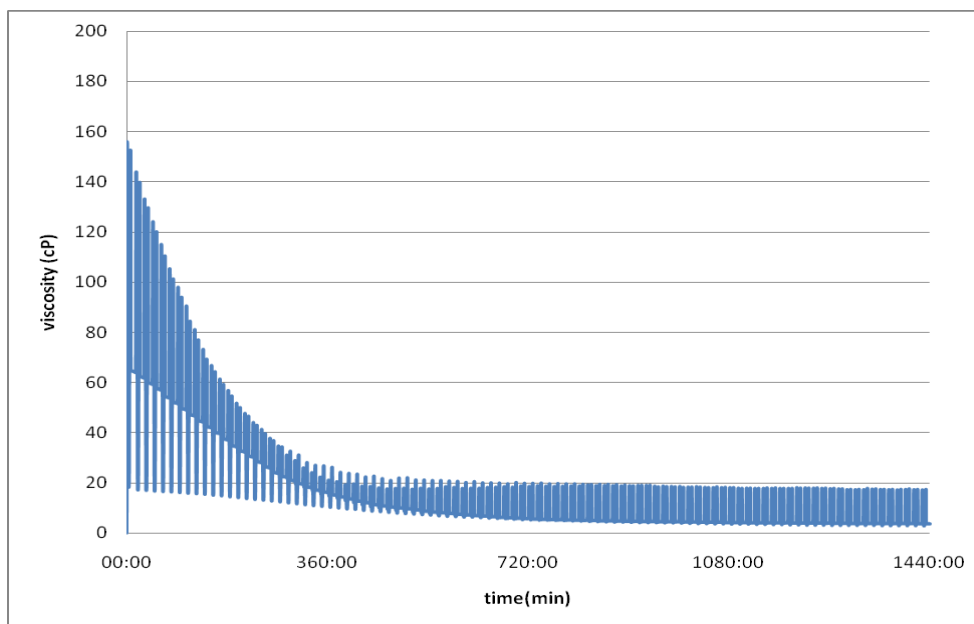


Figure 4.73- 24 hr viscosity profile of 30 ppt gel with 10 ppt ammonium persulfate at room temperature

Based on the 24 hr viscosity tests, an activity curve was also developed for ammonium persulfate at room temperature, shown in Figure 4.74.

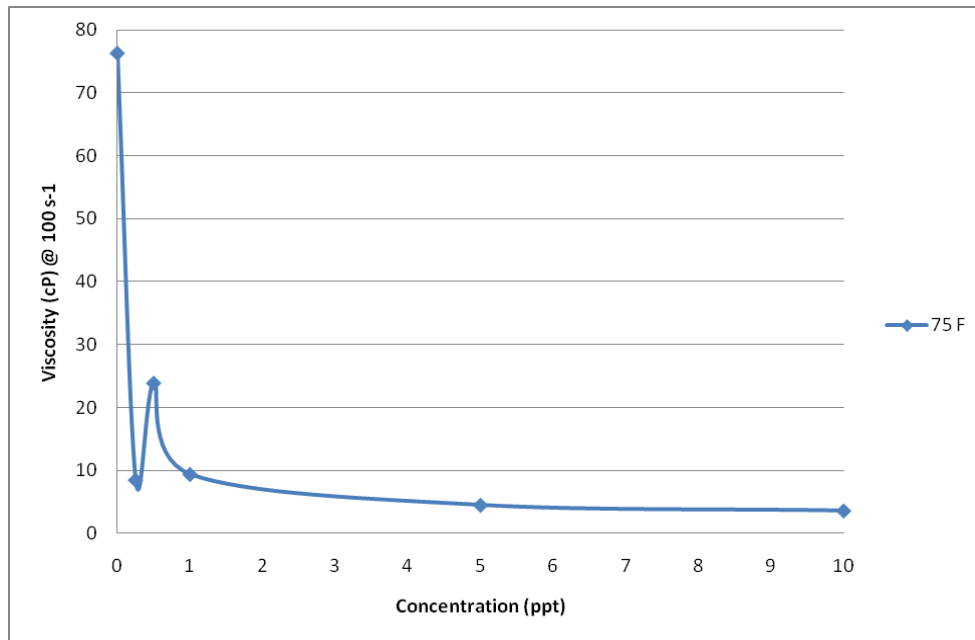


Figure 4.74- Breaker activity curve for 24 hr ammonium persulfate test with 30 ppt guar gel at room temperature

4.7 Residue-After-Break (RAB) Test

The RAB test was conducted using three breakers which have similar working ranges. Ammonium persulfate, sodium persulfate and galactomannanase enzyme were tested. The RAB test, as mentioned earlier, determines the amount of unbroken gel and residue in the fluid after it has been broken. All three breakers were tested with 30 ppt gels at two different working temperatures, i.e 125 °F and 150 °F. The results are shown in Tables 4.11 – 4.16.

Tests at 125 °F

Table 4.11- Residue generated using ammonium persulfate at 125 °F

Conc. (ppt)	sample vol (ml)	wt. of polymer (g)	wt. of filter paper		wt. of residue after break (g)	%RAB
			before (g)	after (g)		
10	200	0.72	0.2794	0.3275	0.0481	6.680556
5	200	0.72	0.2579	0.3133	0.0554	7.694444
1	200	0.72	0.5366	1.0722	0.5356	74.38889
0	200	0.72	0.534	1.1091	0.5751	79.875

Table 4.12- Residue generated using sodium persulfate at 125 °F

Conc. (ppt)	sample vol (ml)	wt. of polymer (g)	wt. of filter paper		wt. of residue after break (g)	%RAB
			empty (g)	final (g)		
10	200	0.72	0.2807	0.327	0.0463	6.430556
5	200	0.72	0.258	0.3093	0.0513	7.653
1	200	0.72	0.5304	0.789	0.2586	35.91667
0	200	0.72	0.534	1.1091	0.5751	79.875

Table 4.13- Residue generated using galactomannanase at 125 °F

Conc.	sample vol	wt. of polymer	wt. of filter paper		wt. of residue after break	%RAB
			empty (g)	final (g)		
(gpt)	(ml)	(g)	(g)	(g)	(g)	
1	200	0.72	0.5123	0.5529	0.0406	5.638889
0.5	200	0.72	0.5203	0.5819	0.0616	8.555556
0	200	0.72	0.534	1.1091	0.5751	79.875

Tests at 150 °F**Table 4.14- Residue generated using ammonium persulfate at 150 °F**

Conc.	sample vol	wt. of polymer	wt. of filter paper		wt. of residue after break	%RAB
			empty (g)	final (g)		
(ppt)	(ml)	(g)	(g)	(g)	(g)	
10	200	0.72	0.1386	0.1773	0.0387	5.375
5	200	0.72	0.2607	0.2985	0.0378	5.25
2	200	0.72	0.5377	0.5728	0.0351	4.875
1	200	0.72	0.2565	0.305	0.0485	6.736111
0.5	200	0.72	0.5306	0.8515	0.3209	44.56944
0	200	0.72	0.538	1.079	0.541	75.13889

Table 4.15- Residue generated using sodium persulfate at 150 °F

Conc.	sample vol	wt. of polymer	wt. of filter paper		wt. of residue after break	%RAB
			empty (g)	final (g)		
(ppt)	(ml)	(g)	(g)	(g)	(g)	
10	200	0.72	0.128	0.1623	0.0343	4.763889
5	200	0.72	0.5419	0.5842	0.0423	5.875
2	200	0.72	0.2562	0.3057	0.0495	6.875
1	200	0.72	0.2529	0.2927	0.0398	5.527778
0.5	200	0.72	0.5309	0.7293	0.1984	27.55556
0	200	0.72	0.538	1.079	0.541	75.13889

Table 4.16- Residue generated using galactomannanase at 150 °F

Conc (gpt)	sample vol (ml)	wt. of polymer (g)	wt. of filter paper		wt. of residue after break (g)	%RAB
			empty (g)	final (g)		
1	200	0.72	0.5407	0.5923	0.0516	7.166667
0.5	200	0.72	0.5299	0.572	0.0421	5.847222
0	200	0.72	0.538	1.079	0.541	75.13889

The results generally show an expected trend with lower concentrations giving higher residue values. Galactomannanase enzyme demonstrates lower residue values compared to the oxidizers. The lower concentrations for both oxidizers (0.5 ppt and 1 ppt), yield very high residue values. The comparison can be drawn from the residue generated for the sample without any breaker in it. The sample without any breaker at 125 °F shows almost 80% as unbroken gel and residue percentage while the sample with no breaker tested at 150 °F yields slightly less residue-unbroken polymer at 75%.

5. CONCLUSIONS AND RECOMMENDATION

The main objective of this research project was to conduct a comprehensive study to evaluate breaker activity as a function of time and temperature. An extensive amount of testing was done with three oxidative breakers (ammonium persulfate, magnesium peroxide, sodium bromate) and one enzymatic breaker (galactomannanase). A wide range of breaker concentrations and temperatures were used. Viscosity measurements were done to evaluate breaker activity. The amount of unbroken gel/residue was determined for three breakers (ammonium persulfate, sodium persulfate and galactomannanase) which are used for the same temperature range in the field. The following conclusions can be drawn from this study:

1. Viscosity break profiles have been developed for the breakers studied based on breaker concentration and temperature for 30 ppt guar gels, and some 60 ppt gels. These break profiles present a comparison between the concentrations of the breaker at all the tested temperatures and provide a guideline for designing fracturing fluids with specific break times using these breakers.
2. Early time viscosity data was plotted from the viscosity profiles, showing the initial 10 minutes of break time. These data show that the greatest reduction in viscosity occurs during the first few minutes of the test. It helps evaluate the breaker performance for a very short break time. The

data showed that a few tested breaker concentrations were slow in reducing the viscosity in the initial few minutes but did break the gel over a longer period of time.

3. Based on the lowest viscosity achieved by every breaker at each tested concentration and temperature, breaker activity curves or S – curves were developed. These curves provide a clear comparison of performance between different concentrations of the same breaker, as well as the same concentrations of different breakers, tested at the same temperatures. These S-curves are a simple tool that can be used to choose the best concentration for a particular breaker while designing a fracturing fluid, and they can also help choose a breaker best suited for the job from the different breakers tested. From the 1ppt S-curves for the breakers tested, ammonium persulfate was found to provide the greatest reduction in viscosity over the range of 125 °F to 225 °F. Magnesium peroxide was better in degrading the gel compared to sodium bromate between 200 °F and 240 °F. While sodium bromate was more effective from 250 °F. Galactomannanase was more effective than ammonium persulfate at temperatures close to ambient temperature.
4. Ammonium persulfate was the most extensively tested breaker during this study. It is one of the most common breakers used in the industry. It is supposed to be inactive below 125 °F without the use of a breaker catalyst. An interesting observation came about while testing this breaker.

It was found to be active at room temperature. 24 hr break rheology tests were conducted with various concentrations, and in all these tests ammonium persulfate was found to degrade the gel viscosity. Increase in concentration showed more degradation in viscosity.

5. Residue-after-break tests showed the amount of residue generated by the three breakers tested. The highest concentrations of the three breakers tested all yielded residues in the range of 5% - 7%. Galactomannanase was found to produce less residue than the ammonium and sodium persulfate breakers especially at lower concentrations (0.5 ppt, 1ppt of oxidizer). The amount of residue for the oxidizers for the lower concentrations was very high. These tests indicate that the enzymatic breaker can provide a cleaner, more homogeneous break of the polymer compared to oxidative breakers, used at the same temperatures. Higher concentrations are required for oxidative breakers to achieve the same results as the enzyme at the same temperature.

REFERENCES

- Alderman, E.N. 1970. Super Thick Fluids Provide New Answers to Old Fracturing Problems. Paper presented at the SPE Practical Aspects of Improved Recovery Techniques Symposium, Fort Worth, Texas. 8-9 March. American Institute of Mining, Metallurgical and Petroleum Engineers 2852-MS.
- Almond, S.W. 1982. Factors Affecting Gelling Agent Residue under Low Temperature Conditions. Paper presented at the SPE Formation Damage Control Symposium, Lafayette, Louisiana, 24-25 March. Society of Petroleum Engineers of AIME 10658-MS.
- Almond, S.W. and Bland, W.E. 1984. The Effect of Break Mechanism on Gelling Agent Residue and Flow Impairment in 20/40 Mesh Sand. Paper presented at the SPE Formation Damage Control Symposium, Bakersfield, California, 13-14 February. Society of Petroleum Engineers of AIME 12485-MS.
- Brannon, H.D. and Pulsinelli, R.J. 1992. Breaker Concentrations Required to Improve the Permeability of Proppant Packs Damaged by Concentrated Linear and Borate-Crosslinked Fracturing Fluids. *SPE Production Engineering* 7(4): 338-342. DOI: 10.2118/21583-PA.
- Brannon, H.D. and Tjon-Joe-Pin, R.M. 1994. Biotechnological Breakthrough Improves Performance of Moderate to High-Temperature Fracturing Applications. Paper presented at the SPE Annual Technical Conference and Exhibition, New Orleans, Louisiana, 25-28 September. Society of Petroleum Engineers 28513-MS.
- Brannon, H.D. and Tjon-Joe-Pin, R.M. 1995. Characterization of Breaker Efficiency Based upon Size Distribution of Polymeric Fragments. Paper presented at the SPE Annual Technical Conference and Exhibition, Dallas, Texas, 22-25 October. Society of Petroleum Engineers 30492-MS.
- Craig, D.P., Fan, Y. and Holditch, S.A. 1992. Viscous Property Measurement of Delayed Titanate Crosslinked Gels Containing Oxidative Breakers. Paper presented at the SPE Rocky Mountain Regional Meeting, Casper, Wyoming, 18-21 May. Society of Petroleum Engineers 24340-MS.
- DeVine, C.S., Tjon-Joe-Pin, R.M., Rickards, A.R. and Carr, M. 1998. Polymeric Damage and a Cost Effective Method for Damage Removal from Wells. Paper presented at the SPE Annual Technical Conference and Exhibition, New Orleans, Louisiana, 27-30 September. Society of Petroleum Engineers 49249-MS.

- Economides, M.J. 1987. How to Engineer a Fracturing Treatment. *SPE Journal of Petroleum Technology* **39**(11): 1343-1345. DOI: 10.2118/17176-PA
- Economides, M.J. and Nolte, K.G. 2000. *Reservoir Stimulation*: Wiley. 3rd edition. ISBN.
- Economides, M.J. 2007. *Modern Fracturing: Enhancing Natural Gas Production*. Gulf Publishing Co. Original edition. ISBN.
- Gall, B.L. and Raible, C.J. 1985. Molecular Size Studies of Degraded Fracturing Fluid Polymers. Paper presented at the SPE Oilfield and Geothermal Chemistry Symposium, Phoenix, Arizona, 9-11 March. Society of Petroleum Engineers 13566-MS.
- Harris, P.C. 1993. Chemistry and Rheology of Borate-Crosslinked Fluids at Temperatures to 300°F. *Journal of Petroleum Technology* **45**(3): 264-269. DOI: 10.2118/24339-PA.
- Nasr-El-Din, H.A., Al-Mohammed, A.M, Al-Aamri, A.D. and Al-Fuwaires, O.A. 2007. A Study of Gel Degradation, Surface Tension, and Their Impact on the Productivity of Hydraulically Fractured Gas Wells. Paper presented at the SPE Annual Technical Conference and Exhibition, Anaheim, California, 11-14 November. Society of Petroleum Engineers 109690-MS.
- Rae, P. and di Lullo, G. 1996. Fracturing Fluids and Breaker Systems - A Review of the State-of-the-Art. Paper presented at the SPE Eastern Regional Meeting, Columbus, Ohio, 23-25 October. Society of Petroleum Engineers 37359-MS.
- Roodhart, L.P., Kulper, T.O.H. and Davies, D.R. 1988. Proppant-Pack and Formation Impairment During Gas-Well Hydraulic Fracturing. *SPE Production Engineering* **3**(4): 438-444. DOI: 10.2118/15629-PA.

APPENDIX A

FLOW PARAMETERS n' and K

Table A.1 – Flow parameters n' and K for 30 ppt guar gel without breaker at 75 °F

Elapsed Time	n'	K
(h:mm)		(lbf-s ^{n'} /ft ²)
0:00	0.4508	0.0193
0:17	0.4487	0.0197
0:32	0.4504	0.0196
0:47	0.4508	0.0195
1:02	0.4527	0.0193
1:17	0.4540	0.0191
1:32	0.4558	0.0189
1:47	0.4578	0.0187
2:02	0.4588	0.0185
2:17	0.4601	0.0183
2:32	0.4603	0.0183
2:47	0.4618	0.0181
3:02	0.4609	0.0181
3:17	0.4637	0.0179
3:32	0.4652	0.0177
3:47	0.4655	0.0176
4:02	0.4681	0.0173
4:17	0.4693	0.0172
4:32	0.4707	0.0170
4:47	0.4723	0.0168
5:02	0.4745	0.0166
5:17	0.4759	0.0165
5:32	0.4769	0.0163
5:47	0.4792	0.0161
6:02	0.4795	0.0161

Table A.2 – Flow parameters n' and K for 30 ppt guar gel without breaker at 100 °F

Elapsed Time (h:mm)	n'	K (lbf-sⁿ/ft²)
0:00	0.4551	0.0172
0:17	0.4839	0.0130
0:32	0.4777	0.0139
0:47	0.4754	0.0141
1:02	0.4755	0.0142
1:17	0.4747	0.0142
1:32	0.4745	0.0143
1:47	0.4748	0.0143
2:02	0.4742	0.0144
2:17	0.4741	0.0143
2:32	0.4735	0.0145
2:47	0.4728	0.0145
3:02	0.4728	0.0145
3:17	0.4731	0.0145
3:32	0.4734	0.0146
3:47	0.4717	0.0147
4:02	0.4724	0.0147
4:17	0.4733	0.0147
4:32	0.4726	0.0148
4:47	0.4736	0.0147
5:02	0.4734	0.0148
5:17	0.4722	0.0149
5:32	0.4724	0.0149
5:47	0.4726	0.0149
6:02	0.4722	0.0150

Table A.3 – Flow parameters n' and K for 30 ppt guar gel without breaker at 125 °F

Elapsed Time	n'	K
(h:mm)		(lbf-sⁿ/ft²)
0:00	0.4522	0.0162
0:17	0.5147	0.0088
0:32	0.5111	0.0091
0:47	0.5111	0.0092
1:02	0.5105	0.0093
1:17	0.5109	0.0093
1:32	0.5115	0.0093
1:47	0.5118	0.0093
2:02	0.5118	0.0093
2:17	0.5119	0.0094
2:32	0.5117	0.0094
2:47	0.5117	0.0094
3:02	0.5136	0.0094
3:17	0.5125	0.0095
3:32	0.5132	0.0095
3:47	0.5131	0.0095
4:02	0.5137	0.0095
4:17	0.5129	0.0096
4:32	0.5126	0.0097
4:47	0.5136	0.0096
5:02	0.5134	0.0097
5:17	0.5131	0.0097
5:32	0.5127	0.0098
5:47	0.5129	0.0098
6:02	0.5134	0.0098

Table A.4 – Flow parameters n' and K for 30 ppt guar gel without breaker at 150 °F

Elapsed Time	n'	K
(h:mm)		(lbf-sⁿ/ft²)
0:00	0.4608	0.0152
0:17	0.5574	0.0059
0:32	0.5692	0.0054
0:47	0.5729	0.0053
1:02	0.5788	0.0051
1:17	0.5872	0.0048
1:32	0.5937	0.0046
1:47	0.6015	0.0044
2:02	0.6068	0.0042
2:17	0.6117	0.0040
2:32	0.6161	0.0039
2:47	0.6195	0.0038
3:02	0.6224	0.0037
3:17	0.6239	0.0036
3:32	0.6258	0.0036
3:47	0.6284	0.0035
4:02	0.6306	0.0034
4:17	0.6330	0.0033
4:32	0.6358	0.0033
4:47	0.6390	0.0032
5:02	0.6436	0.0031
5:17	0.6457	0.0030
5:32	0.6453	0.0030
5:47	0.6503	0.0029
6:02	0.6524	0.0028

Table A.5 – Flow parameters n' and K for 30 ppt guar gel without breaker at 175 °F

Elapsed Time	n'	K
(h:mm)		(lbf-sⁿ/ft²)
0:00	0.4571	0.0163
0:17	0.5872	0.0041
0:32	0.6421	0.0027
0:47	0.6455	0.0025
1:02	0.6508	0.0024
1:17	0.6533	0.0023
1:32	0.6671	0.0020
1:47	0.6709	0.0019
2:02	0.6719	0.0019
2:17	0.6780	0.0017
2:32	0.6877	0.0016
2:47	0.6830	0.0016
3:02	0.6956	0.0014
3:17	0.7002	0.0014
3:32	0.7085	0.0013
3:47	0.7145	0.0012
4:02	0.7098	0.0012
4:17	0.7074	0.0012
4:32	0.7037	0.0012
4:47	0.7084	0.0011
5:02	0.7289	0.0010
5:17	0.7245	0.0010
5:32	0.7051	0.0011
5:47	0.7077	0.0011
6:02	0.6943	0.0011

Table A.6 – Flow parameters n' and K for 30 ppt guar gel with 0.25 ppt ammonium persulfate at 75 °F

Elapsed Time	n'	K
(h:mm)		(lbf-sⁿ/ft²)
0:00	0.4527	0.0190
0:17	0.4543	0.0188
0:32	0.4553	0.0186
0:47	0.4566	0.0184
1:02	0.4586	0.0181
1:17	0.4590	0.0180
1:32	0.4606	0.0178
1:47	0.4618	0.0177
2:02	0.4636	0.0175
2:17	0.4654	0.0173
2:32	0.4671	0.0171
2:47	0.4689	0.0169
3:02	0.4698	0.0167
3:17	0.4710	0.0166
3:32	0.4724	0.0164
3:47	0.4745	0.0162
4:02	0.4756	0.0161
4:17	0.4776	0.0159
4:32	0.4808	0.0156
4:47	0.4818	0.0155
5:02	0.4835	0.0153
5:17	0.4848	0.0152
5:32	0.4870	0.0150
5:47	0.4882	0.0148
6:02	0.4885	0.0147

Table A.7 – Flow parameters n' and K for 30 ppt guar gel with 0.25 ppt ammonium persulfate at 100 °F

Elapsed Time	n'	K
(h:mm)		(lbf-sⁿ/ft²)
0:00	0.5673	0.0077
0:17	0.7139	0.0027
0:32	0.7152	0.0027
0:47	0.7348	0.0024
1:02	0.7644	0.0020
1:17	0.8022	0.0016
1:32	0.8425	0.0013
1:47	0.8825	0.0010
2:02	0.9370	0.0007
2:17	1.0032	0.0005
2:32	1.1060	0.0003
2:47	0.9839	0.0005
3:02	0.7784	0.0015
3:17	0.7991	0.0013
3:32	0.8215	0.0011
3:47	0.8455	0.0009
4:02	0.8637	0.0008
4:17	0.8877	0.0007
4:32	0.9113	0.0006
4:47	0.9375	0.0005
5:02	0.9641	0.0004
5:17	0.9959	0.0003
5:32	1.0220	0.0003
5:47	1.0655	0.0002
6:02	1.1126	0.0002

Table A.8 – Flow parameters n' and K for 30 ppt guar gel with 0.25 ppt ammonium persulfate at 125 °F

Elapsed Time	n'	K
(h:mm)		(lbf-s^{n'}/ft²)
0:00	0.4708	0.0147
0:17	0.5999	0.0037
0:32	0.7321	0.0014
0:47	0.7632	0.0009
1:02	0.7591	0.0008
1:17	0.6522	0.0011
1:32	0.6193	0.0012
1:47	0.5895	0.0012
2:02	0.5365	0.0014
2:17	0.5067	0.0016
2:32	0.4794	0.0017
2:47	0.4766	0.0016
3:02	0.4532	0.0017
3:17	0.4132	0.0020
3:32	0.3878	0.0021
3:47	0.3597	0.0024
4:02	0.3404	0.0026
4:17	0.3164	0.0029
4:32	0.2962	0.0031
4:47	0.3140	0.0026
5:02	0.2833	0.0030
5:17	0.2720	0.0033
5:32	0.2660	0.0033
5:47	0.2515	0.0035
6:02	0.2372	0.0038

Table A.9 – Flow parameters n' and K for 30 ppt guar gel with 0.25 ppt ammonium persulfate at 150 °F

Elapsed Time	n'	K
(h:mm)		(lbf-s^{n'}/ft²)
0:00	0.7061	0.0033
0:17	1.0414	0.0001
0:32	2.7111	0.0000*

*Instrument limit reached.

Table A.10 – Flow parameters n' and K for 30 ppt guar gel with 0.25 ppt ammonium persulfate at 175 °F

Elapsed Time (h:mm)	n'	K (lbf-s ⁿ /ft ²)
0:00	0.4655	0.0151
0:17	0.2729	0.0013
0:32	0.2427	0.0011
0:47	0.2197	0.0013
1:02	0.2080	0.0014
1:17	0.1955	0.0015
1:32	0.1916	0.0016
1:47	0.1776	0.0017
2:02	0.1805	0.0017
2:17	0.1809	0.0017
2:32	0.1696	0.0018
2:47	0.1852	0.0016
3:02	0.1898	0.0016
3:17	0.2021	0.0014
3:32	0.1872	0.0016
3:47	0.1823	0.0017
4:02	0.1978	0.0015
4:17	0.1872	0.0016
4:32	0.1721	0.0018
4:47	0.1790	0.0017
5:02	0.1764	0.0017
5:17	0.2414	0.0011
5:32	0.2197	0.0013
5:47	0.2418	0.0011
6:02	0.2146	0.0013

Table A.11 – Flow parameters n' and K for 30 ppt guar gel with 0.5 ppt ammonium persulfate at 75 °F

Elapsed Time (h:mm)	n'	K (lbf-s ⁿ /ft ²)
0:00	0.4518	0.0181
0:17	0.4586	0.0172
0:32	0.4654	0.0164
0:47	0.4722	0.0156
1:02	0.4821	0.0146
1:17	0.4918	0.0136
1:32	0.5018	0.0127
1:47	0.5160	0.0116
2:02	0.5238	0.0110
2:17	0.5316	0.0105
2:32	0.5392	0.0099
2:47	0.5494	0.0092
3:02	0.5589	0.0087
3:17	0.5670	0.0081
3:32	0.5726	0.0078
3:47	0.5792	0.0074
4:02	0.5834	0.0072
4:17	0.5940	0.0067
4:32	0.6014	0.0064
4:47	0.6055	0.0061
5:02	0.6111	0.0058
5:17	0.6154	0.0056
5:32	0.6220	0.0054
5:47	0.6277	0.0051
6:02	0.6342	0.0049

Table A.12 – Flow parameters n' and K for 30 ppt guar gel with 0.5 ppt ammonium persulfate at 100 °F

Elapsed Time (h:mm)	n'	K (lbf-s ⁿ /ft ²)
0:00	0.6045	0.0060
0:17	1.1167	0.0003
0:32	1.4447	0.0000
0:47	0.8897	0.0007
1:02	0.9881	0.0003
1:17	1.1355	0.0001
1:32	1.2737	0.0000
1:47	1.5672	0.0000
2:02	1.3555	0.0000
2:17	1.4861	0.0000
2:32	1.6032	0.0000
2:47	1.6267	0.0000
3:02	2.3231	0.0000
3:17	1.5100	0.0000
3:32	1.8916	0.0000
3:47	3.0128	0.0000
4:02	1.0149	0.0001
4:17	1.0294	0.0001
4:32	1.0475	0.0001
4:47	1.0750	0.0001
5:02	1.1122	0.0000
5:17	1.1347	0.0000
5:32	1.1671	0.0000
5:47	1.1893	0.0000
6:02	1.2271	0.0000

Table A.13 – Flow parameters n' and K for 30 ppt guar gel with 0.5 ppt ammonium persulfate at 125 °F

Elapsed Time (h:mm)	n'	K (lbf-s ^{n'} /ft ²)
0:00	0.4971	0.0124
0:17	0.8064	0.0009
0:32	0.9745	0.0002
0:47	0.9967	0.0001
1:02	0.9049	0.0001
1:17	0.8991	0.0001
1:32	0.8835	0.0001
1:47	0.8118	0.0001
2:02	0.7862	0.0001
2:17	0.7402	0.0001
2:32	0.7278	0.0001
2:47	0.6901	0.0002
3:02	0.6608	0.0002
3:17	0.5579	0.0003
3:32	0.5534	0.0003
3:47	0.5339	0.0003
4:02	0.5447	0.0002
4:17	0.5413	0.0002
4:32	0.5236	0.0003
4:47	0.4969	0.0003
5:02	0.5239	0.0003
5:17	0.5163	0.0003
5:32	0.5184	0.0003
5:47	0.5184	0.0003
6:02	0.5143	0.0003

Table A.14 – Flow parameters n' and K for 30 ppt guar gel with 0.5 ppt ammonium persulfate at 150 °F

Elapsed Time (h:mm)	n'	K (lbf-s ^{n'} /ft ²)
0:00	0.5334	0.0092
0:17	0.3869	0.0015
0:32	0.3069	0.0017
0:47	0.2319	0.0025
1:02	0.2078	0.0029
1:17	0.2034	0.0029
1:32	0.1846	0.0033
1:47	0.1716	0.0036
2:02	0.1712	0.0036
2:17	0.1697	0.0036
2:32	0.2173	0.0027
2:47	0.2142	0.0027
3:02	0.1783	0.0034
3:17	0.1641	0.0037
3:32	0.1619	0.0038
3:47	0.1605	0.0038
4:02	0.1597	0.0038
4:17	0.1524	0.0040
4:32	0.1509	0.0040
4:47	0.1513	0.0040
5:02	0.1557	0.0039
5:17	0.1519	0.0040
5:32	0.1415	0.0042
5:47	0.1418	0.0042
6:02	0.1381	0.0043

Table A.15 – Flow parameters n' and K for 30 ppt guar gel with 0.5 ppt ammonium persulfate at 175 °F

Elapsed Time (h:mm)	n'	K (lbf-s ^{n'} /ft ²)
0:00	0.4520	0.0157
0:17	0.1193	0.0048
0:32	0.1366	0.0039
0:47	0.1236	0.0041
1:02	0.0728	0.0057
1:17	0.1052	0.0049
1:32	0.1048	0.0050
1:47	0.1011	0.0051
2:02	0.1002	0.0053
2:17	0.1002	0.0053
2:32	0.1064	0.0051
2:47	0.1123	0.0048
3:02	0.1174	0.0047
3:17	0.1283	0.0043
3:32	0.1329	0.0042
3:47	0.1365	0.0042
4:02	0.1419	0.0040
4:17	0.1410	0.0040
4:32	0.1377	0.0041
4:47	0.1408	0.0040
5:02	0.1466	0.0039
5:17	0.1370	0.0041
5:32	0.1362	0.0041
5:47	0.1302	0.0043
6:02	0.1255	0.0045

Table A.16 – Flow parameters n' and K for 30 ppt guar gel with 1 ppt ammonium persulfate at 75 °F

Elapsed Time (h:mm)	n'	K (lbf-s ^{n'} /ft ²)
0:00	0.4721	0.0155
0:17	0.4750	0.0152
0:32	0.4770	0.0150
0:47	0.4784	0.0148
1:02	0.4797	0.0147
1:17	0.4808	0.0145
1:32	0.4819	0.0144
1:47	0.4827	0.0143
2:02	0.4833	0.0142
2:17	0.4845	0.0141
2:32	0.4853	0.0140
2:47	0.4868	0.0139
3:02	0.4890	0.0137
3:17	0.4909	0.0135
3:32	0.4925	0.0134
3:47	0.4926	0.0133
4:02	0.4938	0.0132
4:17	0.4964	0.0129
4:32	0.4981	0.0128
4:47	0.4993	0.0127
5:02	0.5015	0.0125
5:17	0.5025	0.0125
5:32	0.5044	0.0123
5:47	0.5065	0.0121
6:02	0.5073	0.0120

Table A.17 – Flow parameters n' and K for 30 ppt guar gel with 1 ppt ammonium persulfate at 100 °F

Elapsed Time (h:mm)	n'	K (lbf-s ^{n'} /ft ²)
0:00	0.4613	0.0156
0:17	0.5485	0.0075
0:32	0.5609	0.0070
0:47	0.5661	0.0067
1:02	0.5863	0.0058
1:17	0.6055	0.0050
1:32	0.6305	0.0041
1:47	0.6526	0.0035
2:02	0.6732	0.0029
2:17	0.6954	0.0024
2:32	0.7126	0.0021
2:47	0.7297	0.0017
3:02	0.7530	0.0014
3:17	0.7741	0.0012
3:32	0.7854	0.0010
3:47	0.7955	0.0009
4:02	0.8024	0.0008
4:17	0.8083	0.0007
4:32	0.8169	0.0007
4:47	0.8121	0.0006
5:02	0.8154	0.0006
5:17	0.8136	0.0005
5:32	0.8047	0.0005
5:47	0.7973	0.0005
6:02	0.7888	0.0005

Table A.18 – Flow parameters n' and K for 30 ppt guar gel with 1 ppt ammonium persulfate at 150 °F

Elapsed Time (h:mm)	n'	K (lbf-s ^{n'} /ft ²)
0:00	0.5117	0.0106
0:17	0.9357	0.0001
0:32	0.7820	0.0001
0:47	0.6331	0.0001
1:02	0.4347	0.0003
1:17	0.3988	0.0003
1:32	0.3775	0.0003
1:47	0.3669	0.0003
2:02	0.3623	0.0003
2:17	0.3598	0.0003
2:32	0.3497	0.0003
2:47	0.3373	0.0004
3:02	0.3470	0.0004
3:17	0.3497	0.0003
3:32	0.3509	0.0003
3:47	0.3497	0.0003
4:02	0.3522	0.0003
4:17	0.3413	0.0004
4:32	0.3413	0.0004
4:47	0.3427	0.0004
5:02	0.3415	0.0004
5:17	0.3400	0.0004
5:32	0.3413	0.0004
5:47	0.3289	0.0004
6:02	0.3174	0.0004

Table A.19 – Flow parameters n' and K for 30 ppt guar gel with 1 ppt ammonium persulfate at 175 °F

Elapsed Time (h:mm)	n'	K (lbf-s ^{n'} /ft ²)
0:00	0.4810	0.0132
0:17	0.1104	0.0037
0:32	0.1365	0.0031
0:47	0.1353	0.0032
1:02	0.1450	0.0031
1:17	0.1504	0.0030
1:32	0.1473	0.0030
1:47	0.1491	0.0031
2:02	0.1453	0.0032
2:17	0.1414	0.0032
2:32	0.1390	0.0032
2:47	0.1390	0.0032
3:02	0.1391	0.0032
3:17	0.1380	0.0032
3:32	0.1390	0.0032
3:47	0.1339	0.0033
4:02	0.1314	0.0033
4:17	0.1342	0.0033
4:32	0.1312	0.0033
4:47	0.1326	0.0033
5:02	0.1332	0.0033
5:17	0.1339	0.0033
5:32	0.1482	0.0032
5:47	0.1746	0.0028
6:02	0.1522	0.0031

Table A.20 – Flow parameters n' and K for 30 ppt guar gel with 0.5 gpt galactomannanase at 75 °F

Elapsed Time (h:mm)	n'	K (lbf-s ⁿ /ft ²)
0:01	0.6480	0.0036
0:17	0.7894	0.0005
0:32	0.7037	0.0006
0:47	0.6499	0.0007
1:02	0.6053	0.0008
1:17	0.5830	0.0008
1:32	0.5639	0.0009
1:47	0.5431	0.0009
2:02	0.5274	0.0010
2:17	0.5147	0.0010
2:32	0.5033	0.0011
2:47	0.4894	0.0011
3:02	0.4797	0.0012
3:17	0.4640	0.0012
3:32	0.4580	0.0013
3:47	0.4489	0.0013
4:02	0.4429	0.0013
4:17	0.4383	0.0014
4:32	0.4311	0.0014
4:47	0.4309	0.0014
5:02	0.4220	0.0015
5:17	0.4182	0.0015
5:32	0.4132	0.0015
5:47	0.4105	0.0015
6:02	0.4026	0.0016

Table A.21 – Flow parameters n' and K for 30 ppt guar gel with 0.5 gpt galactomannanase at 100 °F

Elapsed Time (h:mm)	n'	K (lbf-s ^{n'} /ft ²)
0:01	0.6981	0.0028
0:17	0.9545	0.0001
0:32	0.7208	0.0003
0:47	0.6747	0.0003
1:02	0.6503	0.0003
1:17	0.6345	0.0003
1:32	0.6218	0.0003
1:47	0.6122	0.0003
2:02	0.5994	0.0003
2:17	0.5961	0.0003
2:32	0.6021	0.0003
2:47	0.5835	0.0004
3:02	0.5720	0.0004
3:17	0.5506	0.0004
3:32	0.5507	0.0004
3:47	0.5549	0.0004
4:02	0.5377	0.0004
4:17	0.5295	0.0005
4:32	0.5271	0.0005
4:47	0.5248	0.0005
5:02	0.5211	0.0005
5:17	0.5308	0.0004
5:32	0.5300	0.0004
5:47	0.5230	0.0005
6:02	0.5266	0.0004

Table A.22 – Flow parameters n' and K for 30 ppt guar gel with 0.5 gpt galactomannanase at 125 °F

Elapsed Time (h:mm)	n'	K (lbf-s ⁿ /ft ²)
0:01	0.5827	0.0042
0:17	0.5922	0.0009
0:32	0.5736	0.0009
0:47	0.5497	0.0011
1:02	0.5361	0.0012
1:17	0.5216	0.0013
1:32	0.5120	0.0013
1:47	0.5078	0.0014
2:02	0.5023	0.0014
2:17	0.4972	0.0015
2:32	0.4959	0.0015
2:47	0.4979	0.0014
3:02	0.4956	0.0015
3:17	0.4965	0.0015
3:32	0.4928	0.0015
3:47	0.4908	0.0015
4:02	0.4913	0.0015
4:17	0.4898	0.0015
4:32	0.4896	0.0015
4:47	0.4897	0.0015
5:02	0.4889	0.0015
5:17	0.4855	0.0015
5:32	0.4823	0.0015
5:47	0.4853	0.0015
6:02	0.4820	0.0015

Table A.23 – Flow parameters n' and K for 30 ppt guar gel with 0.5 gpt galactomannanase at 150 °F

Elapsed Time (h:mm)	n'	K (lbf-s ⁿ /ft ²)
0:01	0.6414	0.0029
0:17	0.7744	0.0002
0:32	0.7618	0.0002
0:47	0.7047	0.0003
1:02	0.6961	0.0004
1:17	0.7005	0.0003
1:32	0.7102	0.0003
1:47	0.7104	0.0003
2:02	0.7131	0.0003
2:17	0.7062	0.0003
2:32	0.7015	0.0003
2:47	0.7016	0.0003
3:02	0.6851	0.0004
3:17	0.6679	0.0004
3:32	0.6545	0.0004
3:47	0.6530	0.0004
4:02	0.6437	0.0004
4:17	0.6422	0.0004
4:32	0.6594	0.0004
4:47	0.6791	0.0003
5:02	0.6658	0.0004
5:17	0.6567	0.0004
5:32	0.6590	0.0004
5:47	0.6493	0.0004
6:02	0.6331	0.0004

Table A.24 – Flow parameters n' and K for 30 ppt guar gel with 0.5 gpt galactomannanase at 175 °F

Elapsed Time	n'	K
(h:mm)		(lbf-s^{n'}/ft²)
0:01	0.5174	0.0050
0:17	0.4950	0.0013
0:32	0.4950	0.0014
0:47	0.4689	0.0016
1:02	0.4517	0.0018
1:17	0.4421	0.0019
1:32	0.4334	0.0019
1:47	0.4285	0.0020
2:02	0.4274	0.0020
2:17	0.4212	0.0020
2:32	0.4194	0.0021
2:47	0.4158	0.0021
3:02	0.4121	0.0021
3:17	0.4092	0.0021
3:32	0.4064	0.0021
3:47	0.4073	0.0021
4:02	0.4048	0.0021
4:17	0.4053	0.0021
4:32	0.4036	0.0021
4:47	0.4011	0.0021
5:02	0.3989	0.0021
5:17	0.3958	0.0021
5:32	0.3934	0.0021
5:47	0.3925	0.0021
6:02	0.3890	0.0022

Table A.25 – Flow parameters n' and K for 30 ppt guar gel with 1 gpt galactomannanase at 75 °F

Elapsed Time (h:mm)	n'	K (lbf-s ^{n'} /ft ²)
0:01	0.6615	0.0031
0:17	0.9000	0.0001
0:32	0.7124	0.0003
0:47	0.6699	0.0004
1:02	0.6446	0.0004
1:17	0.6237	0.0004
1:32	0.6097	0.0004
1:47	0.5939	0.0004
2:02	0.6059	0.0004
2:17	0.6134	0.0003
2:32	0.6146	0.0003
2:47	0.6216	0.0003
3:02	0.6342	0.0003
3:17	0.6288	0.0003
3:32	0.5986	0.0004
3:47	0.5894	0.0004
4:02	0.5788	0.0004
4:17	0.5699	0.0004
4:32	0.5705	0.0004
4:47	0.5622	0.0004
5:02	0.5622	0.0004
5:17	0.5512	0.0005
5:32	0.5507	0.0005
5:47	0.5474	0.0005
6:02	0.5486	0.0005

Table A.26 – Flow parameters n' and K for 30 ppt guar gel with 1 gpt galactomannanase at 100 °F

Elapsed Time (h:mm)	n'	K (lbf-s ^{n'} /ft ²)
0:01	0.5968	0.0035
0:17	0.5126	0.0009
0:32	0.4508	0.0011
0:47	0.4140	0.0013
1:02	0.3775	0.0015
1:17	0.3580	0.0016
1:32	0.3356	0.0018
1:47	0.3200	0.0020
2:02	0.3121	0.0020
2:17	0.3079	0.0021
2:32	0.2981	0.0022
2:47	0.2901	0.0022
3:02	0.2881	0.0023
3:17	0.2852	0.0023
3:32	0.2816	0.0023
3:47	0.2794	0.0024
4:02	0.2745	0.0024
4:17	0.2729	0.0024
4:32	0.2689	0.0025
4:47	0.2649	0.0025
5:02	0.2699	0.0025
5:17	0.2655	0.0025
5:32	0.2624	0.0026
5:47	0.2576	0.0026
6:02	0.2604	0.0026

Table A.27 – Flow parameters n' and K for 30 ppt guar gel with 1 gpt galactomannanase at 125 °F

Elapsed Time (h:mm)	n'	K (lbf-s ⁿ /ft ²)
0:01	0.6076	0.0031
0:17	0.6013	0.0004
0:32	0.4891	0.0008
0:47	0.4690	0.0009
1:02	0.4466	0.0011
1:17	0.4273	0.0011
1:32	0.4208	0.0012
1:47	0.4196	0.0012
2:02	0.4170	0.0012
2:17	0.4168	0.0012
2:32	0.4146	0.0012
2:47	0.4150	0.0012
3:02	0.4166	0.0012
3:17	0.4118	0.0012
3:32	0.4142	0.0012
3:47	0.4171	0.0012
4:02	0.4134	0.0012
4:17	0.4154	0.0012
4:32	0.4049	0.0013
4:47	0.4008	0.0013
5:02	0.3967	0.0013
5:17	0.4024	0.0013
5:32	0.4024	0.0013
5:47	0.3980	0.0013
6:02	0.4015	0.0013

Table A.28 – Flow parameters n' and K for 30 ppt guar gel with 1 gpt galactomannanase at 150 °F

Elapsed Time (h:mm)	n'	K (lbf-s ^{n'} /ft ²)
0:01	0.4896	0.0052
0:17	0.4674	0.0013
0:32	0.4553	0.0015
0:47	0.4146	0.0020
1:02	0.4008	0.0022
1:17	0.4086	0.0021
1:32	0.4067	0.0021
1:47	0.3890	0.0024
2:02	0.3870	0.0024
2:17	0.3891	0.0024
2:32	0.3878	0.0024
2:47	0.4045	0.0021
3:02	0.4035	0.0021
3:17	0.4037	0.0021
3:32	0.4027	0.0021
3:47	0.4022	0.0021
4:02	0.4013	0.0021
4:17	0.4011	0.0021
4:32	0.4026	0.0021
4:47	0.4034	0.0021
5:02	0.4014	0.0021
5:17	0.4007	0.0021
5:32	0.3971	0.0022
5:47	0.3956	0.0022
6:02	0.3973	0.0021

Table A.29 – Flow parameters n' and K for 30 ppt guar gel without breaker at 150 °F
(CHANDLER 5550)

Elapsed Time (h:mm)	n'	K (lbf-s ^{n'} /ft ²)
0:15	0.6004	0.0050
0:31	0.5845	0.0052
0:46	0.5763	0.0053
1:02	0.5750	0.0053
1:17	0.5713	0.0054
1:33	0.5675	0.0055
1:49	0.5648	0.0055
2:04	0.5648	0.0055
2:20	0.5591	0.0055
2:35	0.5590	0.0055
2:51	0.5681	0.0053
3:07	0.5626	0.0060
3:22	0.5575	0.0067
3:38	0.5534	0.0073
3:53	0.5486	0.0079
4:09	0.5465	0.0083
4:25	0.5407	0.0089
4:40	0.5351	0.0094
4:56	0.5233	0.0100

Table A.30 – Flow parameters n' and K for 30 ppt guar gel without breaker at 175 °F
(CHANDLER 5550)

Elapsed Time	n'	K
(h:mm)		(lbf-s^{n'}/ft²)
0:15	0.5023	0.0059
0:31	0.4317	0.0069
0:46	0.2885	0.0113
1:02	0.2539	0.0132
1:18	0.2143	0.0161
1:33	0.1555	0.0203
1:49	0.1185	0.0233
2:04	0.1022	0.0247
2:20	0.0817	0.0268
2:36	0.0621	0.0287
2:51	0.0621	0.0287
3:07	0.0516	0.0307
3:22	0.0537	0.0319
3:38	0.0600	0.0331
3:54	0.0723	0.0332
4:09	0.0772	0.0341
4:25	0.0814	0.0356
4:40	0.0871	0.0370
4:56	0.1006	0.0374

Table A.31 – Flow parameters n' and K for 30 ppt guar gel without breaker at 200 °F
(CHANDLER 5550)

Elapsed Time (h:mm)	n'	K (lbf-s^{n'}/ft²)
0:15	0.5848	0.3641
0:31	0.5269	0.4169
0:46	0.4729	0.4844
1:02	0.4224	0.5764
1:17	0.3921	0.6291
1:33	0.3660	0.6765
1:49	0.3424	0.7214
2:04	0.3164	0.7783
2:20	0.2932	0.8307
2:35	0.2838	0.8247
2:51	0.2735	0.8469
3:07	0.2556	0.9224
3:22	0.3381	0.7569
3:38	0.4219	0.6246
3:53	0.4666	0.5842

Table A.32 – Flow parameters n' and K for 30 ppt guar gel without breaker at 225 °F
(CHANDLER 5550)

Elapsed Time (h:mm)	n'	K (lbf-s ⁿ /ft ²)
0:15	0.6185	0.0019
0:31	0.5627	0.0020
0:46	0.4945	0.0024
1:02	0.4558	0.0027
1:17	0.4014	0.0032
1:33	0.3184	0.0044
1:49	0.2754	0.0051
2:04	0.2119	0.0065
2:20	0.1969	0.0068
2:35	0.1941	0.0068
2:51	0.1802	0.0071
3:07	0.1923	0.0069
3:22	0.2646	0.0060
3:38	0.3300	0.0055
3:54	0.4203	0.0044

Table A.33 – Flow parameters n' and K for 30 ppt guar gel without breaker at 250 °F
(CHANDLER 5550)

Elapsed Time (h:mm)	n'	K (lbf-s ⁿ /ft ²)
0:15	0.2462	0.0066
0:31	0.0477	0.0123*

* Instrument limit reached.

Table A.34– Flow parameters n' and K for 30 ppt guar gel without breaker at 275 °F
(CHANDLER 5550)

Elapsed Time (h:mm)	n'	K (lbf-s ⁿ /ft ²)
0:15	0.2997	0.0028
0:31	0.1906	0.0031
0:46	0.0732	0.0053
1:02	0.0652	0.0054
1:17	0.0691	0.0053
1:33	0.0951	0.0050
1:49	0.0077	0.0075
3:07	0.0311	0.0069
3:38	0.0104	0.0075
3:54	0.1017	0.0057
4:09	0.1656	0.0048
4:25	0.1562	0.0052
4:40	0.2320	0.0040
4:56	0.2348	0.0041

Table A.35 – Flow parameters n' and K for 30 ppt guar gel without breaker at 300 °F
(CHANDLER 5550)

Elapsed Time (h:mm)	n'	K (lbf-s ⁿ /ft ²)
0:15	0.0249	0.0167
0:31	0.0000	0.0171
0:46	0.0048	0.0181
1:02	0.0030	0.0169*

*Instrument limit reached.

Table A.36 – Flow parameters n' and K for 60 ppt guar gel without breaker at 200 °F
(CHANDLER 5550)

Elapsed Time (h:mm)	n'	K (lbf-s ^{n'} /ft ²)
0:15	0.4398	0.0481
0:31	0.4806	0.0369
0:46	0.5018	0.0319
1:02	0.5198	0.0282
1:17	0.5290	0.0259
1:33	0.5448	0.0233
1:48	0.5528	0.0217
2:04	0.5643	0.0199
2:19	0.5733	0.0185
2:35	0.5770	0.0175
2:51	0.5861	0.0163
3:06	0.5918	0.0154
3:22	0.5921	0.0149
3:37	0.5981	0.0140
3:53	0.5953	0.0137
4:08	0.6005	0.0129
4:24	0.5952	0.0128
4:40	0.5889	0.0127
4:56	0.5853	0.0125
5:11	0.5689	0.0130
5:27	0.5323	0.0147
5:42	0.4620	0.0193
5:58	0.3528	0.0299
6:13	0.3635	0.0332
6:29	0.5028	0.0226
6:44	0.5428	0.0223
7:00	0.5425	0.0249
7:16	0.5346	0.0281
7:31	0.5260	0.0311
7:47	0.5148	0.0343
8:03	0.5082	0.0368

Table A.37– Flow parameters n' and K for 60 ppt guar gel without breaker at 225 °F
(CHANDLER 5550)

Elapsed Time (h:mm)	n'	K (lbf-s ^{n'} /ft ²)
0:15	0.5498	0.0205
0:31	0.6168	0.0122
0:46	0.6339	0.0096
1:02	0.6462	0.0078
1:17	0.6354	0.0071
1:33	0.6132	0.0069
1:49	0.6007	0.0065
2:04	0.5944	0.0063
2:20	0.5749	0.0066
2:35	0.5720	0.0066
2:51	0.5611	0.0068
3:06	0.5550	0.0069
3:22	0.5418	0.0071
3:38	0.5326	0.0073
3:53	0.5179	0.0076
4:09	0.4956	0.0083
4:25	0.4659	0.0093
4:40	0.3958	0.0125
4:56	0.3250	0.0167
5:11	0.2439	0.0235
5:27	0.1885	0.0296
5:42	0.1394	0.0365
5:58	0.1002	0.0427
6:13	0.1474	0.0387
6:29	0.3473	0.0210
6:45	0.5045	0.0142
7:01	0.5491	0.0141
7:16	0.5638	0.0160
7:32	0.5668	0.0183
7:47	0.5605	0.0208
8:03	0.5553	0.0227

Table A.38 – Flow parameters n' and K for 60 ppt guar gel without breaker at 250 °F
(CHANDLER 5550)

Elapsed Time (h:mm)	n'	K (lbf-s ⁿ /ft ²)
0:15	0.6526	0.0096
0:31	0.6961	0.0034
0:46	0.5631	0.0035
1:02	0.4402	0.0045
1:18	0.3971	0.0051
1:33	0.3732	0.0055
1:49	0.3515	0.0058
2:04	0.3398	0.0060
2:20	0.2686	0.0079
2:36	0.2546	0.0083
2:51	0.2514	0.0083
3:07	0.2361	0.0087
3:23	0.2273	0.0089
3:38	0.2194	0.0092
3:54	0.2073	0.0095
4:09	0.2047	0.0096
4:25	0.1957	0.0099
4:41	0.1644	0.0111
4:56	0.1635	0.0113
5:12	0.1499	0.0118
5:27	0.1369	0.0122
5:43	0.1606	0.0110
5:59	0.1173	0.0132
6:14	0.1806	0.0111
6:30	0.2684	0.0092
6:45	0.3664	0.0073
7:01	0.4632	0.0059
7:17	0.5392	0.0050
7:32	0.6173	0.0041
7:48	0.6658	0.0039
8:03	0.7209	0.0035

Table A.39 – Flow parameters n' and K for 60 ppt guar gel without breaker at 300 °F
(CHANDLER 5550)*

Elapsed Time (h:mm)	n'	K (lbf-s ^{n'} /ft ²)
0:15	0.3737	0.0061
0:31	0.0597	0.0111
0:46	0.0203	0.0125
1:02	0.0005	0.0133
4:40	0.0190	0.0119
4:56	0.0223	0.0120
5:11	0.0069	0.0130
6:14	0.0074	0.0117
6:29	0.0120	0.0115
6:45	0.0148	0.0111
7:00	0.0070	0.0117
7:47	0.0049	0.0119
8:03	0.0075	0.0118

*Instrument limit reached.

Table A.40 – Flow parameters n' and K for 30 ppt guar gel with 0.25 ppt ammonium persulfate at 200 °F (CHANDLER 5550)

Elapsed Time (h:mm)	n'	K (lbf-s ^{n'} /ft ²)
0:17	0.3466	0.0023
0:34	0.1950	0.0037
0:52	0.1945	0.0043
1:09	0.1674	0.0056
1:27	0.1424	0.0066
1:44	0.1438	0.0066
2:01	0.0988	0.0084
2:18	0.1256	0.0076
2:36	0.1301	0.0075
2:53	0.1534	0.0064
3:10	0.1366	0.0071
3:28	0.0887	0.0088
3:45	0.1268	0.0076
4:02	0.1177	0.0081
4:20	0.1121	0.0082
4:37	0.1183	0.0080
4:55	0.1244	0.0077
5:12	0.1303	0.0073
5:29	0.1500	0.0065
5:46	0.1511	0.0067
6:04	0.1538	0.0066

Table A.41 – Flow parameters n' and K for 30 ppt guar gel with 0.25 ppt ammonium persulfate at 225 °F (CHANDLER 5550)

Elapsed Time	n'	K
(h:mm)		(lbf-s^{n'}/ft²)
0:17	0.1674	0.0048
0:35	0.1731	0.0044
0:52	0.1520	0.0053
1:10	0.1383	0.0058
1:27	0.1225	0.0065
1:44	0.1300	0.0063
2:02	0.1329	0.0063
2:19	0.1363	0.0062
2:37	0.1405	0.0061
2:54	0.1358	0.0062
3:12	0.1414	0.0062
3:29	0.1469	0.0061
3:46	0.1302	0.0066
4:04	0.1392	0.0063
4:21	0.1153	0.0070
4:38	0.1133	0.0072
4:56	0.1074	0.0076
5:13	0.1062	0.0076
5:31	0.0969	0.0080
5:48	0.0950	0.0081
6:06	0.1096	0.0074

Table A.42 – Flow parameters n' and K for 30 ppt guar gel with 0.25 ppt ammonium persulfate at 250 °F (CHANDLER 5550)

Elapsed Time (h:mm)	n'	K (lbf-s ^{n'} /ft ²)
0:17	0.2357	0.0023
0:35	0.1976	0.0031
0:52	0.1795	0.0036
1:10	0.1876	0.0036
1:28	0.1836	0.0039
1:45	0.1645	0.0046
2:02	0.1669	0.0046
2:19	0.1491	0.0051
2:37	0.1487	0.0054
2:54	0.1479	0.0055
3:12	0.1527	0.0054
3:29	0.1493	0.0055
3:47	0.1505	0.0054
4:04	0.1481	0.0055
4:21	0.1600	0.0053
4:38	0.1564	0.0054
4:56	0.1464	0.0057
5:13	0.1522	0.0055
5:31	0.1390	0.0059
5:48	0.1291	0.0062
6:06	0.1491	0.0055

Table A.43 – Flow parameters n' and K for 30 ppt guar gel with 0.5 ppt ammonium persulfate at 200 °F (CHANDLER 5550)

Elapsed Time (h:mm)	n'	K (lbf-s ^{n'} /ft ²)
0:17	0.2742	0.0021
0:34	0.2994	0.0019
0:52	0.3260	0.0018
1:09	0.3118	0.0020
1:27	0.3031	0.0022
1:44	0.2975	0.0024
2:02	0.2897	0.0024
2:19	0.2847	0.0026
2:36	0.3021	0.0024
2:54	0.2869	0.0026
3:11	0.2781	0.0028
3:28	0.2649	0.0030
3:46	0.2891	0.0026
4:21	0.2692	0.0029
4:38	0.2826	0.0027
4:55	0.2728	0.0029
5:13	0.2396	0.0034
5:30	0.2607	0.0031
5:47	0.2568	0.0032
6:05	0.2587	0.0031

Table A.44 – Flow parameters n' and K for 30 ppt guar gel with 0.5 ppt ammonium persulfate at 225 °F (CHANDLER 5550)

Elapsed Time (h:mm)	n'	K (lbf-s ^{n'} /ft ²)
0:17	0.2305	0.0025
0:34	0.1784	0.0036
0:52	0.1740	0.0038
1:09	0.1718	0.0038
1:27	0.1633	0.0042
1:44	0.1679	0.0041
2:02	0.1491	0.0048
2:19	0.1557	0.0047
2:36	0.1508	0.0048
2:54	0.1511	0.0048
3:11	0.1453	0.0049
3:28	0.1572	0.0047
3:46	0.1502	0.0048
4:03	0.1533	0.0048
4:21	0.1494	0.0048
4:38	0.1514	0.0048
4:56	0.1507	0.0048
5:13	0.1439	0.0049
5:30	0.1492	0.0048
5:48	0.1519	0.0048
6:05	0.1518	0.0048

Table A.45– Flow parameters n' and K for 30 ppt guar gel with 0.5 ppt ammonium persulfate at 250 °F (CHANDLER 5550)

Elapsed Time (h:mm)	n'	K (lbf-s ^{n'} /ft ²)
0:17	0.1397	0.0044
0:35	0.1707	0.0045
0:52	0.1687	0.0049
1:10	0.1546	0.0055
1:28	0.1325	0.0064
1:45	0.1279	0.0066
2:03	0.1354	0.0066
2:20	0.1197	0.0073
2:38	0.1129	0.0074
2:55	0.1178	0.0074
3:12	0.1239	0.0072
3:30	0.1194	0.0074
3:47	0.1223	0.0073
4:04	0.1186	0.0073
4:22	0.1232	0.0071
4:39	0.1222	0.0073
4:57	0.1194	0.0072
5:14	0.1001	0.0079
5:31	0.0863	0.0083
5:48	0.0820	0.0084
6:06	0.0822	0.0085

Table A.46 – Flow parameters n' and K for 30 ppt guar gel with 1 ppt ammonium persulfate at 200 °F (CHANDLER 5550)

Elapsed Time	n'	K
(h:mm)		(lbf-s^{n'}/ft²)
0:17	0.2244	0.0033
0:34	0.2011	0.0037
0:52	0.1867	0.0041
1:09	0.1908	0.0042
1:27	0.1771	0.0047
1:44	0.1767	0.0049
2:02	0.1747	0.0049
2:19	0.1724	0.0051
2:36	0.1456	0.0060
2:53	0.1476	0.0060
3:11	0.1406	0.0061
3:28	0.1398	0.0061
3:46	0.1416	0.0061
4:03	0.1439	0.0060
4:21	0.1392	0.0060
4:38	0.1432	0.0061
4:55	0.1388	0.0061
5:13	0.1417	0.0061
5:30	0.1397	0.0061
5:47	0.1410	0.0061
6:05	0.1411	0.0061

Table A.47 – Flow parameters n' and K for 30 ppt guar gel with 1 ppt ammonium persulfate at 225 °F (CHANDLER 5550)

Elapsed Time (h:mm)	n'	K (lbf-s ^{n'} /ft ²)
0:17	0.4368	0.0000
0:34	1.0201	0.0000
0:52	2.6660	0.0000
1:09	2.5754	0.0000
1:27	2.2276	0.0000
1:44	1.4232	0.0000
2:02	0.2889	0.0007
2:19	0.3280	0.0003
2:36	0.3659	0.0005
2:53	0.3569	0.0005
3:11	0.2442	0.0005
3:28	0.3281	0.0006
3:46	0.2588	0.0008
4:03	0.3632	0.0003
4:21	0.3588	0.0005
4:38	0.3572	0.0003
4:55	0.1943	0.0010
5:13	0.2273	0.0009
5:30	0.2582	0.0008
5:47	0.3284	0.0003
6:05	0.2890	0.0007

Table A.48 – Flow parameters n' and K for 30 ppt guar gel with 1 ppt ammonium persulfate at 250 °F (CHANDLER 5550)

Elapsed Time	n'	K
(h:mm)		(lbf-s^{n'}/ft²)
0:17	0.1025	0.0084
0:34	0.1031	0.0080
0:52	0.0886	0.0088
1:09	0.0910	0.0087
1:27	0.0862	0.0089
1:44	0.0801	0.0096
2:01	0.0748	0.0098
2:18	0.0773	0.0097
2:36	0.0786	0.0096
2:53	0.0826	0.0095
3:11	0.0815	0.0095
3:28	0.0825	0.0095
3:46	0.0818	0.0095
4:03	0.0850	0.0094
4:21	0.0834	0.0095
4:38	0.0744	0.0098
4:55	0.0789	0.0096
5:12	0.0846	0.0095
5:30	0.0754	0.0098
5:47	0.0798	0.0096
6:05	0.0754	0.0098

Table A.49 – Flow parameters n' and K for 30 ppt guar gel with 1 ppt magnesium peroxide at 175 °F (CHANDLER 5550)

Elapsed Time (h:mm)	n'	K (lbf-s ^{n'} /ft ²)
0:17	0.5573	0.0051
0:35	0.5867	0.0040
0:52	0.5765	0.0041
1:10	0.5322	0.0051
1:28	0.5204	0.0054
1:45	0.5093	0.0058
2:03	0.5103	0.0056
2:21	0.5101	0.0056
2:38	0.5447	0.0045
2:56	0.5991	0.0032
3:14	0.5932	0.0033
3:31	0.4801	0.0065
3:49	0.4248	0.0094
4:06	0.4118	0.0101
4:24	0.4099	0.0106
4:42	0.4076	0.0105
4:59	0.4258	0.0093
5:17	0.4455	0.0081
5:35	0.4507	0.0078
5:52	0.4425	0.0105
6:10	0.4646	0.0092

Table A.50 – Flow parameters n' and K for 30 ppt guar gel with 1 ppt magnesium peroxide at 200 °F (CHANDLER 5550)

Elapsed Time (h:mm)	n'	K (lbf-s ^{n'} /ft ²)
0:17	0.7265	0.1463
0:35	0.7311	0.1216
0:52	0.7095	0.1262
1:10	0.6892	0.1329
1:28	0.6817	0.1319
1:45	0.6722	0.1359
2:03	0.6676	0.1354
2:21	0.6615	0.1367
2:38	0.6573	0.1367
2:56	0.6535	0.1386
3:14	0.6487	0.1396
3:31	0.6503	0.1358
3:49	0.6454	0.1382
4:07	0.6427	0.1383
4:24	0.6426	0.1367
4:42	0.6387	0.1384
4:59	0.6351	0.1397
5:17	0.6360	0.1375
5:35	0.6333	0.1381
5:52	0.6271	0.1415
6:10	0.6233	0.1440

Table A.51– Flow parameters n' and K for 30 ppt guar gel with 1 ppt magnesium peroxide at 225 °F (CHANDLER 5550)

Elapsed Time (h:mm)	n'	K (lbf-s ^{n'} /ft ²)
0:17	0.8085	0.0006
0:35	0.7085	0.0007
0:52	0.7406	0.0004
1:10	0.6890	0.0005
1:28	0.6245	0.0007
1:45	0.5920	0.0008
2:03	0.5576	0.0009
2:21	0.5028	0.0011
2:38	0.4499	0.0015
2:56	0.4287	0.0016
3:13	0.4435	0.0014
3:31	0.4335	0.0014
3:49	0.3787	0.0020
4:06	0.3989	0.0017
4:24	0.3955	0.0017
4:42	0.3876	0.0017
4:59	0.3707	0.0018
5:17	0.3668	0.0018
5:35	0.3649	0.0018
5:52	0.3457	0.0019
6:10	0.3757	0.0016

Table A.52 – Flow parameters n' and K for 30 ppt guar gel with 1 ppt magnesium peroxide at 250 °F (CHANDLER 5550)

Elapsed Time (h:mm)	n'	K (lbf-s ^{n'} /ft ²)
0:17	0.7431	0.0007
0:35	0.6362	0.0008
0:52	0.5184	0.0013
1:10	0.4515	0.0018
1:28	0.4247	0.0021
1:45	0.3721	0.0027
2:03	0.3507	0.0029
2:21	0.3363	0.0031
2:38	0.3232	0.0032
2:56	0.3106	0.0034
3:14	0.3005	0.0035
3:31	0.2887	0.0037
3:49	0.2731	0.0039
4:06	0.2714	0.0040
4:24	0.2612	0.0042
4:41	0.2511	0.0044
4:59	0.2563	0.0042
5:17	0.2543	0.0042
5:34	0.2357	0.0046
5:52	0.2309	0.0048
6:09	0.2169	0.0051

Table A.53 – Flow parameters n' and K for 30 ppt guar gel with 5 ppt magnesium peroxide at 175 °F (CHANDLER 5550)

Elapsed Time (h:mm)	n'	K (lbf-s ^{n'} /ft ²)
0:17	0.5785	0.0044
0:35	0.5802	0.0040
0:52	0.5484	0.0047
1:10	0.5391	0.0050
1:28	0.5253	0.0054
1:45	0.5379	0.0050
2:03	0.5530	0.0045
2:21	0.5422	0.0047
2:38	0.5549	0.0044
2:56	0.5654	0.0041
3:14	0.5726	0.0039
3:31	0.5687	0.0040
3:49	0.5685	0.0040
4:07	0.5678	0.0040
4:24	0.5772	0.0037
4:42	0.5718	0.0039
5:00	0.5609	0.0041
5:17	0.5826	0.0036
5:35	0.5861	0.0035
5:53	0.5866	0.0035
6:10	0.5766	0.0037

Table A.54 – Flow parameters n' and K for 30 ppt guar gel with 5 ppt magnesium peroxide at 200 °F (CHANDLER 5550)

Elapsed Time (h:mm)	n'	K (lbf-s ^{n'} /ft ²)
0:17	0.5867	0.0032
0:35	0.5569	0.0031
0:52	0.5437	0.0031
1:10	0.5222	0.0034
1:28	0.4878	0.0040
1:45	0.5118	0.0033
2:03	0.5231	0.0030
2:21	0.5169	0.0030
2:38	0.5125	0.0029
2:56	0.4839	0.0033
3:14	0.4261	0.0045
3:31	0.4222	0.0046
3:49	0.4391	0.0040
4:07	0.4311	0.0041
4:24	0.4323	0.0039
4:42	0.4098	0.0043
5:00	0.4195	0.0039
5:17	0.4339	0.0034
5:35	0.4169	0.0036
5:52	0.4467	0.0028
6:10	0.4458	0.0025

Table A.55 – Flow parameters n' and K for 30 ppt guar gel with 5 ppt magnesium peroxide at 225 °F (CHANDLER 5550)

Elapsed Time (h:mm)	n'	K (lbf-s ⁿ /ft ²)
0:17	0.5955	0.0023
0:35	0.5208	0.0027
0:52	0.4949	0.0025
1:10	0.4765	0.0024
1:28	0.4313	0.0029
1:45	0.3933	0.0034
2:03	0.3635	0.0039
2:21	0.3046	0.0053
2:38	0.3011	0.0049
2:56	0.2807	0.0053
3:14	0.2857	0.0051
3:31	0.2737	0.0052
3:49	0.2630	0.0053
4:07	0.2495	0.0056
4:24	0.2377	0.0059
4:42	0.2323	0.0058
4:59	0.2271	0.0060
5:17	0.2172	0.0062
5:35	0.2109	0.0063
5:52	0.2037	0.0064
6:10	0.2062	0.0063

Table A.56 – Flow parameters n' and K for 30 ppt guar gel with 5 ppt magnesium peroxide at 250 °F (CHANDLER 5550)

Elapsed Time (h:mm)	n'	K (lbf-s ^{n'} /ft ²)
0:17	0.6287	0.0011
0:35	0.3449	0.0040
0:52	0.2839	0.0042
1:10	0.2576	0.0043
1:28	0.2357	0.0042
1:45	0.1929	0.0049
2:03	0.2015	0.0050
2:21	0.1465	0.0065
2:38	0.1720	0.0051
2:56	0.1715	0.0048
3:13	0.2279	0.0037
3:31	0.1841	0.0045
3:49	0.1601	0.0058
4:06	0.1610	0.0060
4:24	0.1626	0.0058
4:42	0.1747	0.0052
4:59	0.1772	0.0053
5:17	0.1564	0.0060
5:35	0.1761	0.0052
5:52	0.1573	0.0056
6:10	0.1630	0.0055

Table A.57 – Flow parameters n' and K for 30 ppt guar gel with 10 ppt magnesium peroxide at 175 °F (CHANDLER 5550)

Elapsed Time (h:mm)	n'	K (lbf-s ^{n'} /ft ²)
0:17	0.6386	0.0031
0:35	0.6514	0.0026
0:52	0.6730	0.0022
1:10	0.6358	0.0025
1:28	0.6193	0.0027
1:45	0.6373	0.0024
2:03	0.6300	0.0025
2:21	0.6493	0.0021
2:38	0.6487	0.0021
2:56	0.7002	0.0015
3:13	0.6838	0.0016
3:31	0.6766	0.0016
3:49	0.6800	0.0016
4:06	0.6578	0.0018
4:24	0.6683	0.0016
4:42	0.6515	0.0018
4:59	0.6639	0.0016
5:17	0.6166	0.0021
5:35	0.6274	0.0020
5:52	0.6347	0.0018
6:10	0.6085	0.0021

Table A.58 – Flow parameters n' and K for 30 ppt guar gel with 10 ppt magnesium peroxide at 200 °F (CHANDLER 5550)

Elapsed Time (h:mm)	n'	K (lbf-s ^{n'} /ft ²)
0:17	0.7160	0.0014
0:35	0.7000	0.0011
0:52	0.6777	0.0011
1:10	0.6429	0.0012
1:28	0.6338	0.0011
1:45	0.6125	0.0012
2:03	0.5946	0.0012
2:20	0.5703	0.0014
2:38	0.5529	0.0014
2:55	0.5369	0.0015
3:13	0.5125	0.0016
3:31	0.4962	0.0017
3:48	0.4806	0.0018
4:06	0.4627	0.0019
4:24	0.4504	0.0020
4:41	0.4364	0.0021
4:59	0.4191	0.0023
5:16	0.4114	0.0023
5:34	0.3960	0.0024
5:52	0.3922	0.0024
6:09	0.3730	0.0025

Table A.59 – Flow parameters n' and K for 30 ppt guar gel with 10 ppt magnesium peroxide at 225 °F (CHANDLER 5550)

Elapsed Time (h:mm)	n'	K (lbf-s ⁿ /ft ²)
0:17	0.6414	0.0016
0:35	0.5585	0.0018
0:52	0.5012	0.0021
1:10	0.4552	0.0023
1:28	0.3747	0.0032
1:45	0.3508	0.0035
2:03	0.3025	0.0043
2:21	0.2863	0.0045
2:38	0.2599	0.0050
2:56	0.2538	0.0050
3:14	0.2293	0.0054
3:31	0.2102	0.0057
3:49	0.2061	0.0060
4:07	0.2063	0.0060
4:24	0.1901	0.0066
4:42	0.1532	0.0074
5:00	0.1819	0.0068
5:17	0.1816	0.0066
5:35	0.1784	0.0068
5:52	0.1793	0.0066
6:10	0.1818	0.0067

Table A.60 – Flow parameters n' and K for 30 ppt guar gel with 10 ppt magnesium peroxide at 250 °F (CHANDLER 5550)

Elapsed Time (h:mm)	n'	K (lbf-s ^{n'} /ft ²)
0:17	0.6541	0.0009
0:35	0.4888	0.0016
0:52	0.3943	0.0024
1:10	0.3263	0.0032
1:28	0.2813	0.0039
1:45	0.2634	0.0041
2:03	0.2510	0.0045
2:21	0.2317	0.0048
2:38	0.2350	0.0047
2:56	0.2238	0.0049
3:14	0.2419	0.0044
3:31	0.2205	0.0048
3:49	0.2076	0.0049
4:07	0.2237	0.0043
4:24	0.1981	0.0051
4:42	0.1964	0.0055
5:00	0.1969	0.0052
5:17	0.1936	0.0050
5:35	0.2049	0.0047
5:53	0.1804	0.0055
6:10	0.1959	0.0052

Table A.61 – Flow parameters n' and K for 30 ppt guar gel with 1 ppt sodium bromate at 150 °F (CHANDLER 5550)

Elapsed Time (h:mm)	n'	K (lbf-s ⁿ /ft ²)
0:15	0.3679	0.0131
0:31	0.2725	0.0196
0:46	0.2218	0.0252
1:02	0.2370	0.0235
1:17	0.1970	0.0279
1:33	0.1724	0.0310
1:49	0.1557	0.0294
2:04	0.0914	0.0402
2:20	0.0597	0.0462
2:35	0.0528	0.0476
2:51	0.0381	0.0500
3:07	0.0299	0.0522
3:22	0.0286	0.0537
3:38	0.0291	0.0547
3:54	0.0348	0.0543
4:09	0.0350	0.0552
4:25	0.0306	0.0570
4:40	0.0346	0.0566
4:56	0.0315	0.0581

Table A.62 – Flow parameters n' and K for 30 ppt guar gel with 1 ppt sodium bromate at 200 °F (CHANDLER 5550)

Elapsed Time (h:mm)	n'	K (lbf-s ⁿ /ft ²)
0:15	0.8990	0.0797
0:30	0.8246	0.0887
0:46	0.7515	0.1080
1:02	0.6874	0.1276
1:17	0.6289	0.1501
1:33	0.5709	0.1793
1:48	0.5272	0.2030
2:04	0.4858	0.2311
2:20	0.4030	0.3067
2:35	0.3638	0.3461
2:51	0.3293	0.3880
3:06	0.4703	0.2564
3:22	0.6191	0.1768
3:37	0.7627	0.1195
3:53	0.8420	0.1009
4:09	0.8329	0.1186
4:24	0.8388	0.1267
4:40	0.8403	0.1348
4:55	0.8293	0.1484

Table A.63 – Flow parameters n' and K for 30 ppt guar gel with 1 ppt sodium bromate at 225 °F (CHANDLER 5550)

Elapsed Time (h:mm)	n'	K (lbf-s ^{n'} /ft ²)
0:15	0.2459	0.0106
0:31	0.1391	0.0140
0:46	0.1233	0.0143
1:02	0.1018	0.0151
1:17	0.0924	0.0156
1:33	0.0879	0.0157
1:48	0.0617	0.0171
2:04	0.0548	0.0173
2:20	0.0440	0.0178
2:35	0.0379	0.0180
2:51	0.0379	0.0180
3:06	0.0440	0.0178
3:22	0.0617	0.0171
3:37	0.1018	0.0151
3:53	0.0857	0.0167
4:08	0.1195	0.0152
4:24	0.1435	0.0145
4:40	0.1396	0.0152
4:56	0.1690	0.0140

Table A.64– Flow parameters n' and K for 30 ppt guar gel with 1 ppt sodium bromate at 250 °F (CHANDLER 5550)

Elapsed Time (h:mm)	n'	K (lbf-s ^{n'} /ft ²)
0:15	0.5232	0.0015
0:31	0.3678	0.0018
0:46	0.2261	0.0027
1:02	0.1366	0.0033
1:17	0.1011	0.0037
1:33	0.0855	0.0039
1:48	0.0661	0.0042
2:04	0.0145	0.0050
2:19	0.0058	0.0052
2:35	0.0000	0.0053
2:51	0.0460	0.0045
3:06	0.1065	0.0038
3:22	0.0622	0.0049
3:37	0.1193	0.0040
3:53	0.1115	0.0043
4:08	0.1370	0.0042
4:24	0.1549	0.0041
4:39	0.2086	0.0035
4:55	0.1759	0.0042

Table A.65 – Flow parameters n' and K for 30 ppt guar gel with 1 ppt sodium bromate at 275 °F (CHANDLER 5550)*

Elapsed Time (h:mm)	n'	K (lbf-s ⁿ /ft ²)
0:15	0.3129	0.0027
0:31	0.0901	0.0050
0:46	0.1012	0.0049
1:02	0.1008	0.0050
1:18	0.0036	0.0077
3:38	0.0542	0.0065
3:54	0.0582	0.0066
4:09	0.0332	0.0077
4:25	0.0427	0.0075
4:40	0.0628	0.0071
4:56	0.0465	0.0076

*Instrument limit reached.

Table A.66 – Flow parameters n' and K for 30 ppt guar gel with 1 ppt sodium bromate at 300 °F (CHANDLER 5550)*

Elapsed Time (h:mm)	n'	K (lbf-s ⁿ /ft ²)
0:15	0.2084	0.0038
0:31	0.0000	0.0071
0:46	0.0567	0.0067
1:02	0.0040	0.0084
1:33	0.0065	0.0083
2:04	0.0627	0.0065
2:20	0.0620	0.0065
2:51	0.0060	0.0083
4:25	0.0704	0.0068
4:41	0.0729	0.0067
4:56	0.1024	0.0064

*Instrument limit reached.

Table A.67 – Flow parameters n' and K for 30 ppt guar gel with 5 ppt sodium bromate at 150 °F (CHANDLER 5550)

Elapsed Time (h:mm)	n'	K (lbf-s ⁿ /ft ²)
0:15	0.5975	0.0048
0:31	0.5941	0.0047
0:46	0.5928	0.0048
1:02	0.5973	0.0047
1:17	0.5955	0.0048
1:33	0.5823	0.0050
1:49	0.5830	0.0050
2:04	0.5925	0.0048
2:20	0.5760	0.0051
2:36	0.5746	0.0051
2:51	0.5864	0.0048
3:07	0.5762	0.0056
3:22	0.5787	0.0060
3:38	0.5827	0.0064
3:54	0.5724	0.0071
4:09	0.5592	0.0078
4:25	0.5637	0.0079
4:41	0.5609	0.0082
4:56	0.5594	0.0085

Table A.68 – Flow parameters n' and K for 30 ppt guar gel with 5 ppt sodium bromate at 200 °F (CHANDLER 5550)

Elapsed Time (h:mm)	n'	K (lbf-s ^{n'} /ft ²)
0:15	0.6971	0.1636
0:31	0.6444	0.1767
0:46	0.6008	0.1939
1:02	0.5723	0.2091
1:17	0.5442	0.2222
1:33	0.5144	0.2428
1:49	0.4961	0.2497
2:04	0.4594	0.2763
2:20	0.4322	0.3007
2:35	0.4198	0.3054
2:51	0.4168	0.2972
3:07	0.4991	0.2535
3:22	0.5654	0.2409
3:38	0.5697	0.2772
3:54	0.5633	0.3246
4:09	0.5749	0.3434
4:25	0.5844	0.3582
4:40	0.5396	0.4581
4:56	0.5440	0.4785

Table A.69– Flow parameters n' and K for 30 ppt guar gel with 5 ppt sodium bromate at 225 °F (CHANDLER 5550)

Elapsed Time (h:mm)	n'	K (lbf-s ⁿ /ft ²)
0:15	0.6037	0.2159
0:31	0.5136	0.2431
0:46	0.3979	0.3367
1:02	0.3349	0.4020
1:17	0.2873	0.4647
1:33	0.2192	0.5605
1:48	0.2010	0.5846
2:04	0.1579	0.6715
2:20	0.1512	0.6827
2:35	0.1092	0.7643
2:51	0.1068	0.7633
3:06	0.1421	0.6961
3:22	0.1981	0.5896
3:37	0.2777	0.4715
3:53	0.3707	0.3662
4:09	0.3716	0.4045
4:24	0.4345	0.3433
4:40	0.4650	0.3260
4:56	0.5090	0.2920

Table A.70– Flow parameters n' and K for 30 ppt guar gel with 5 ppt sodium bromate at 250 °F (CHANDLER 5550)*

Elapsed Time (h:mm)	n'	K (lbf-s ⁿ /ft ²)
0:15	0.1286	0.0097
0:31	0.0485	0.0120
0:46	0.0249	0.0124
1:02	0.0000	0.0127
1:17	0.0296	0.0103
2:35	0.0166	0.0120
3:22	0.0370	0.0103
3:37	0.0592	0.0097
3:53	0.0528	0.0099
4:09	0.0591	0.0098
4:24	0.0376	0.0108
4:40	0.0397	0.0108
4:55	0.0270	0.0114

*Instrument limit reached.

Table A.71 – Flow parameters n' and K for 30 ppt guar gel with 5 ppt sodium bromate at 275 °F (CHANDLER 5550)*

Elapsed Time (h:mm)	n'	K (lbf-s ⁿ /ft ²)
0:15	0.2519	0.0024
0:31	0.0023	0.0055
2:20	0.0433	0.0049
2:51	0.0246	0.0051
3:07	0.0314	0.0051
3:38	0.0304	0.0069
3:53	0.0291	0.0069
4:09	0.0299	0.0060
4:25	0.0361	0.0058
4:40	0.0299	0.0059
4:56	0.0297	0.0059

*Instrument limit reached.

Table A.72 – Flow parameters n' and K for 30 ppt guar gel with 5 ppt sodium bromate at 300 °F (CHANDLER 5550)*

Elapsed Time (h:mm)	n'	K (lbf-s ^{n'} /ft ²)
0:15	0.0345	0.0123
1:02	0.0224	0.0118
1:17	0.0060	0.0139
2:35	0.0013	0.0128
3:22	0.0902	0.0086
3:38	0.0715	0.0084
3:54	0.0587	0.0082
4:09	0.0171	0.0094

*Instrument limit reached.

Table A.73 – Flow parameters n' and K for 30 ppt guar gel with 10 ppt sodium bromate at 150 °F (CHANDLER 5550)

Elapsed Time (h:mm)	n'	K (lbf-s ⁿ /ft ²)
0:15	0.2970	0.0180
0:31	0.2819	0.0188
0:46	0.2180	0.0243
1:02	0.1176	0.0358
1:17	0.0684	0.0437
1:33	0.0337	0.0500
1:49	0.0233	0.0521
2:04	0.0160	0.0537
2:20	0.0160	0.0537
2:36	0.0087	0.0554
2:51	0.0087	0.0554
3:07	0.0138	0.0545
3:22	0.0153	0.0545
3:38	0.0195	0.0540
3:54	0.0102	0.0564
4:09	0.0146	0.0559
4:25	0.0121	0.0569
4:40	0.0126	0.0575
4:56	0.0098	0.0591

Table A.74 – Flow parameters n' and K for 30 ppt guar gel with 10 ppt sodium bromate at 200 °F (CHANDLER 5550)

Elapsed Time (h:mm)	n'	K (lbf-s ^{n'} /ft ²)
0:15	0.4795	0.4357
0:31	0.4093	0.5052
0:46	0.3867	0.5023
1:02	0.3382	0.5628
1:17	0.3030	0.6159
1:33	0.2528	0.7158
1:49	0.2226	0.7727
2:04	0.1897	0.8502
2:20	0.2064	0.7779
2:35	0.1878	0.8135
2:51	0.1795	0.8132
3:07	0.1829	0.8630
3:22	0.2547	0.7065
3:38	0.3065	0.6328
3:54	0.3437	0.6048
4:09	0.3453	0.6433
4:25	0.3828	0.5896
4:40	0.3918	0.6068
4:56	0.4220	0.5612

Table A.75– Flow parameters n' and K for 30 ppt guar gel with 10 ppt sodium bromate at 225 °F (CHANDLER 5550)*

Elapsed Time	n'	K
(h:mm)		(lbf-s^{n'}/ft²)
0:17	0.3079	0.0123
0:35	0.1706	0.0219
0:52	0.0825	0.0404
1:10	0.0733	0.0421
1:28	0.0759	0.0399
1:45	0.0544	0.0435
2:56	0.0014	0.0515
3:13	0.0045	0.0506

*Instrument limit reached.

Table A.76– Flow parameters n' and K for 30 ppt guar gel with 10 ppt sodium bromate at 250 °F (CHANDLER 5550)

Elapsed Time (h:mm)	n'	K (lbf-s ^{n'} /ft ²)
0:17	0.5869	0.0019
0:35	0.4756	0.0026
0:52	0.4046	0.0034
1:10	0.3298	0.0050
1:28	0.2778	0.0064
1:45	0.2525	0.0071
2:03	0.2283	0.0077
2:21	0.2039	0.0085
2:38	0.1801	0.0094
2:56	0.1796	0.0090
3:14	0.1720	0.0093
3:31	0.1657	0.0095
3:49	0.1655	0.0092
4:07	0.1527	0.0098
4:24	0.1591	0.0093
4:42	0.1469	0.0097
5:00	0.1458	0.0097
5:17	0.1458	0.0097
5:35	0.1315	0.0102
5:53	0.1345	0.0101
6:10	0.1386	0.0099

Table A.77– Flow parameters n' and K for 30 ppt guar gel with 10 ppt sodium bromate at 275 °F (CHANDLER 5550)

Elapsed Time (h:mm)	n'	K (lbf-s ^{n'} /ft ²)
0:17	0.4564	0.0028
0:35	0.2832	0.0050
0:52	0.2047	0.0070
1:10	0.1610	0.0087
1:28	0.1264	0.0103
1:45	0.1262	0.0102
2:03	0.1069	0.0114
2:21	0.0844	0.0124
2:38	0.0591	0.0138
2:56	0.0675	0.0132
3:14	0.0535	0.0140
3:31	0.0442	0.0146
3:49	0.0619	0.0137
4:07	0.0579	0.0139
4:24	0.0358	0.0150
4:42	0.0281	0.0155
5:00	0.0400	0.0148
5:17	0.0274	0.0156
5:35	0.0337	0.0152
5:53	0.0007	0.0172

Table A78 – Flow parameters n' and K for 30 ppt guar gel with 10 ppt sodium bromate at 300 °F (CHANDLER 5550)

Elapsed Time (h:mm)	n'	K (lbf-s ⁿ /ft ²)
0:17	0.4133	0.0019
0:35	0.2156	0.0038
0:52	0.1517	0.0058
1:10	0.1234	0.0067
1:28	0.0927	0.0080
1:45	0.0929	0.0080
2:03	0.0762	0.0085
2:21	0.0850	0.0082
2:38	0.0986	0.0078
2:56	0.0994	0.0078
3:14	0.0970	0.0078
3:31	0.0959	0.0079
3:49	0.1002	0.0078
4:07	0.1006	0.0077
4:24	0.0945	0.0079
4:42	0.0961	0.0079
4:59	0.0983	0.0079
5:17	0.0856	0.0082
5:35	0.0933	0.0080
5:52	0.0983	0.0079
6:10	0.1014	0.0077

Table A.79 – Flow parameters n' and K for 60 ppt guar gel with 1 ppt magnesium peroxide at 175 °F (CHANDLER 5550)

Elapsed Time (h:mm)	n'	K (lbf-s ⁿ /ft ²)
0:15	0.4204	6.0369
0:31	0.4615	4.6647
0:46	0.4791	4.1155
1:02	0.4982	3.6785
1:18	0.5114	3.4037
1:33	0.5179	3.2456
1:49	0.5269	3.0781
2:04	0.5290	3.0076
2:20	0.5340	2.9077
2:36	0.5382	2.8269
2:51	0.5431	2.7423
3:07	0.5451	2.6973
3:22	0.5507	2.6133
3:38	0.5532	2.5627
3:54	0.5557	2.5180
4:09	0.5587	2.4728
4:25	0.5632	2.4093
4:41	0.5644	2.3859
4:56	0.5610	2.3980
5:12	0.5678	2.3218
5:27	0.5728	2.2618
5:43	0.5755	2.2191
5:59	0.5739	2.2243
6:14	0.5480	2.8226
6:30	0.5089	3.7056
6:45	0.4852	4.4375
7:01	0.4662	5.1272
7:17	0.4529	5.6810
7:32	0.4381	6.2489
7:48	0.4284	6.7137
8:03	0.4194	7.1490

Table A.80 – Flow parameters n' and K for 60 ppt guar gel with 1 ppt magnesium peroxide at 200 °F (CHANDLER 5550)

Elapsed Time	n'	K
(h:mm)		(lbf-s^{n'}/ft²)
0:15	0.5247	2.9257
0:31	0.6253	1.4787
0:46	0.6694	1.0262
1:02	0.6935	0.7964
1:17	0.7039	0.6595
1:33	0.7261	0.5267
1:49	0.7315	0.4502
2:04	0.7187	0.4190
2:20	0.6999	0.3970
2:35	0.6714	0.3897
2:51	0.6414	0.3876
3:07	0.5957	0.4108

Table A.81 – Flow parameters n' and K for 60 ppt guar gel with 1 ppt magnesium peroxide at 225 °F (CHANDLER 5550)

Elapsed Time (h:mm)	n'	K (lbf-s ⁿ /ft ²)
0:15	0.5877	0.0168
0:31	0.6585	0.0082
0:46	0.6696	0.0060
1:02	0.6434	0.0055
1:17	0.6178	0.0053
1:33	0.5934	0.0052
1:48	0.5631	0.0054
2:04	0.5174	0.0061
2:20	0.0489	0.0578
2:35	0.0574	0.0538
2:51	0.0576	0.0530
3:06	0.0536	0.0537
3:22	0.0496	0.0541
3:38	0.0423	0.0556
3:54	0.0346	0.0572
4:09	0.0297	0.0584
4:25	0.0175	0.0613
4:40	0.0132	0.0622
4:56	0.0128	0.0623
5:11	0.0125	0.0625
5:27	0.0127	0.0625
5:43	0.0131	0.0624
5:58	0.0124	0.0624
6:14	0.0125	0.0626
6:29	0.0248	0.0596
6:45	0.0743	0.0508
7:00	0.1632	0.0380
7:16	0.3015	0.0237
7:32	0.4500	0.0143
7:47	0.5105	0.0122
8:03	0.5357	0.0119

Table A.82 – Flow parameters n' and K for 60 ppt guar gel with 1 ppt magnesium peroxide at 250 °F (CHANDLER 5550)

Elapsed Time	n'	K
(h:mm)		(lbf-s^{n'}/ft²)
0:15	0.5388	0.0088
0:31	0.2357	0.0115
0:46	0.0927	0.0153
1:02	0.0434	0.0171
1:17	0.0318	0.0175
1:33	0.0142	0.0185
1:48	0.0120	0.0187
2:04	0.0000	0.0195

*Instrument limit reached.

Table A.83 – Flow parameters n' and K for 60 ppt guar gel with 1 ppt sodium bromate at 200 °F (CHANDLER 5550)

Elapsed Time (h:mm)	n'	K (lbf-s ⁿ /ft ²)
0:15	0.4762	0.0379
0:31	0.5223	0.0282
0:46	0.5416	0.0242
1:02	0.5629	0.0210
1:18	0.5764	0.0189
1:33	0.5907	0.0169
1:49	0.6033	0.0153
2:04	0.6116	0.0142
2:20	0.6216	0.0130
2:36	0.6265	0.0122
2:51	0.6327	0.0114
3:07	0.6361	0.0108
3:23	0.6456	0.0099
3:38	0.6591	0.0089
3:54	0.6545	0.0087
4:09	0.6579	0.0082
4:25	0.6653	0.0076
4:41	0.6651	0.0074
4:56	0.6647	0.0071
5:12	0.6682	0.0067
5:27	0.6666	0.0065
5:43	0.6537	0.0066
5:59	0.6615	0.0061
6:14	0.6826	0.0069
6:30	0.6699	0.0089
6:45	0.6604	0.0109
7:01	0.6457	0.0130
7:17	0.6304	0.0152
7:32	0.6171	0.0172
7:48	0.6091	0.0189
8:04	0.6010	0.0203

Table A.84 – Flow parameters n' and K for 60 ppt guar gel with 1 ppt sodium bromate at 225 °F (CHANDLER 5550)

Elapsed Time (h:mm)	n'	K (lbf-s ^{n'} /ft ²)
0:15	0.5359	0.0242
0:31	0.6096	0.0137
0:46	0.6485	0.0094
1:02	0.6711	0.0072
1:18	0.6626	0.0064
1:33	0.6588	0.0056
1:49	0.6355	0.0055
2:04	0.6100	0.0054
2:20	0.5893	0.0054
2:36	0.5580	0.0058
2:51	0.5492	0.0057
3:07	0.5307	0.0058
3:22	0.5032	0.0062
3:38	0.4768	0.0067
3:54	0.4643	0.0068

Table A.85 – Flow parameters n' and K for 60 ppt guar gel with 1 ppt sodium bromate at 250 °F (CHANDLER 5550)

Elapsed Time (h:mm)	n'	K (lbf-s ⁿ /ft ²)
0:15	0.6598	0.0085
0:31	0.6341	0.0041
0:46	0.4935	0.0044
1:02	0.4009	0.0051
1:17	0.3538	0.0057
1:33	0.3063	0.0065
1:49	0.2576	0.0075
2:04	0.2282	0.0082
2:20	0.2022	0.0088
2:36	0.1802	0.0093
2:51	0.1464	0.0104
3:07	0.1412	0.0104
3:22	0.1366	0.0103
3:38	0.1206	0.0108
3:54	0.1278	0.0104
4:09	0.1093	0.0109
4:25	0.0979	0.0114
4:40	0.0989	0.0113
4:56	0.0973	0.0112
5:12	0.0751	0.0120
5:27	0.0758	0.0120
5:43	0.0734	0.0121
5:58	0.0642	0.0124
6:14	0.0868	0.0119
6:30	0.0991	0.0119
6:45	0.1555	0.0102
7:01	0.1688	0.0103
7:17	0.2331	0.0086
7:32	0.2657	0.0081
7:48	0.3054	0.0074
8:03	0.3309	0.0071

APPENDIX B
EARLY TIME VISCOSITY CHARTS

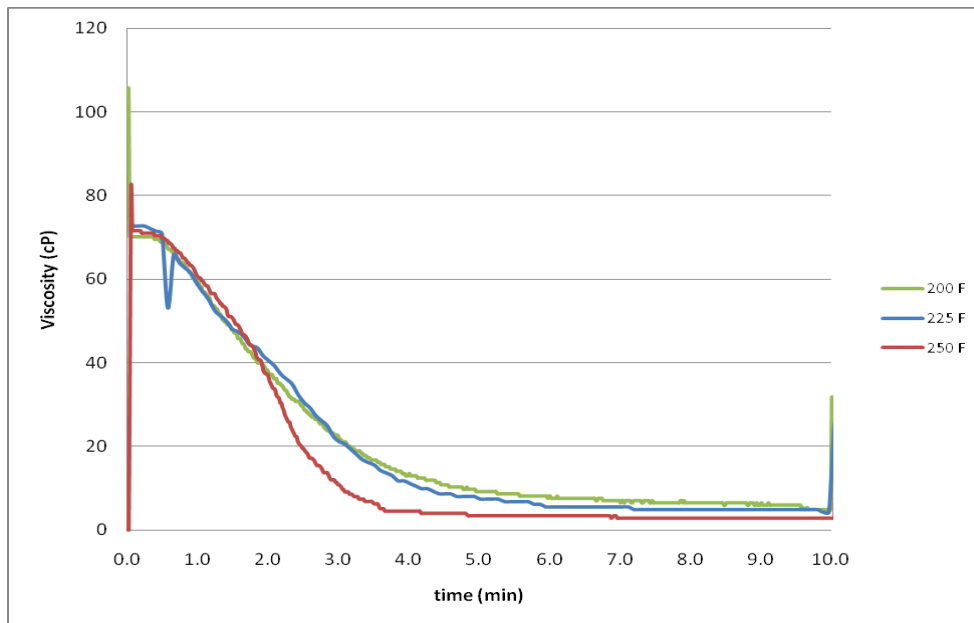


Figure B.1– Early time viscosity of 30 ppt guar gel with 0.25 ppt ammonium persulfate

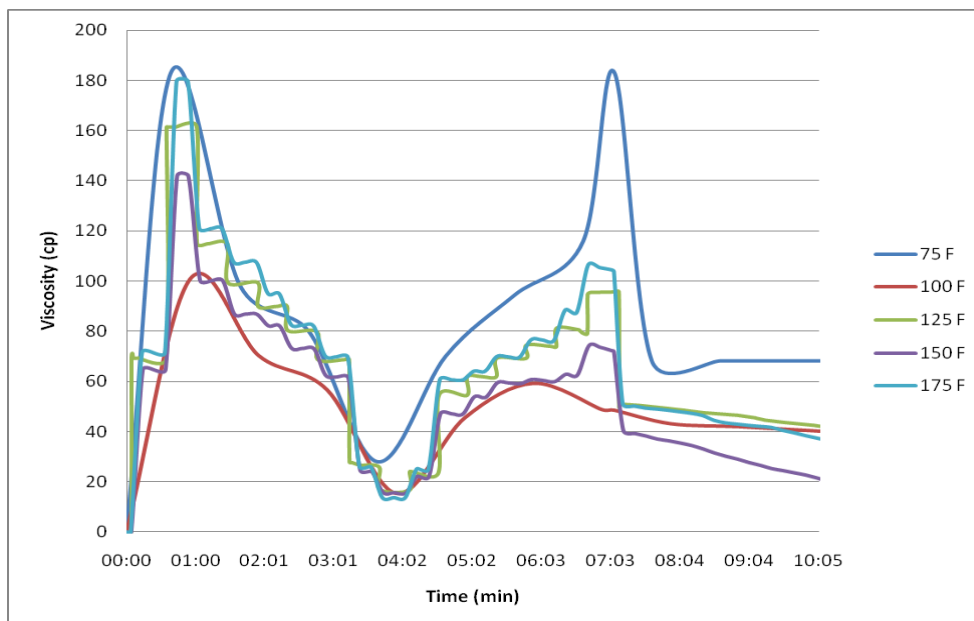


Figure B.2– Early time viscosity of 30 ppt guar gel with 0.5 ppt ammonium persulfate

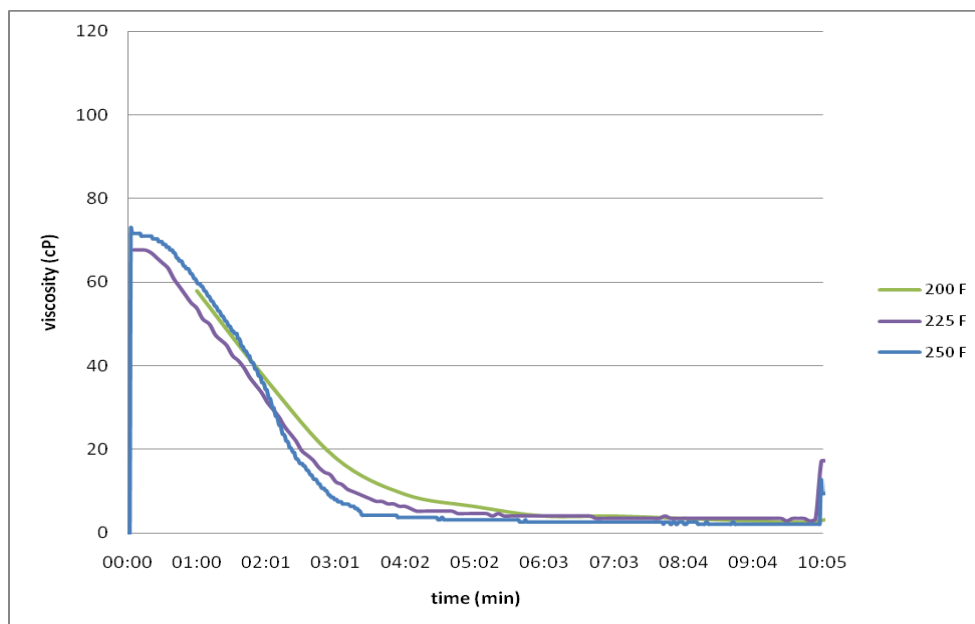


Figure B.3 – Early time viscosity of 30 ppt guar gel with 0.5 ppt ammonium persulfate

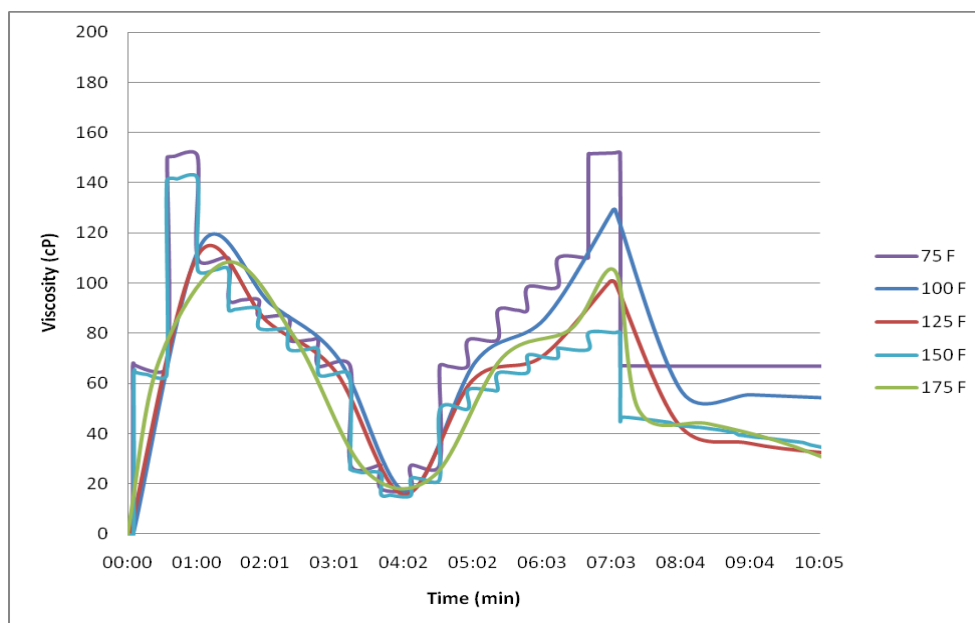


Figure B.4– Early time viscosity of 30 ppt guar gel with 1 ppt ammonium persulfate

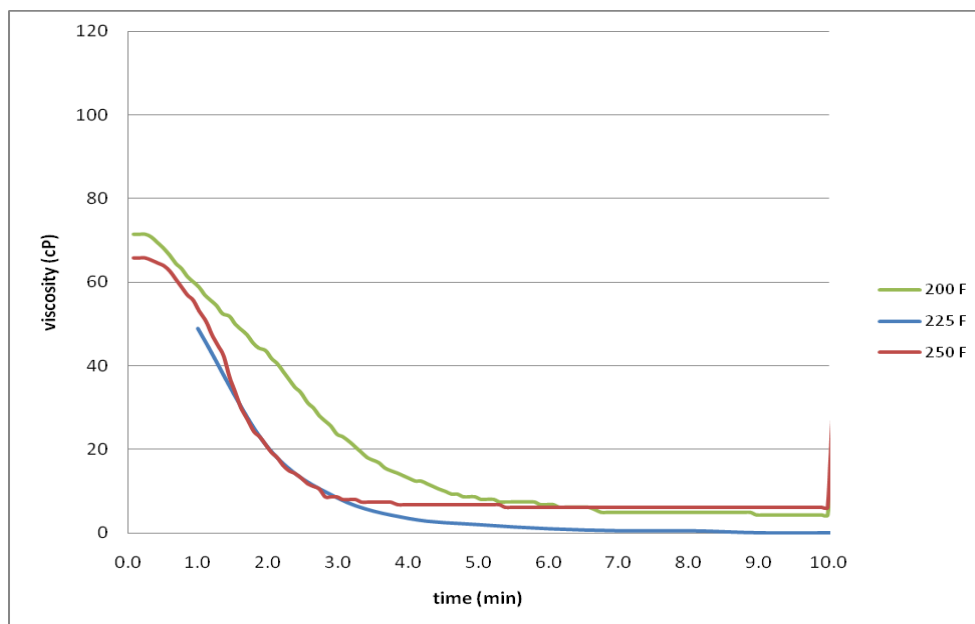


Figure B.5– Early time viscosity of 30 ppt guar gel with 1 ppt ammonium persulfate

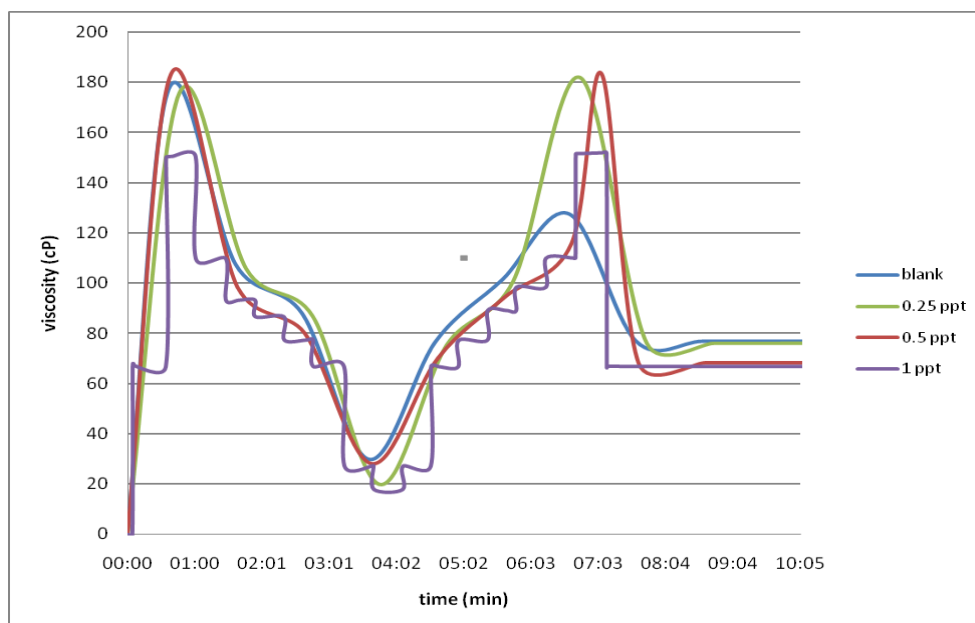


Figure B.6– Early time viscosity of 30 ppt guar gel with ammonium persulfate at 75 °F

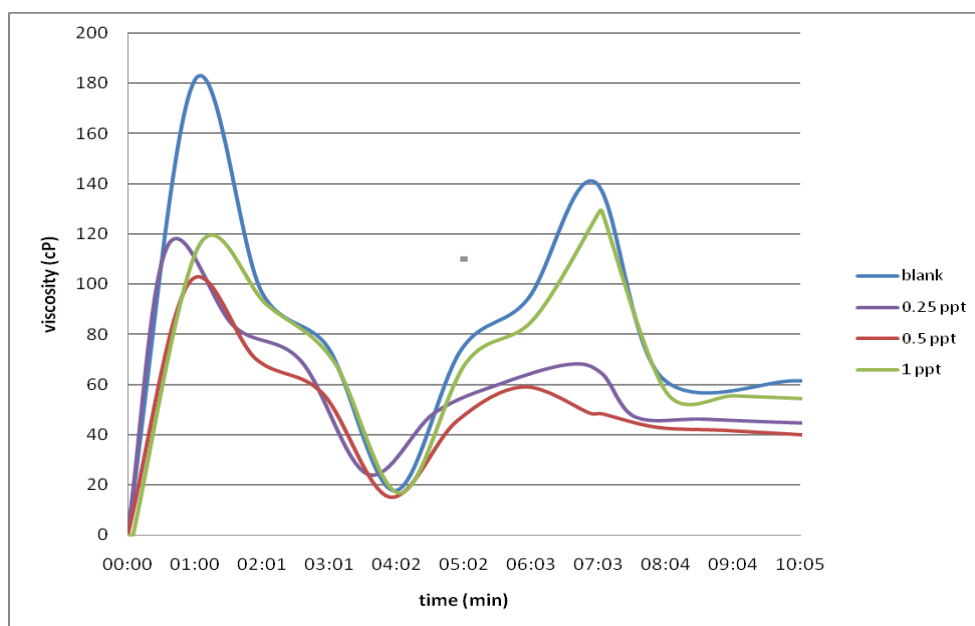


Figure B.7– Early time viscosity of 30 ppt guar gel with ammonium persulfate at 100 °F

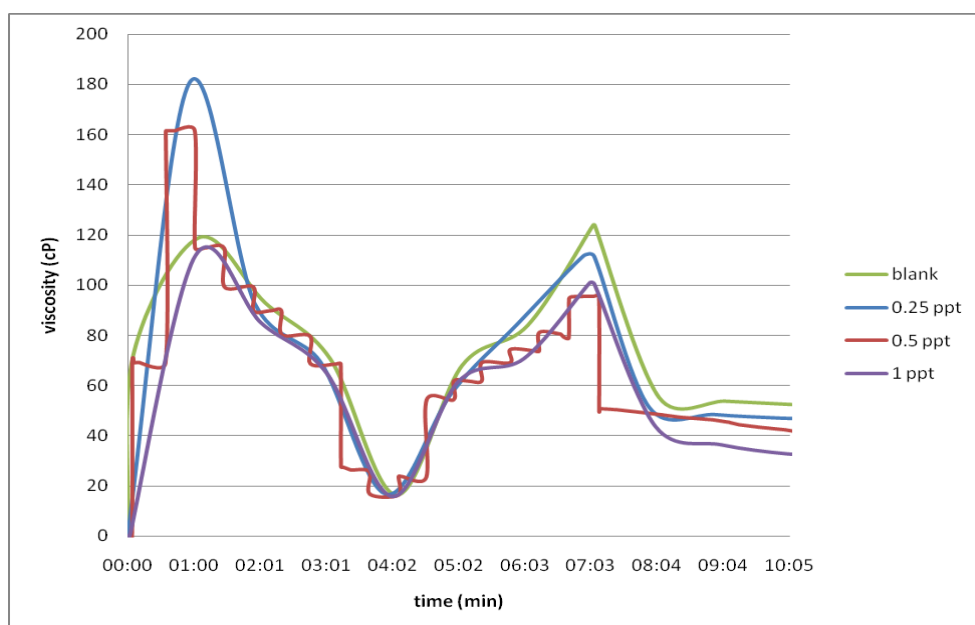


Figure B.8– Early time viscosity of 30 ppt guar gel with ammonium persulfate at 125 °F

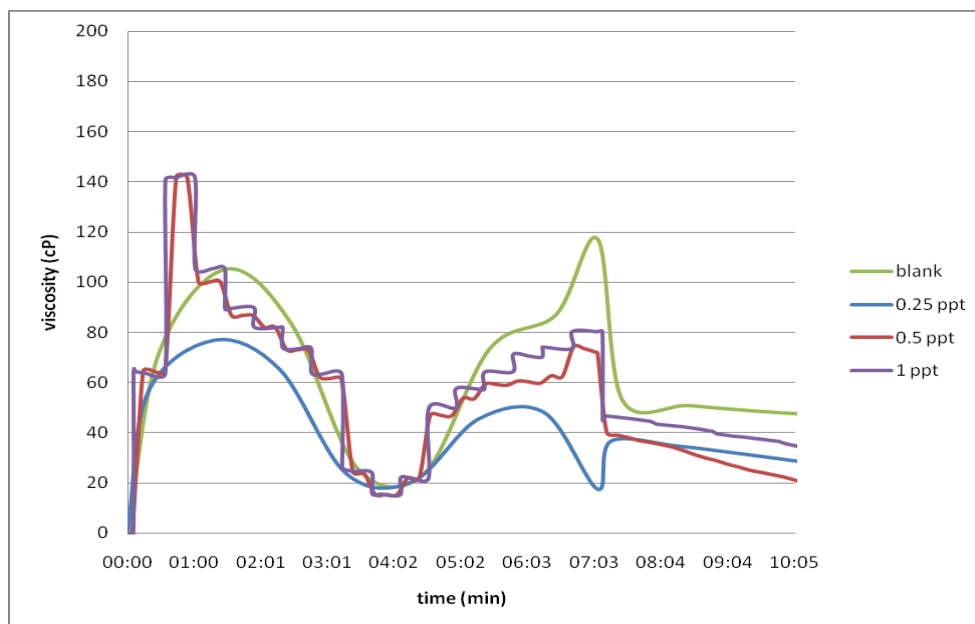


Figure B.9– Early time viscosity of 30 ppt guar gel with ammonium persulfate at 150 °F

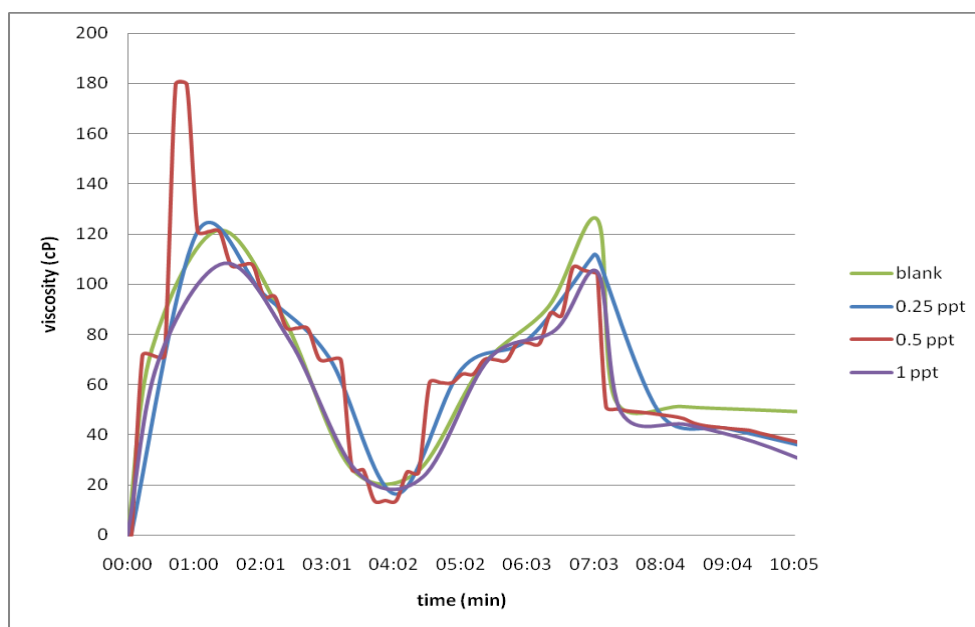


Figure B.10– Early time viscosity of 30 ppt guar gel with ammonium persulfate at 175

°F

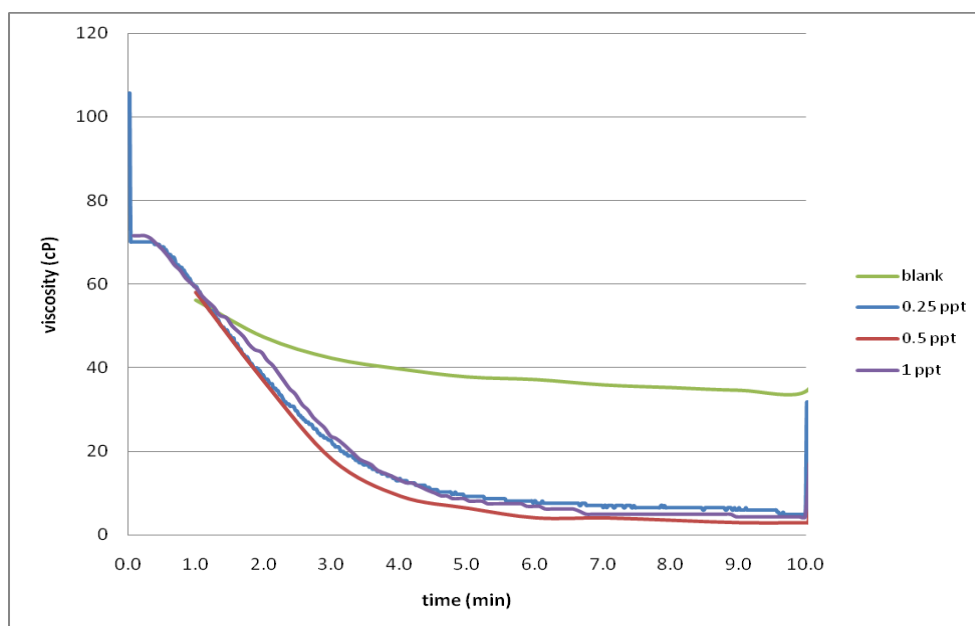


Figure B.11– Early time viscosity of 30 ppt guar gel with ammonium persulfate at 200

°F

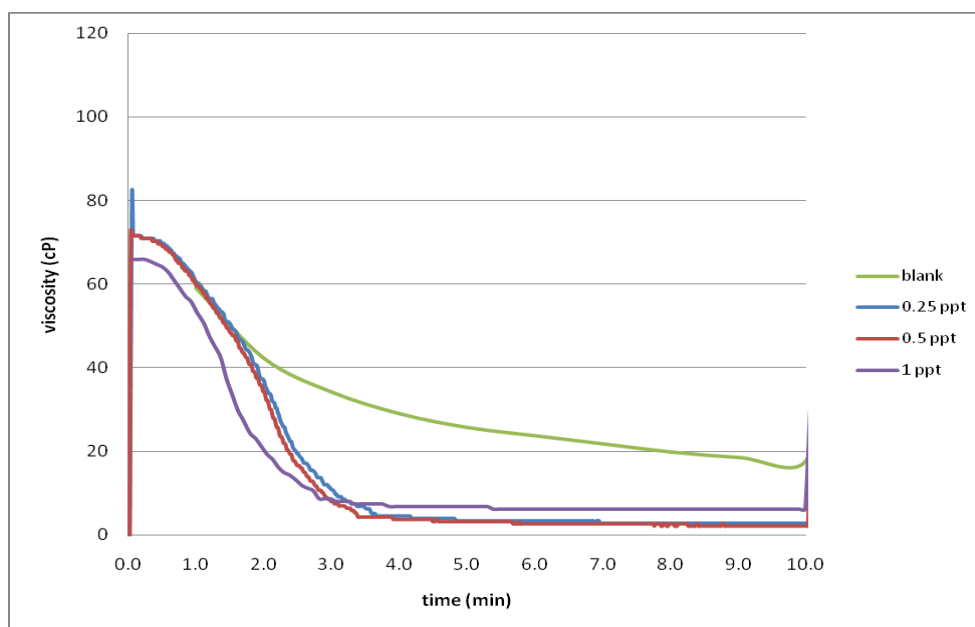


Figure B.12– Early time viscosity of 30 ppt guar gel with ammonium persulfate at 250

°F

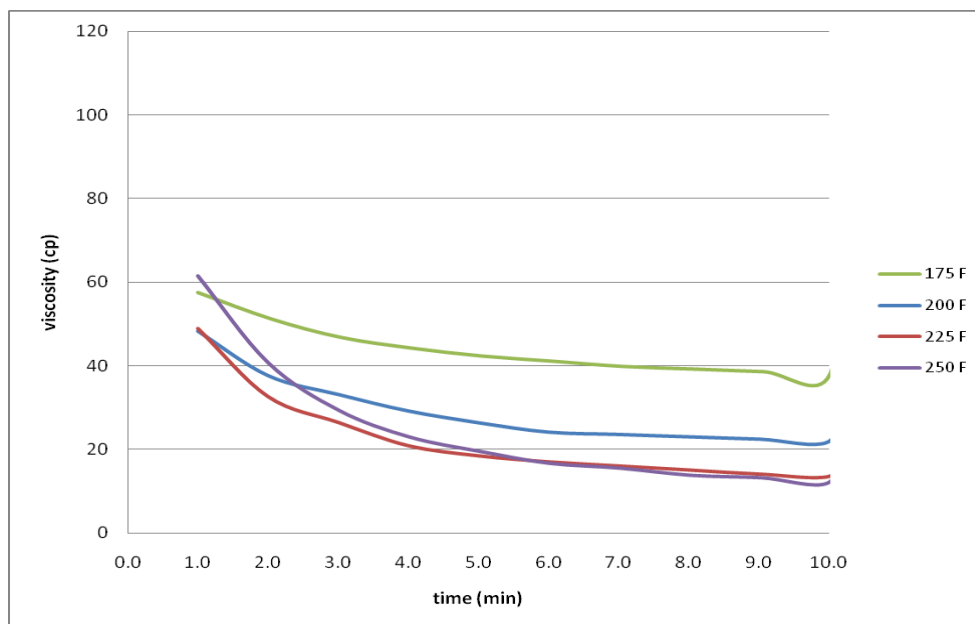


Figure B.13– Early time viscosity of 30 ppt guar gel with 1 ppt magnesium peroxide

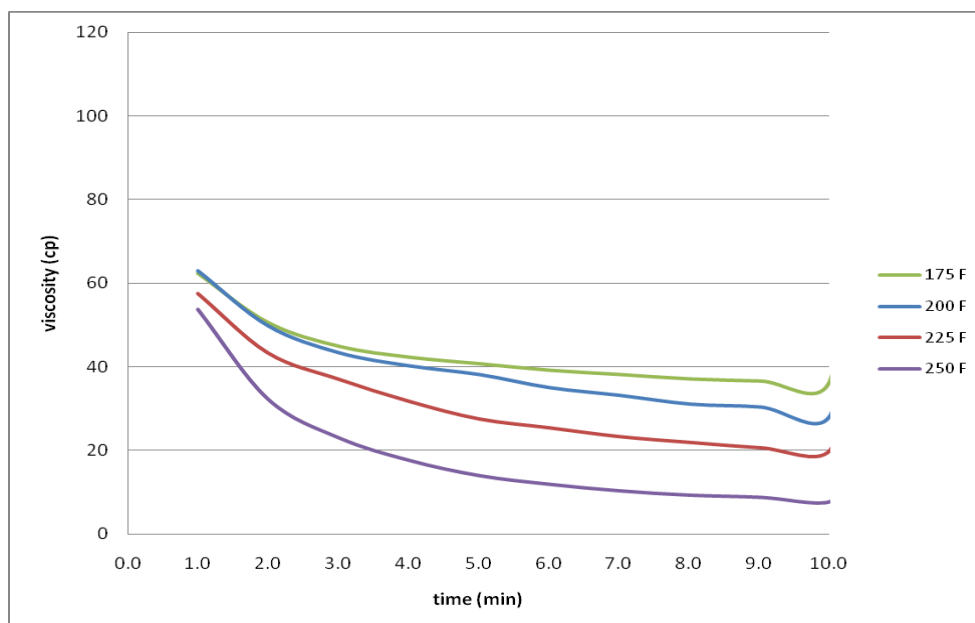


Figure B.14– Early time viscosity of 30 ppt guar gel with 5 ppt magnesium peroxide

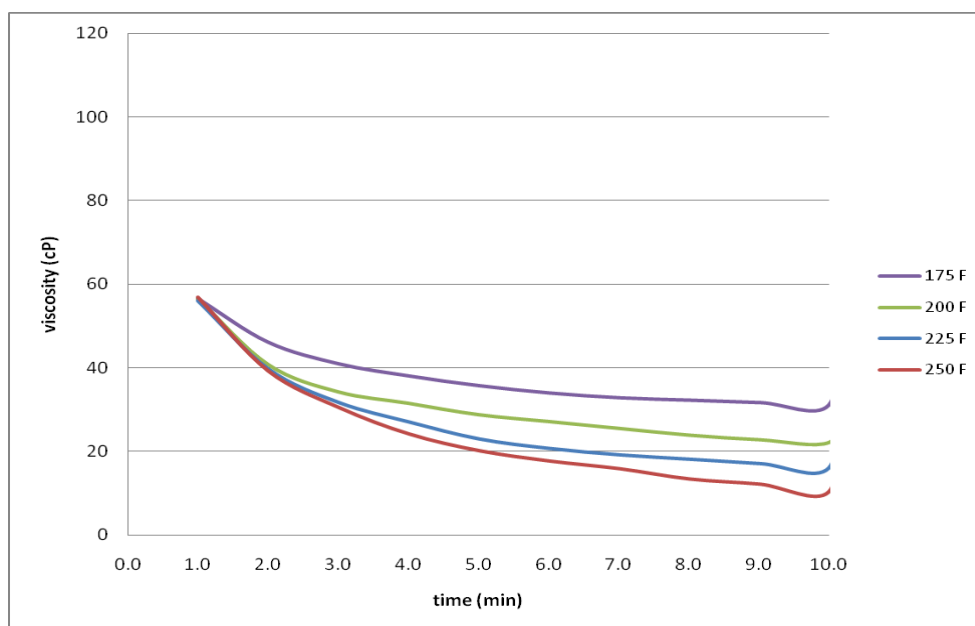


Figure B.15– Early time viscosity of 30 ppt guar gel with 10 ppt magnesium peroxide

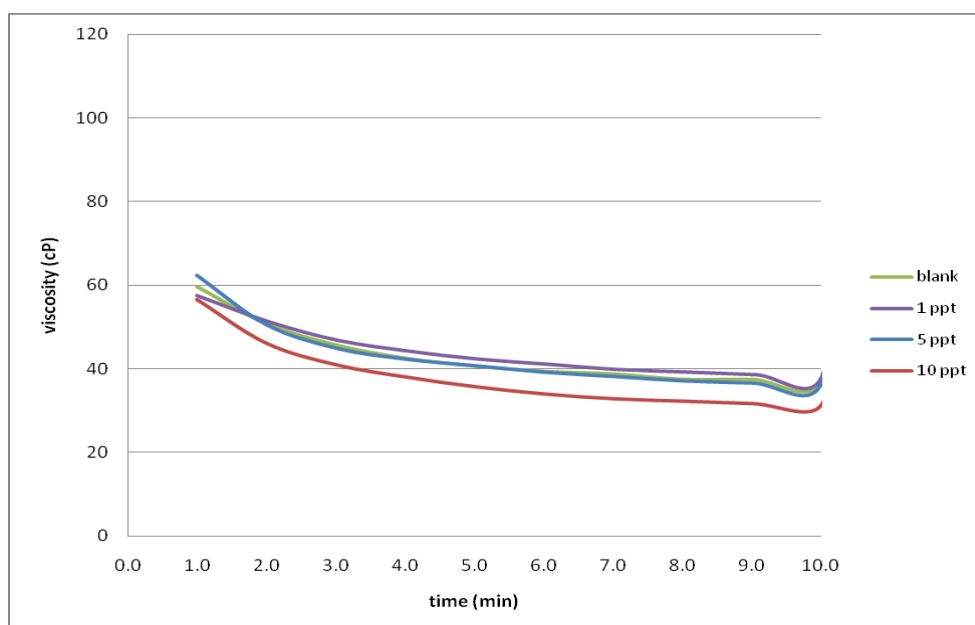


Figure B.16– Early time viscosity of 30 ppt guar gel with magnesium peroxide at 175 °F

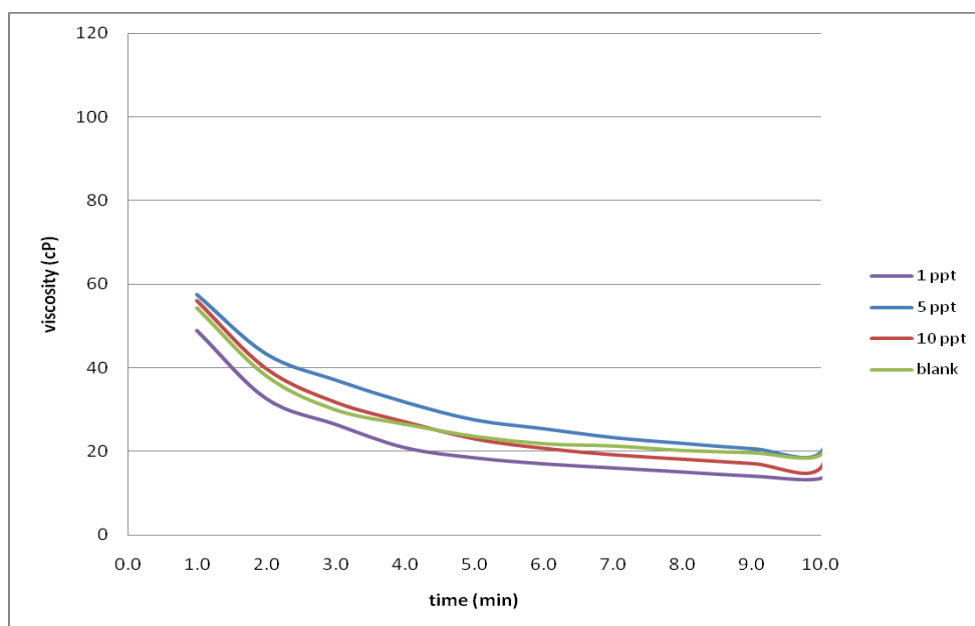


Figure B.17– Early time viscosity of 30 ppt guar gel with magnesium peroxide at 225 °F

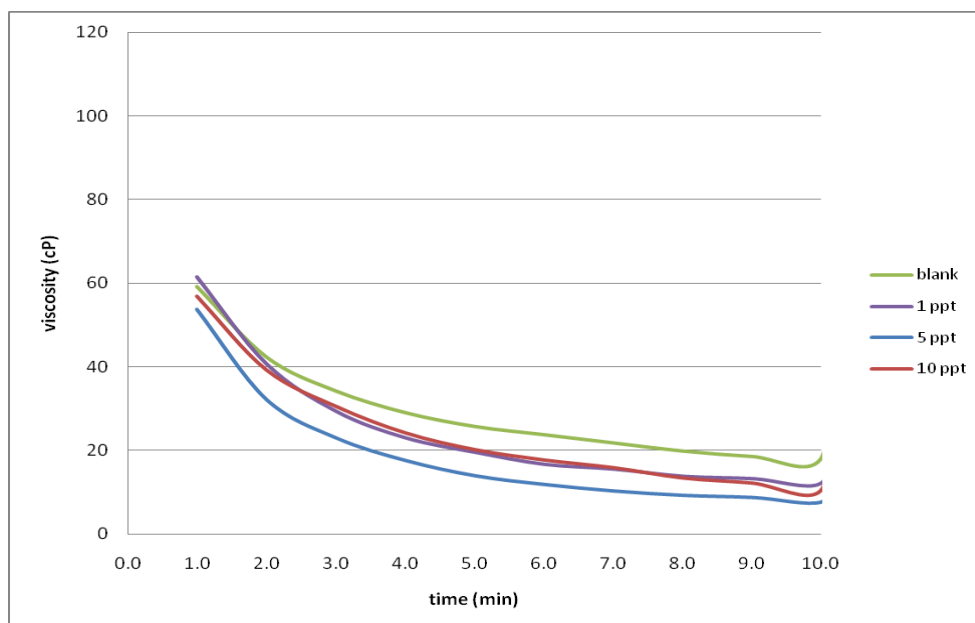


Figure B.18– Early time viscosity of 30 ppt guar gel with magnesium peroxide at 250 °F

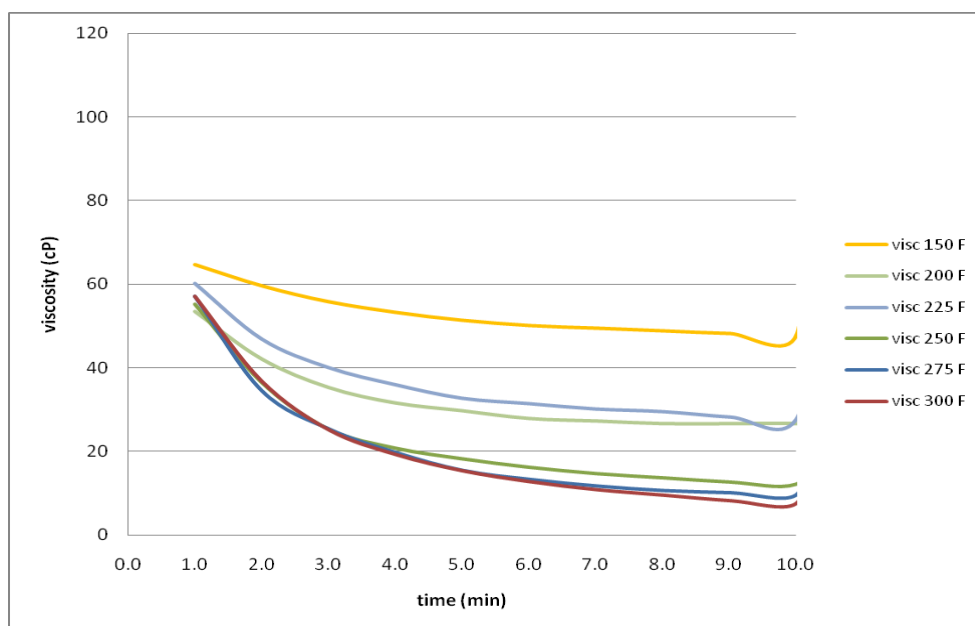


Figure B.19– Early time viscosity of 30 ppt guar gel with 1 ppt sodium bromate

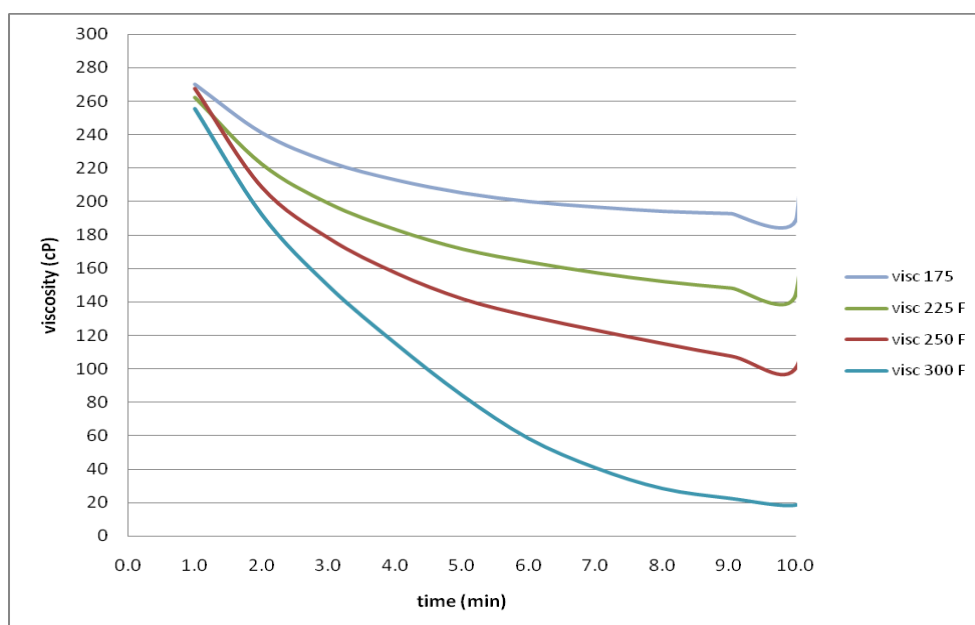


Figure B.20– Early time viscosity of 60 ppt guar gel with 1 ppt sodium bromate

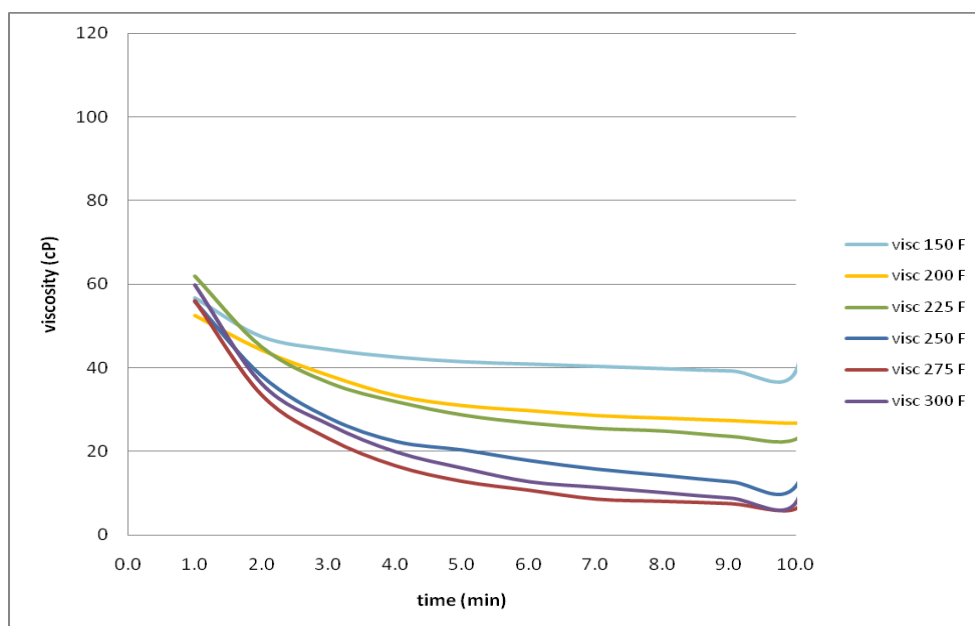


Figure B.21– Early time viscosity of 30 ppt guar gel with 5 ppt sodium bromate

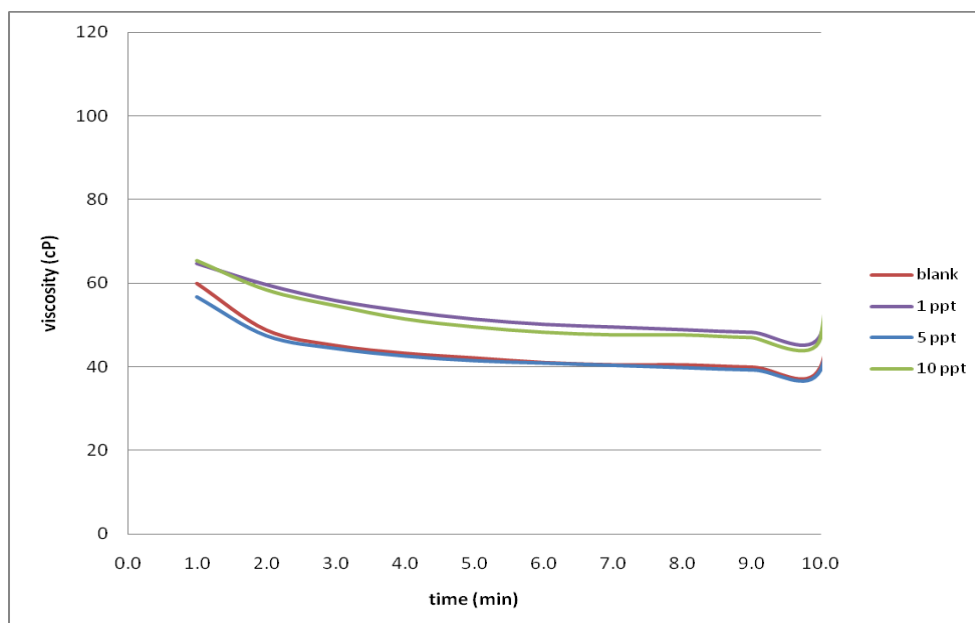


Figure B.22– Early time viscosity of 30 ppt guar gel with sodium bromate at 150 °F

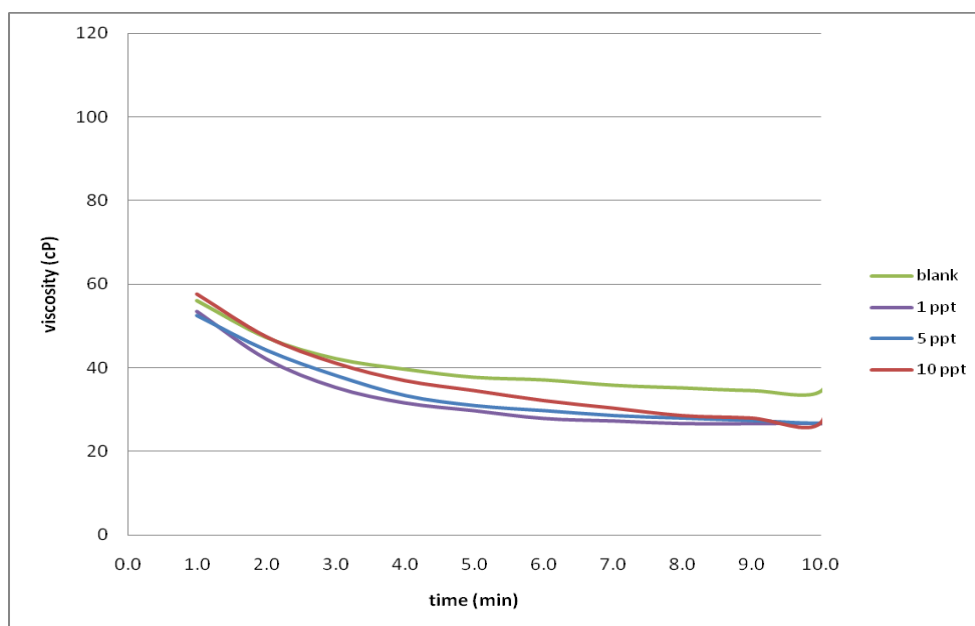


Figure B.23– Early time viscosity of 30 ppt guar gel with sodium bromate at 200 °F

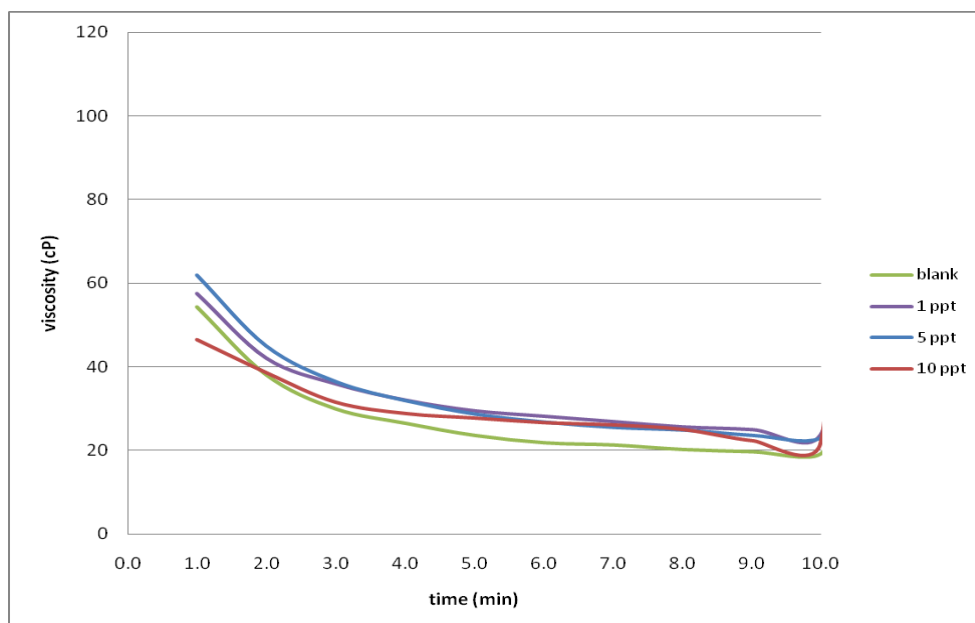


Figure B.24– Early time viscosity of 30 ppt guar gel with sodium bromate at 225 °F

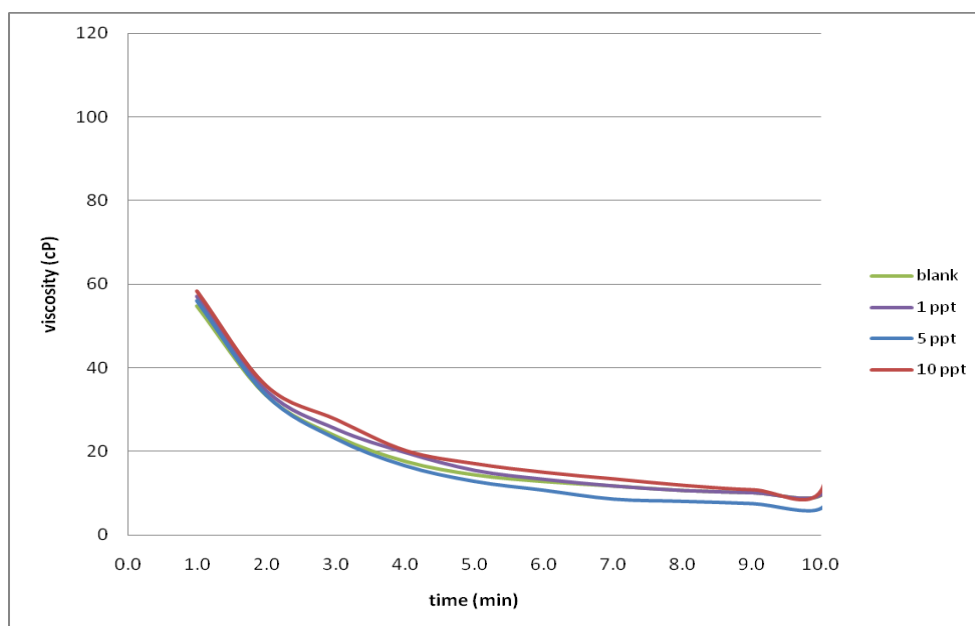


Figure B.25– Early time viscosity of 30 ppt guar gel with sodium bromate at 275 °F

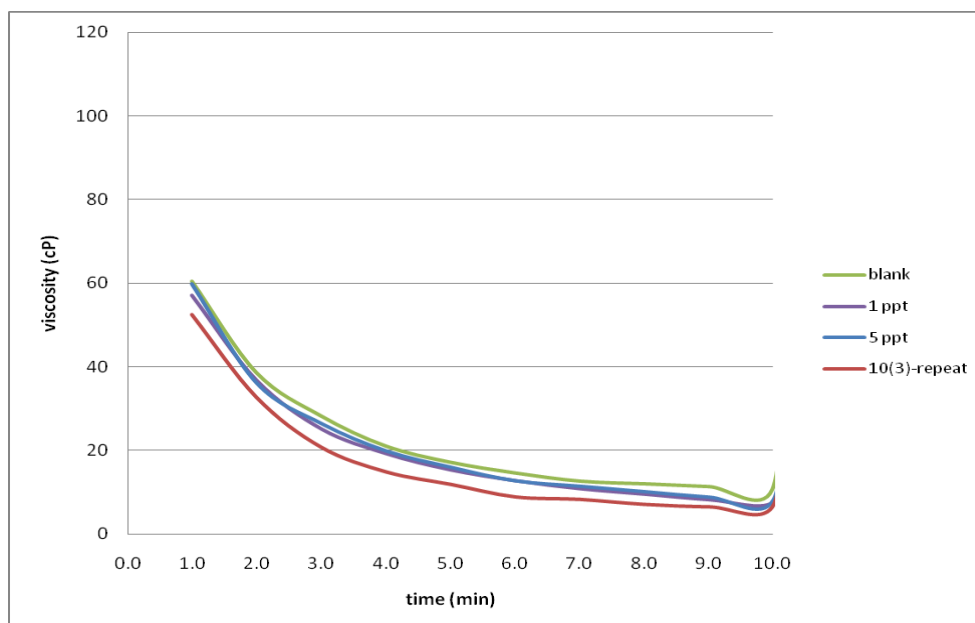


Figure B.26– Early time viscosity of 30 ppt guar gel with sodium bromate at 300 °F

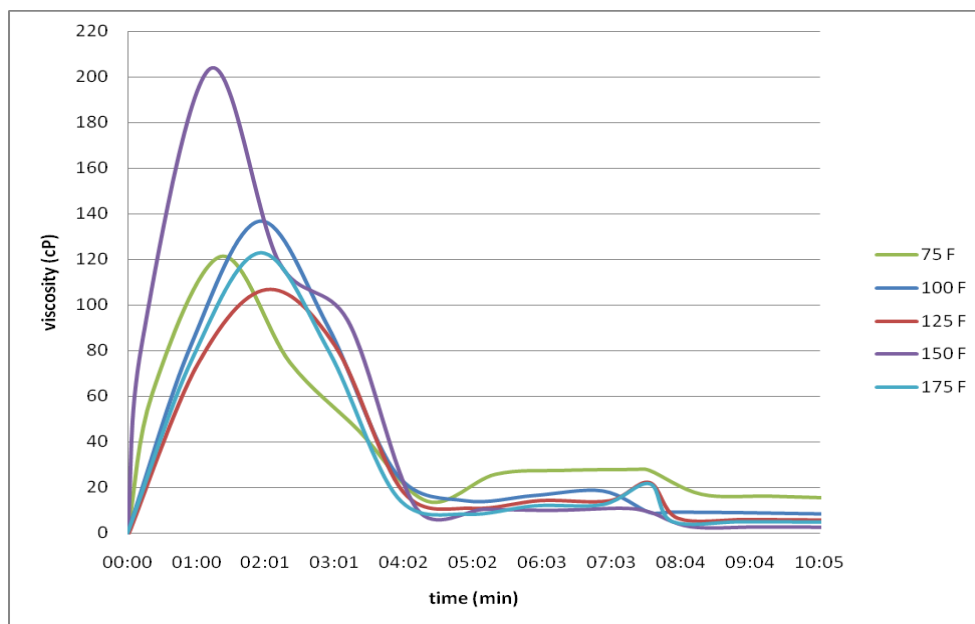


Figure B.27– Early time viscosity of 30 ppt guar gel with 0.5 gpt galactomannanase

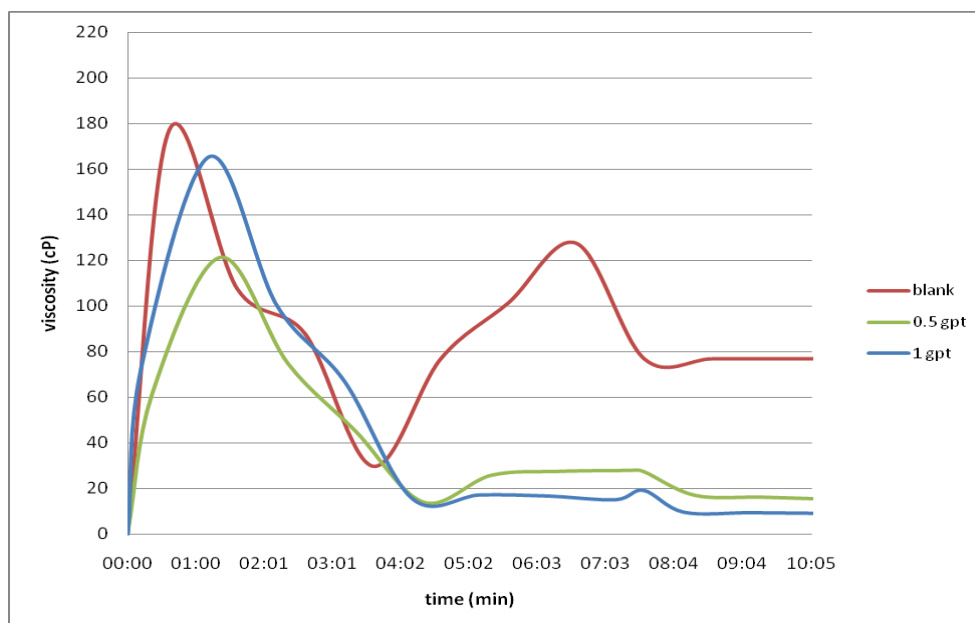


Figure B.28– Early time viscosity of 30 ppt guar gel with galactomannanase at 75 °F

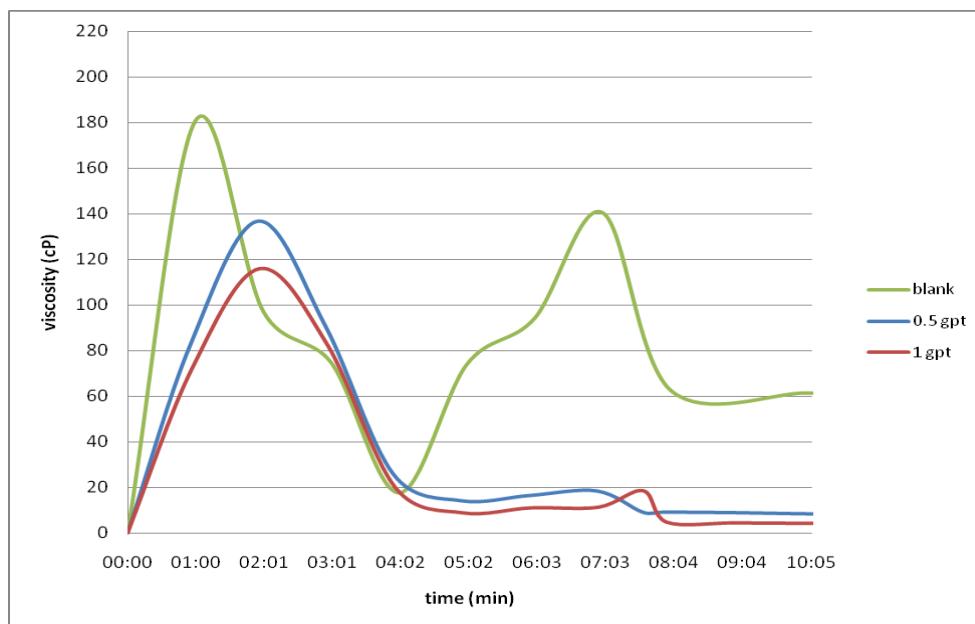


Figure B.29– Early time viscosity of 30 ppt guar gel with galactomannanase at 100 °F

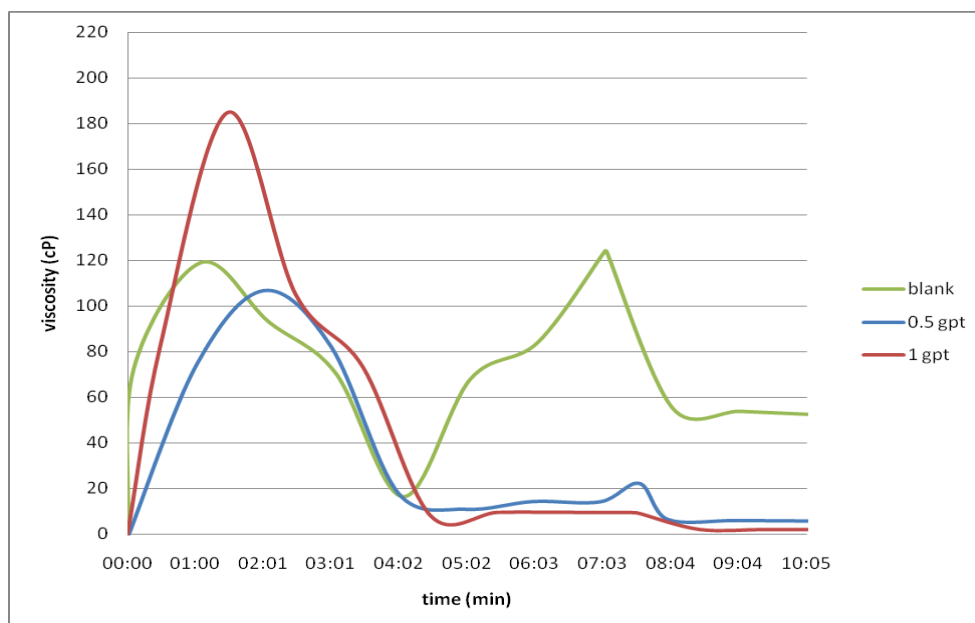


Figure B.30– Early time viscosity of 30 ppt guar gel with galactomannanase at 125 °F

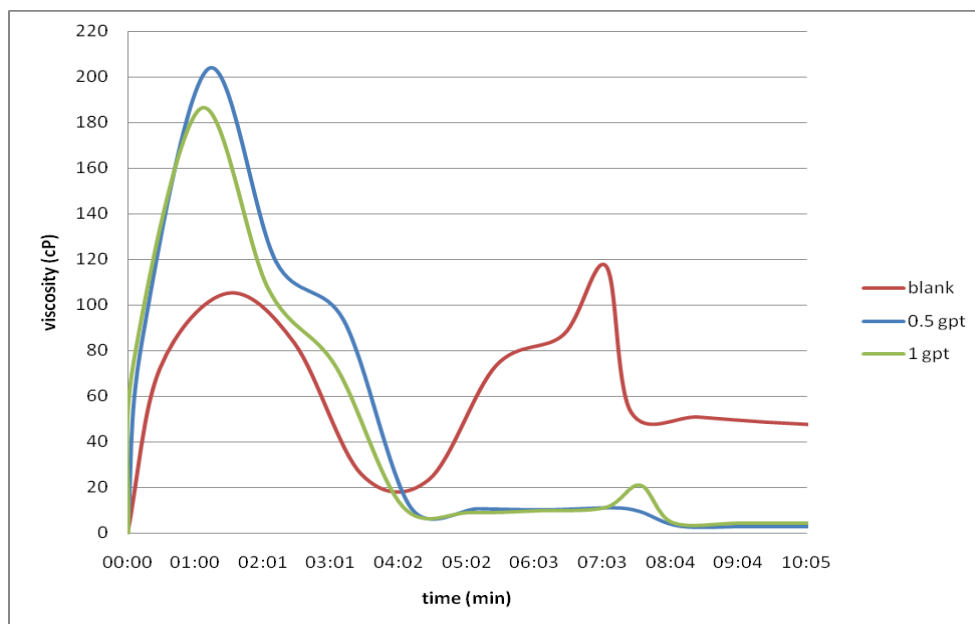


Figure B.31– Early time viscosity of 30 ppt guar gel with galactomannanase at 150 °F

VITA

Name: Muhammad Usman Sarwar

Address: Harold Vance Department of Petroleum Engineering
Texas A&M University
3116 TAMU - 603 Richardson Building
College Station, TX 77843-3116

Email Address: musarwar@hotmail.com

Education: B.E., Mechanical Engineering, NED University of Engineering
and Technology, Karachi, Pakistan, February 2007
M.S., Petroleum Engineering, Texas A&M University, TX, USA,
December 2010